INFLUENCE OF LARGE DEFORMATIONS AND MIDPLANE FORCES ON THE PLASTIC BEHAVIOR OF IMPULSIVELY LOADED PLATES

By

Edwin T. Kruszewski

Dissertation submitted to the Graduate Faculty of the

Virginia Polytechnic Institute

in partial fulfillment for the degree of

DOCTOR OF PHILOSOPHY

in

Engineering Mechanics

April 1968

INFLUENCE OF LARGE DEFORMATIONS AND MIDPLANE FORCES ON THE PLASTIC BEHAVIOR OF IMPULSIVELY LOADED PLATES

By

Edwin T. Kruszewski

ABSTRACT

This dissertation deals with an analysis of impulsively loaded plastic plates that includes effects of large deformations and midplane forces. Specifically, it deals with a circular plate of uniform thickness simply supported at its edges. The impulsive loading is characterized by an initial velocity distribution.

The analysis assumes that the plate is an isotropic, rigid, ideally plastic material. Shear deformations and longitudinal inertia are neglected. Both bending and midplane forces are considered. The midplane forces can be either applied prior to the impulse or generated by deformations of the midplane. Deformations of the cross section are based on the assumption that a line initially normal to the midplane remains straight and normal after deformation. Strains are nonlinear with respect to transverse displacements but contain only linear radial displacement terms. Finally, the Tresca yield criteria are used.

An interaction equation is derived between the plastic moment and normal force. The relationship indicates that the greater the midplane force the smaller the required bending moment for plastic flow. When the

midplane force reaches a maximum value, the plate no longer carries a moment.

Equilibrium equations are derived for the motion of the plate which are consistent with the von Karman plate theory. Governing equations are then developed for the three possible phases of motion. The initial Phase 1 includes a bending hinge that travels from the support to the center of the plate. Phase 2, which is initiated when the hinge reaches the center, continues until either the motion ceases or a portion of the plate becomes a membrane. Phase 3 described the motion of the membrane hinge from its initial point of origin to its final stopping point.

These governing equations are solved for two types of bending-moment—midplane-force interaction relationships. One relationship is based on displacement of the neutral surface from the midplane surface. The second is based on the magnitude of the midplane forces. Both types of plastic plate behavior are examined.

Plots of final central deformation for various applied midplane forces and impulses are presented that clearly illustrate that even small amounts of midplane forces have a significant effect on the final deformation of plastic plates. Numerical results of the large deformational analyses are also presented. Plots are given showing the influence of the magnitude of the impulse on bending hinge velocity, initiation of membrane behavior, location of the membrane hinge, and the final deformation of the plate.

A comparison is made between results of the large deformational analysis and experimental data. It shows excellent agreement. For the

small and intermediate range of impulses the agreement is within experimental scatter. For the large impulses the calculated deformations are slightly conservative. Reasons for this deviation are discussed. Finally a critical examination is made of the various other suggested approaches that have possible application to the behavior of plastic plates.

INFLUENCE OF LARGE DEFORMATIONS AND MIDPLANE FORCES ON THE PLASTIC BEHAVIOR OF IMPULSIVELY LOADED PLATES

by

Edwin T. Kruszewski

Dissertation submitted to the Graduate Faculty of the

Virginia Polytechnic Institute

in partial fulfillment for the degree of

DOCTOR OF PHILOSOPHY

in

Engineering Mechanics

APPROVED:

Chairman Dr. Daniel F. Frederick

Prof. F. J. Maher

Dr. R. Chicurel

Dr. S. T. Gormsen

Dr. T. E. Leinhardt

April 1968

Blacksburg, Virginia

II. TABLE OF CONTENTS

III. ACKNOWLEDGMENTS

The author wishes to express his appreciation to the National Aeronautics and Space Administration for permitting him to conduct this research as part of his work assignment at Langley Research Center; and to Dr. Daniel Frederick, Professor of the Engineering Mechanics Department, Virginia Polytechnic Institute, and to Dr. Robert G. Thomson of the NASA for their helpful criticisms and suggestions. He also wishes to express his appreciation to Martha Robinson, Mathematician, Structures Research Division, Langley Research Center, for her assistance in programing of the numerical solution and the subsequent calculation of the results. Finally, the author wishes to express his gratitude to his wife and children for their patience and consideration throughout his entire doctorate program.

IV. LIST OF FIGURES AND TABLES

V. INTRODUCTION

The problem of the impulsively loaded plastic structure is of interest to designers in several diversified areas. As early as 1951, (see ref. 1) the U.S. Navy undertook a study of this problem in order to provide information to its ship designers about proper torpedo protection. The purpose of this study was to understand the response and to predict the damage done to steel plates of ships and submarines by underwater explosions. The development of high energy explosive devices that can be detonated above ground has caused the designers of buildings to become interested in the problem. Here the impulsive loads are generated by shock waves traveling through the atmosphere rather than water. Rather recently, solutions to this problem have been sought by the designers of spacecraft.

The outer shell of a spacecraft must be designed to withstand the rather harsh environment of space. Meteoroids are one of the more severe environmental hazards. Meteoroids are extra terrestrial particles, in orbit about the sun, which travel at velocities as high as 210,000 feet per second. Because of their extremely high velocity, even the smaller meteoroids can do a considerable amount of damage. For example, the large hole in the 3/16-inch aluminum plate, shown in figure 1, was made by the small 1/16-inch-diameter projectile (also shown in fig. 1) at an impact velocity of only 30,000 feet per second. At the highest meteoroid velocity this small projectile could penetrate a plate over an inch and a quarter thick.

Figure 1.- Damage to a 3/16-inch aluminum target by a 1/16-inch-diameter projectile.

In order to alleviate this damage, spacecraft designers use a so-called "bumper" concept. This concept is based on the fact that wher a high velocity particle impacts a thin sheet of material both the projectile and the sheet material are shattered and vaporized into a cloud of debris. The use of this exterior wall or bumper thus changes the design consideration of the main wall from a penetration problem to one dealing with the momentum exchange between this cloud of debris and the main wall.

Until recently, two basic approaches were used for the analyses of impulsive loaded plates: a pure membrane approach (refs. 1 and 2) and a pure bending approach (refs. 3 and 4). Neither gives an entirely satisfactory answer. The former results in calculated deformations that are less than those experienced by the actual plate, hence unconservative. The latter gives deformations that are much greater than actual and hence too conservative.

Recently, N. Jones (ref. 5) linked the two types of behavior. He permitted the plate to carry both maximum plastic moment and maximum plastic normal force during the first stage of deformation and full plastic normal force in the last stage. This, therefore, results in final deformations that are less than those of the membrane approaches and hence should be in poorer agreement with experiment.

The purpose of this investigation is to develop a method of analysis that includes both bending and midplane forces and permits both flexural and membrane behavior of the plate. The analysis will deal specifically with a simply supported circular plate with an initial uniform velocity.

The equilibrium equations will be those appropriate to large deflections of plates as discussed in reference 6. The yield condition used in the analysis has been used by many investigators for moment axial-force interaction (see, for example, refs. 7 and 8). This yield condition defines the moment midplane-force interaction by examining the stress distribution in the cross section. It permits both to occur simultaneously; however, both forces can never be maximum at the same time. Furthermore, one cannot exist if the other is at its maximum.

VI. REVIEW OF PERTINENT LITERATURE

General Considerations and Background

There exists in literature only a limited number of theoretical analyses dealing with impulsively loaded plastic plates. The majority of the work that does exist is based on the assumption that the material is an isotropic, rigid plastic material whose behavior is consistent with the Tresca yield condition. The impulsive loading is characterized in these studies by the assumption that the structure is subjected only to an initial velocity distribution.

The first analytical study of a plastic plate with such an initial condition was made by G. E. Hudson (see ref. 1). In this study, the author treated a simply supported plate as a membrane, neglecting all bending loads and bending displacements. Initially, the entire plate was assumed to be plastic and traveling at a uniform velocity of V_o. A hinge developed at the boundary and traveled normal to it.

The assumed deformation of the membrane is shown in figure 2. The hinge, at a distance $\bar{\rho}$ from the center, separates the circular membrane into two regions: a flat circular inner region that moves with a uniform transverse velocity of V_o; and an outer region that is assumed to be rigid and conical in shape. Thus, plastic flow takes place only in the central or inner region. The hinge, with its associated discontinuity of slope, then travels with a uniform velocity until the inner circle is reduced to a point. Once the hinge reaches the center, it is assumed to remain there until the plate ceases to move.

An evaluation of this pure membrane approach is found in reference 2. Using an analysis similar to Hudson, Frederick compared his calculated results with experimental data on steel plates. Some of these results are reproduced in figure 3. In this figure experimental and theoretical deflection profiles are compared. Note that the calculated deflections are somewhat lower in value than those found experimentally. This, of course, is due in part to the assumption of a rigid outer region and the omission of all bending deformations.

Frederick also examined two other factors that could influence the theoretically calculated deformations of the impulsively loaded membrane: the inclusion in the analysis of work hardening effects and the consideration of the Von Mises yield condition in place of the Tresca condition. Neither factor, however, was found to be of great importance. As shown in figure 3, work hardening has little effect on the final deformation. In fact, it tends to reduce the calculated deflections and hence, for this analysis, causes a poorer comparison with experiment.

In direct contrast to the approaches discussed in references 1 and 2, which considered only the membrane response of the plate, A. J. Wang (ref. 3) proposed an analysis of the deflections of a plastic plate under impulse loading that considered only the small deflection bending response of the plate. His analysis, like those of references 1 and 2, was based on the Tresca yield condition. His resulting flow rules, however, were different.

The plastic flow rules, used by Wang, were first discussed by Prager in reference 9. Hopkins and Prager (ref. 10) applied

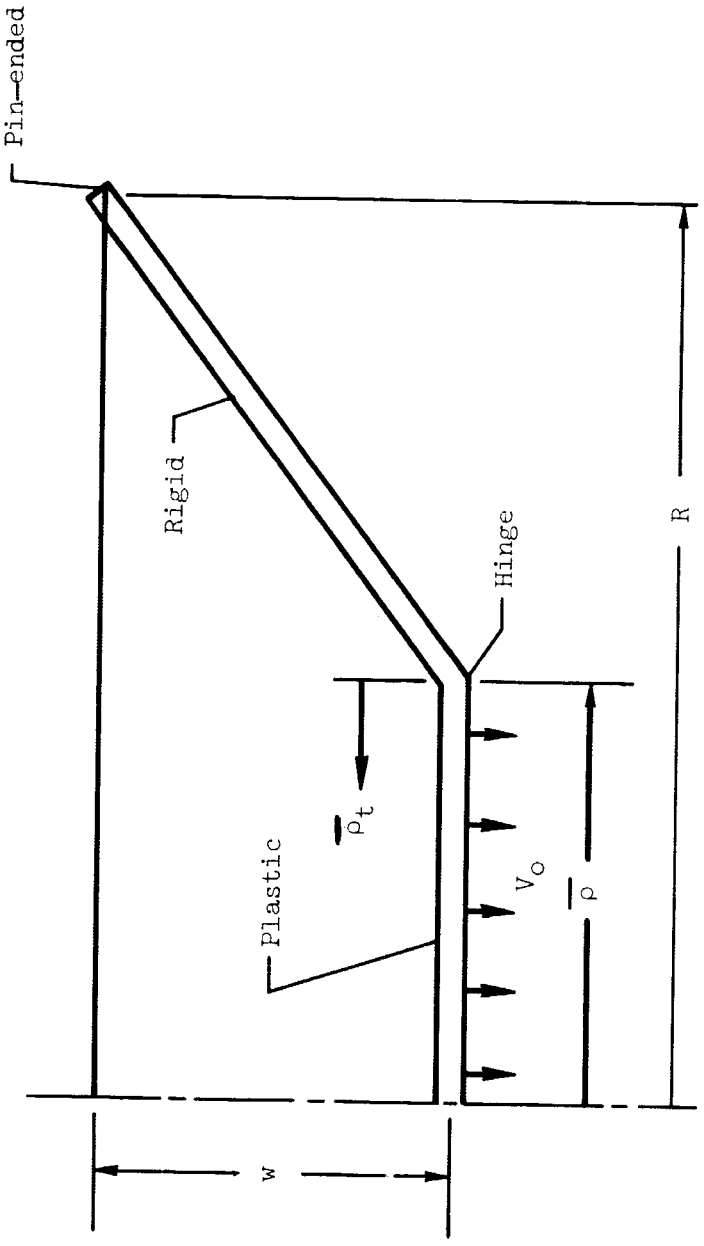

Figure 2.- Membrane mechanisms of Hudson and Frederick.

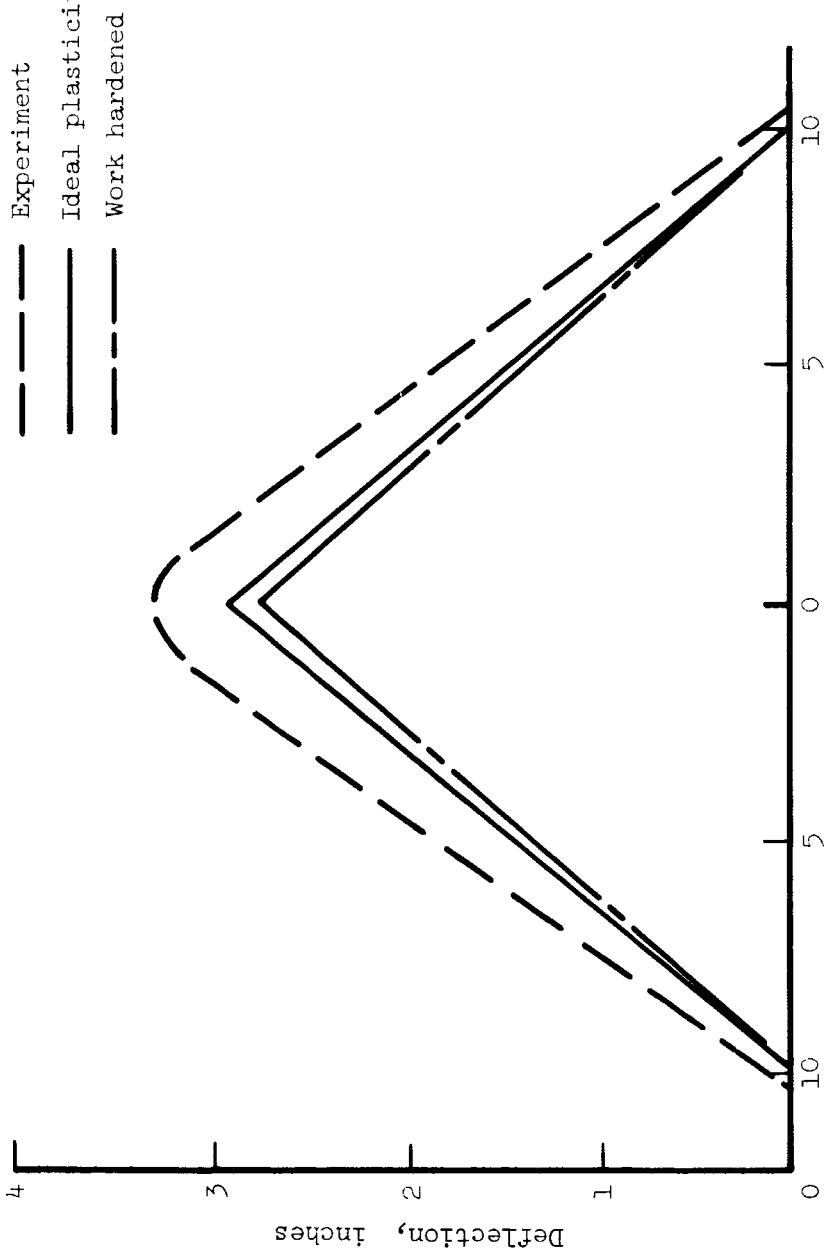

Figure 3.- Membrane deflection profiles.

these rules to dynamic problems, and developed a criteria for the existence and subsequent behavior of discontinuities across a hinge.

In this work the author pointed out that if both the plate displacement and velocity are continuous, the following conditions across the hinge must be maintained. For a stationary hinge circle, the slope across a hinge in the radial direction is discontinuous, as, for example, in the case of the statically loaded plate in reference 11. For a moving hinge circle, the slope in the radial direction must be continuous. The accelerations for this case, however, can be discontinuous.

Consequently, the pure bending solution presented by Wang (ref. 3) differs from the pure membrane approach in references 1 and 2 in several respects. The slope in the radial direction is continuous across the hinge. Plastic flow occurs in both the inner and outer regions of the plate. Finally, the velocity of the hinge is not uniform.

Through the use of an extensive experimental program, A. L. Florence (ref. 4) made a critical evaluation of the small deflection bending analysis. In this experimental program, 22 aluminum and 20 steel plates were subjected to impulsive loadings. The final measured deformations of these plates were then compared to theoretical calculations based on an analysis of Wang.

Some of the results of reference 4 have been reproduced in figures 4 and 5. In figure 4 theoretical and experimental nondimensionalized deflections are plotted as a function of a nondimensional

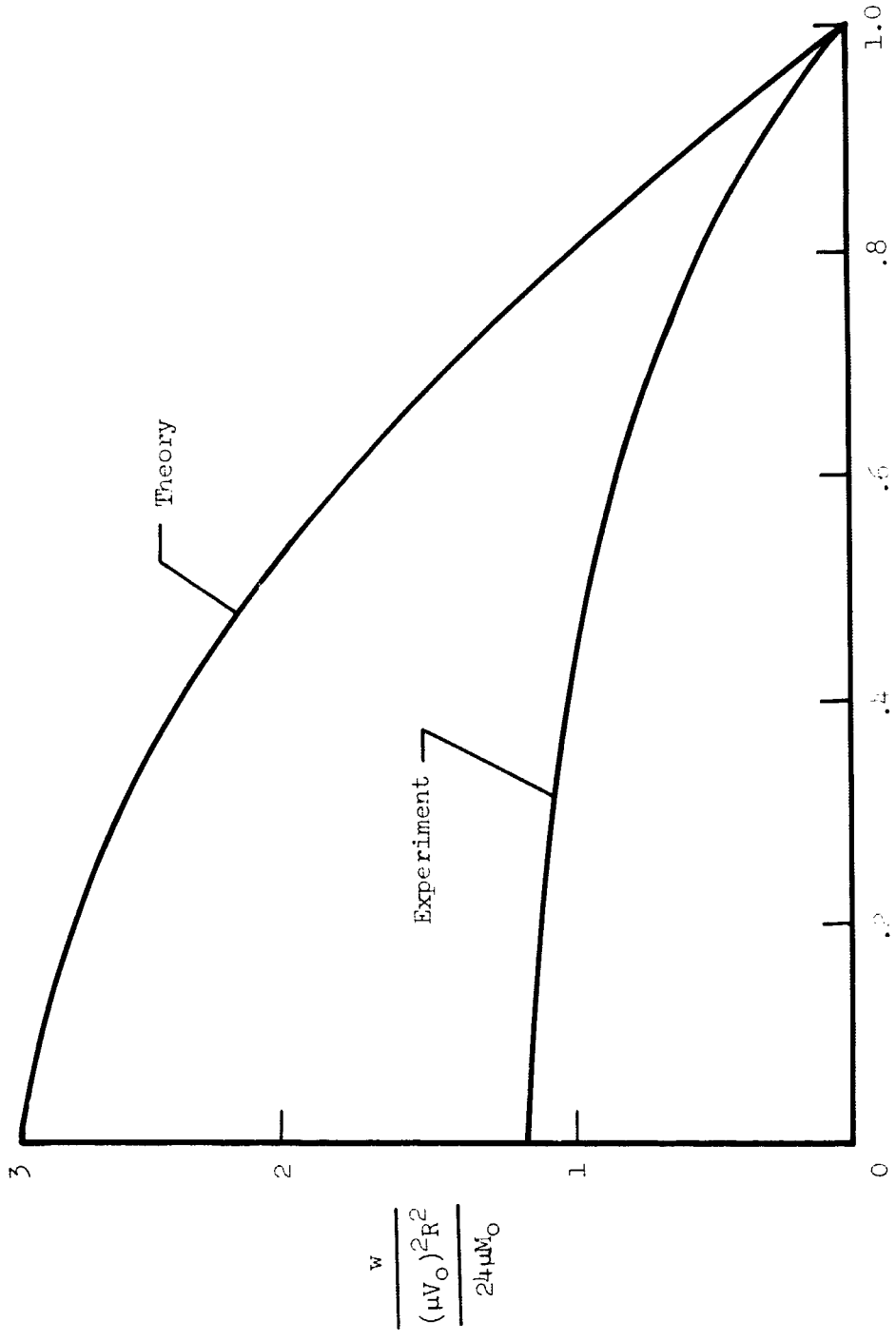

Figure 4.- Bending deflection profiles.

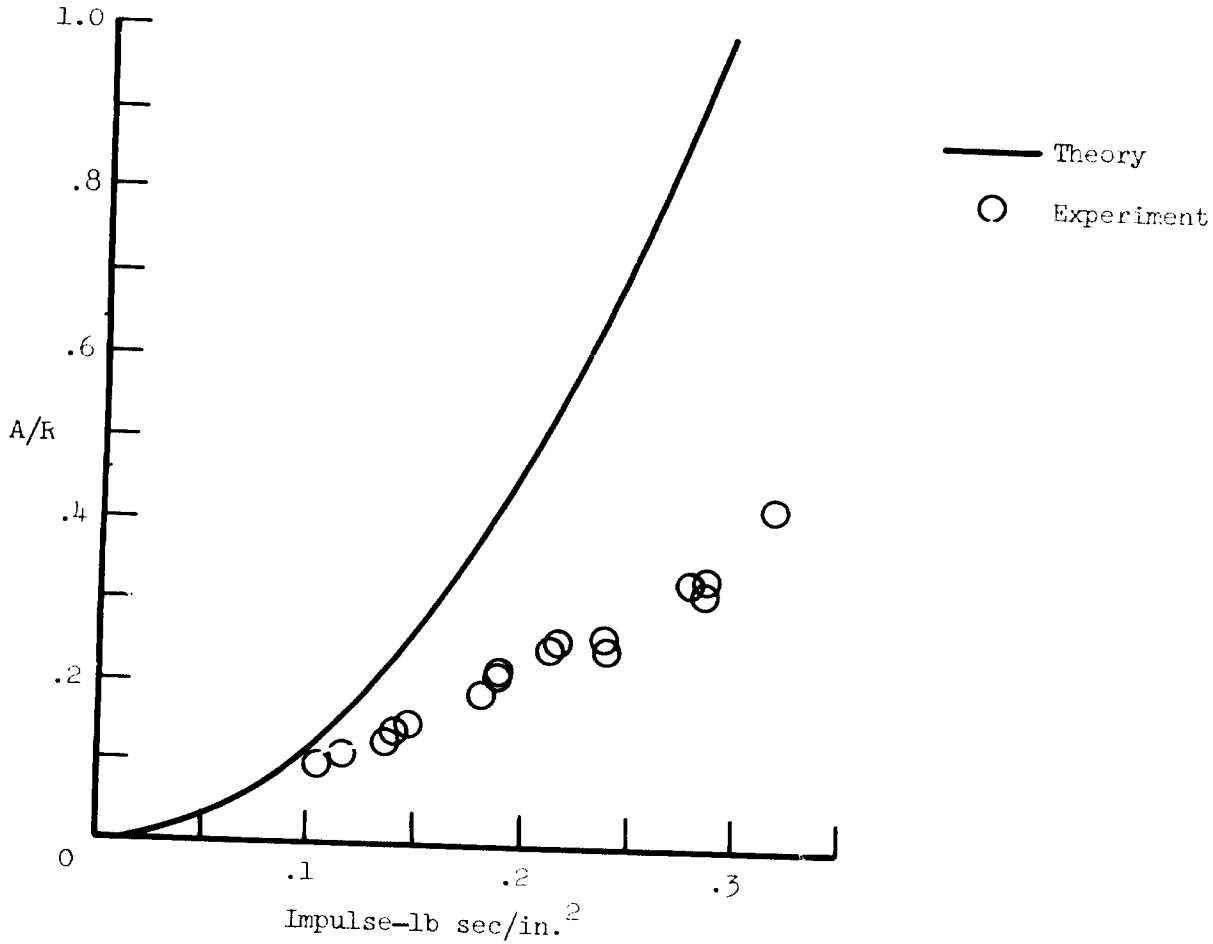

Figure 5.- Comparison of bending theory and experiments for aluminum plates.

radial position, $\frac{r}{R}$. These results show that, when only small deflection bending loads and curvatures are considered, the theoretical results considerably overestimate the experimentally obtained deflections.

Results in figure 4 are for one value of impulsive loading. How these comparisons are affected by changes in the magnitude of the impulsive loading is shown in figure 5. Here both theoretical and experimental deflections at the center of the plate are plotted as a function of the magnitude of the impulse. These results show that the correlation rapidly deteriorates with increasing deflection. This is primarily due to the increased importance of membrane forces and midplane distortion. Florence concluded from these results that a full treatment of the problem requires inclusion of membrane forces.

Overestimations of calculated deflections by a bending analysis were also found by Gerald May and Kurt Gerstle (ref. 12) for the case of statically loaded plates. Here, a finite element approach was used in which elements were considered to be either entirely elastic or plastic.

Jones (ref. 5) realizing the importance of the interaction of bending and midplane forces, attempted to link the bending and membrane behavior of plates in an analysis of impulsively loaded, simply supported plates. Similarly to the other investigators, he divided the motion of the plate into two phases.

The first phase consisted of the initial deformations in which the hinge circle traveled from the support to the center of the plate. The analysis of this phase assumed that the central portion could resist

both a plastic moment, $\bar{M}_p$, and a plastic midplane force, $\bar{N}_p$. The magnitude of each of the forces, however, was assumed to be large enough to cause plastic behavior by themselves. In the outer region of this Phase 1 motion, the midplane force was assumed to be the maximum plastic value while the plastic moment ranged from full maximum value at the hinge to zero at the support. Jones also assumed that the motion of the hinge was the same as that obtained by Wang for the pure bending assumption.

In Phase 2 of the motion Jones assumed that only membrane forces were acting, that is, $\bar{M}_p = 0$. Consequently, in Jones' analysis, the plate always carried the maximum plastic midplane force, $\bar{N}_p$. In addition for a large portion of its motion, it also carries a plastic moment, $\bar{M}_p$.

The question of plastic midplane force and bending-moment interaction has been quite extensively examined for beams (see, for example, refs. 7, 13, and 14). (Reference 14 is an excellent survey of analyses for plastic behavior; it is restricted, however, to work done on beams.) This interaction has also been examined for statically loaded plates (see, for example, refs. 15, 16, and 17). The yield condition that has evolved from all these studies relates the plastic loads present at any point in a structure by the following relationship: $\frac{\bar{M}_p}{\bar{M}_o} + \left(\frac{\bar{N}_p}{\bar{N}_o}\right)^2 = 1$ where $\bar{M}_o$ and $\bar{N}_o$ are the maximum plastic moment and axial force. It is this yield condition that will be used herein.

Review of Literature In Associated Areas

An excellent review of all the phases of plasticity essential to development of plasticity analyses is given by Olszak, Mroz, and Perzyna in reference 15. This summary deals not only with the fundamental basic approaches and constitutive equations but also stresses the application of the theory to various practical problem areas such as plates and shells, soil mechanics, three-dimensional problems, and axially symmetric problems. This reference also devoted a whole chapter to dynamical problems. Each section is followed by a complete bibliography.

An equally thorough survey, but limited only to analyses of beams under dynamic loading, is found in reference 13.

The preceding section dealt only with the state of the art pertaining to the specific problem being analyzed herein; that is, a simply supported circular plate constructed of a perfect rigid plastic material and subjected to an initial uniform velocity. There are, however, analyses dealing with other problems that need mentioning both for the sake of completeness and, in some cases, for their possible application to the large deformation aspect of the present analysis.

In references 18 and 19, Thomson studied the plastic behavior of simply supported circular plates under nonuniform transverse impulses. Only the bending behavior of the plates was considered. The plate was assumed to be impacted by an axisymmetric impulse that induced an initial velocity with a general radial Gaussian distribution.

Perzyna (ref. 20) investigated the effects of a time variation of a loading on plastic deformations of a simply supported circular plate. This analysis, like Thomson's, assumed that the material was a rigid plastic behaving in a manner consistent with the Tresca yield criteria, and considered only the bending mode of deformations. The pressure loading was taken to be uniform in both the radial and tangential directions. The magnitude of the pressure, however, varied with time. Perzyna found that for a given total impulse the character of the time pressure function had little effect on the final shape of the plate.

Plastic behavior of plates with other types of boundary conditions has also been investigated for the bending case. Wang and Hopkins (ref. 21) gave results for circular plates with built-in edges. Shapiro (ref. 22) investigated the plastic response of an annular plate. This rigid plastic plate was assumed fixed at inner radius and the outer rim was subjected to a constant velocity for a finite length of time. Finally Mroz (ref. 22) investigated the case of simply supported annular plates for two different conditions: for a uniform lateral loading with simply supported inner ring and for a uniform shear force applied to the inner periphery whose edges are considered free.

VII. SYMBOLS

A	nondimensional central deformation of the plate
A_F	value of A when plate motion stops
C_1, C_2, C_3	constants of integration (see eqs. (103), (115), and (129))
$F(n)$	function of n defined by equation (131)
I	nondimensional impulse defined in equations (16) and (17)
J_o	Bessel function of the first kind of order 0
K_r, K_θ	curvature of plate in r and θ directions, respectively
M	bending-moment resultant
M_p	value of M for plastic behavior
M_ρ	value of M at the hinge circle
M_o	maximum bending moment plate can sustain, $\sigma_o h^2$
M_r, M_θ	value of M in the r and θ directions
$M_{r\theta}$	twisting moment
N	midplane force
N_p	value of N for plastic behavior
N_ρ	value of N at the hinge circle
N_o	maximum midplane force plate can sustain, $2\sigma_o h$
N_r, N_θ	value of N in the r and θ direction
Q_r, Q_θ	shear force in r and θ direction
R	radius of plate
V_o	initial velocity of plate
W	nondimensional displacement of plate, $\frac{w}{h}$

$\bar{W}$	function defined by equation (46)
Z	nondimensional distance between midplane and neutral surface, $\frac{z_o}{h}$
h	half depth of plate
log	natural logarithm
n	nondimensional membrane radius
n_o	initial value of n
n_F	final value of n
p	loading per unit area of plate
r	radial coordinate
s	distance along midplane in radial direction
t	dimensional time
u	radial displacement of middle surface
w	transverse deflection of middle surface of plate
z	coordinate along axis of symmetry
z_o	distance between middle surface and neutral surface of the plate
β	angle between the neutral surface and r coordinate
$\bar{\epsilon}_r, \bar{\epsilon}_\theta$	strains at any point of cross section in r and θ directions, respectively
$\epsilon_r, \epsilon_\theta$	strains in midplane surface in r and θ directions, respectively
ζ	dummy variable
Ψ	dummy variable
θ	tangential coordinate

λ	constant
μ	mass of plate per unit area
ξ	nondimensional radial coordinate, $\frac{r}{R}$
ρ	plastic bending hinge circle radius
ρ_1	value of ρ at the initiation of the membrane hinge
$\sigma_r, \sigma_\theta, \sigma_z$	normal stress in r, θ, and z direction, respectively
σ_o	yield stress
$\sigma_I, \sigma_{II}, \sigma_{III}$	principal stresses $\sigma_I > \sigma_{II} > \sigma_{III}$
$\tau_{r\theta}, \tau_{z\theta}, \tau_{rz}$	shear stresses
τ	nondimensional time, $\frac{V_o t}{2h}$
τ_1	value of τ when plastic bending hinge reaches center of plate
τ_2	value of τ when plastic membrane hinge is initiated

Subscripts

r	radial direction
θ	circumferential direction
t	differentiation with respect to t
τ	differentiation with respect to τ

A line over the symbol M denotes a dimensional moment such that $\overline{M} = \frac{M}{M_o}$. A line over the symbol N denotes a dimensional midplane such that $\overline{N} = \frac{N}{N_o}$. A dot over the symbol denotes differentiation with respect to time, t.

VIII. DERIVATION OF BASIC EQUATIONS

Assumptions

The purpose of the present work is to develop an analytical method for the prediction of the plastic behavior of impulsively loaded plates that will combine both membrane forces and bending. To do this the analysis must contain large deflection effects and permit midplane distortions along with bending distortions.

The plate that is to be analyzed and the coordinate system that is to be used is shown in figure 6. The plate is circular, has a radius R, a thickness 2h, and is simply supported at its edges. The imposed initial conditions are that the displacement, $w(r,0)$, is zero and the initial velocity, $w_t(r,0)$, is a constant, V_o.

The analytical method will be based on the following assumptions. The plate is assumed to be an isotropic, rigid, ideally plastic material. Consequently, both elastic and work hardening effects will not be included in the analysis. Although midplane forces and distortions are permitted, inertia effects in the radial direction are omitted. Shear deformations and rotary inertia effects are also neglected. The equilibrium and resulting governing equations used in this analysis will be consistent with those of the von Karman plate theory. This theory, as discussed in reference 24, neglects third and higher order terms of the dependent variable so that

$$\sin \beta \approx \beta$$

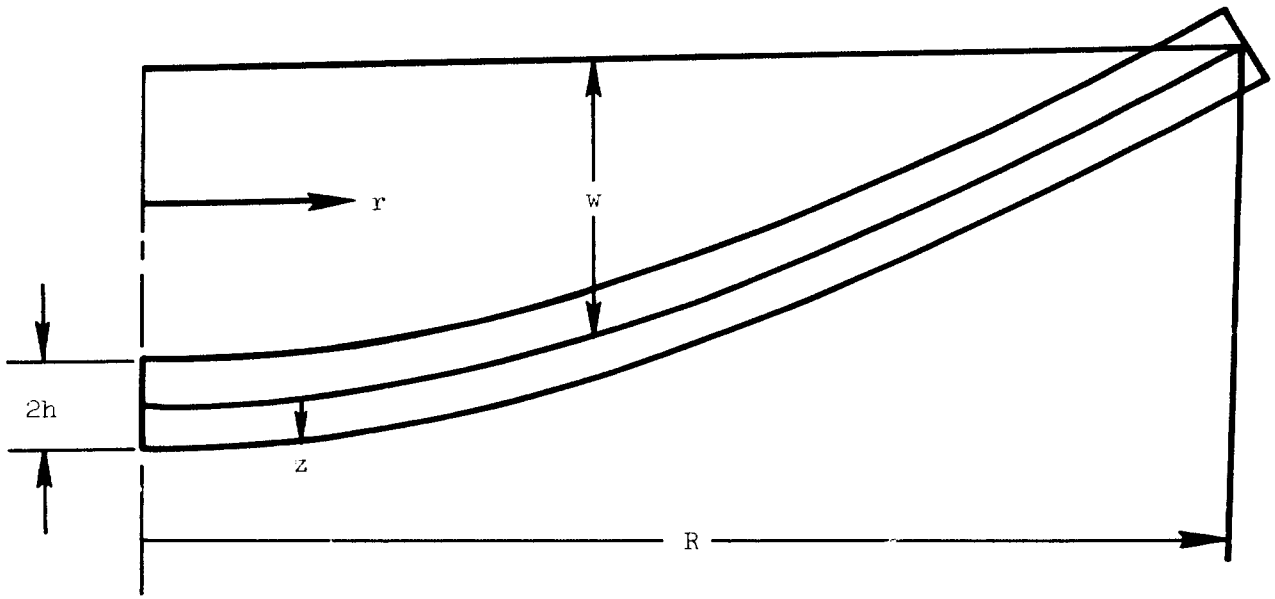

Boundary conditions

$w(R, t) = 0$
$M_r(R, t) = 0$
$u(R, t) = 0$

Initial conditions

$w(r, 0) = 0$
$w_t(r, 0) = V_o$

Figure 6.- Plastic plate and its coordinate system.

and

$$\cos \beta \approx 1 - \frac{1}{2} \beta^2$$

The following sections will discuss some of the basic governing equations for such behavior.

Equilibrium Considerations

The forces acting on the plate and on a typical element are shown in figure 7. These forces consist of bending moments $\bar{M}_r$ and $\bar{M}_\theta$, midplane forces $\bar{N}_r$ and $\bar{N}_\theta$, a shear force $\bar{Q}_r$, and a uniformly distributed loading $\bar{p}$. In the case of the loading symbols, all symbols with bars above will denote dimensional forces, while the force symbols without the bars will represent nondimensional forces. All forces are shown in figure 7 in their positive direction and all are specified per unit length of line element in the middle surface of the plate. Due to the cylindrical symmetry of loading, the shear stresses $\tau_{r\theta}$ and $\tau_{z\theta}$ vanish. Consequently the shear forces $\bar{Q}_\theta$ and the torque $\bar{M}_{\theta r}$ also vanish. With the assumption that the plate thickness (2h) is much smaller than the radius R, the influence of stresses σ_z and τ_{rz} is small and hence negligible.

From figure 7(a) the summation of forces in the midplane direction results in

$$\frac{\partial}{\partial r}(r\bar{N}_r) - \bar{N}_\theta = 0 \qquad (1)$$

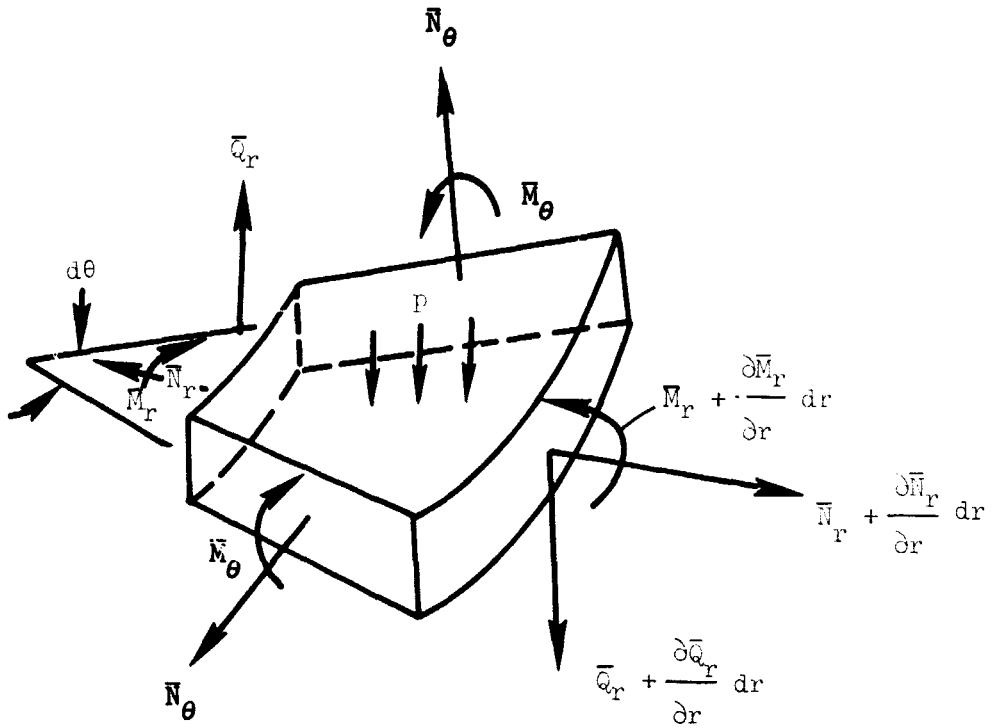

(a) Forces on differential element.

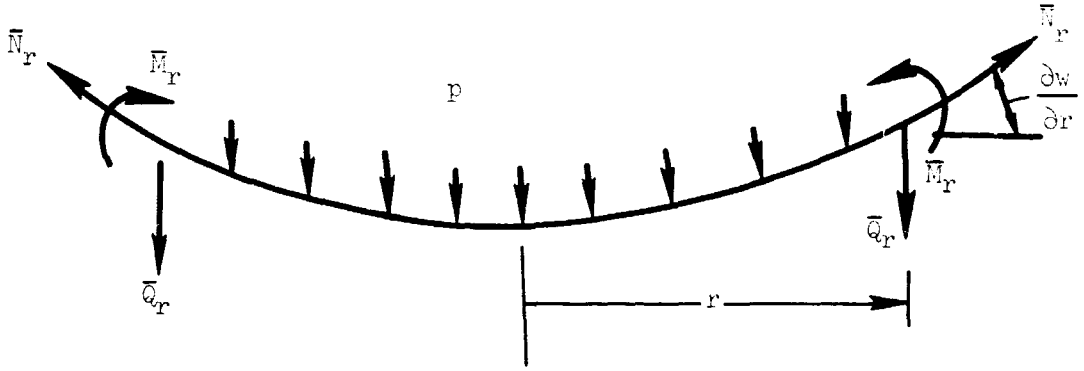

(b) Forces on finite central portion of plate.

Figure 7.- Forces on plate elements.

From figure 7(b) the summation of forces in the transverse direction gives an expression for the transverse shear, $\bar{Q}_r$,

$$\bar{Q}_r = -\bar{N}_r \frac{\partial w}{\partial r} - \frac{1}{r} \int_o^r (\bar{p} - \mu w_{tt})\zeta \, d\zeta \tag{2}$$

where the term μw_{tt} represents the inertial loading due to transverse motion, and μ is the mass of the plate per unit area. The problem discussed herein deals only with the impulsive loading that results in an initial velocity of the plastic plate. The loading term, $\bar{p}$, therefore, is zero and will not be included in the remainder of the analyses.

The summation of moments in figure 7(a) results in the equation

$$\bar{M}_r + r \frac{\partial \bar{M}_r}{\partial r} - \bar{M}_\theta = r\bar{Q}_r \tag{3}$$

Eliminating the shear force $\bar{Q}_r$ from equation (3) (see eq. (2)) results in the equilibrium equation

$$\frac{\partial}{\partial r}(r\bar{M}_r) - \bar{M}_\theta = -rN_r \frac{\partial w}{\partial r} + \int_o^r \mu w_{tt}\zeta \, d\zeta \tag{4}$$

Equations (1) and (4), therefore, represent the equilibrium equations for the plastic plate with midplane forces. These equations, of course, are identical to the von Karman plate equations obtained by considering large deflections of circular plates (see, for example, ref. 6).

Nondimensionalization

In order to simplify the derivations and to obtain the natural parameters of the mechanism involved, the remaining analyses will be written in nondimensional terms. The following nondimensional parameters are therefore defined.

The moment is normalized with respect to $\bar{M}_o$ where

$$\bar{M}_o = h^2\sigma_o \tag{5}$$

and σ_o is the critical yield stress. More will be said about this stress in the section on Plastic Flow Considerations. $\bar{M}_o$ represents the maximum bending moment the plate can possibly carry. Consequently, the absolute value of the nondimensionalized bending moment

$$M = \frac{\bar{M}}{M_o} \tag{6}$$

can never be greater than unity. Similarly the nondimensionalized normal force is

$$N = \frac{\bar{N}}{N_o} \tag{7}$$

where

$$\bar{N}_o = 2h\sigma_o \tag{8}$$

$\bar{N}_o$ is the maximum normal force possible and, similarly to M, $|N|$ can never exceed unity. The nondimensional form of the shear force, Q_r, is

$$Q_r = \frac{R\bar{Q}_r}{h\bar{N}_o} \tag{9}$$

The nondimensionalized radial coordinate, ξ, displacement, W, and time, τ, are defined as follows

$$\xi = \frac{r}{R} \tag{10}$$

$$W = \frac{w}{h} \tag{11}$$

and

$$\tau = \frac{V_o t}{2h} \tag{12}$$

Equilibrium equations (1), (2), and (4) can now be written in nondimensional form as

$$\frac{\partial}{\partial \xi}(\xi N_r) - N_\theta = 0 \tag{13}$$

$$Q_r = -N_r \frac{\partial W}{\partial \xi} + \frac{3I}{\xi} \int_o^\xi W_{\tau\tau} \psi \, d\psi \tag{14}$$

$$\frac{\partial}{\partial \xi}(\xi M_r) - M_\theta = -2\xi N_r \frac{\partial W}{\partial \xi} + 6I \int_0^\xi W_{\tau\tau} \psi \, d\psi \tag{15}$$

where I is a nondimensionalized momentum defined as

$$I = \frac{\mu V_o^2 R^2}{12h^2 N_o} \tag{16}$$

or

$$I = \frac{\mu V_o^2 R^2}{24h^3 \sigma_o} \tag{17}$$

Deformation Considerations

Consistent with all of the previously mentioned analyses on the plastic behavior of plates, the deformations of the cross section will be based on the assumption that a line initially normal to the midplane remains straight and normal after deformation. Consequently the strain at any point in the cross section of the plate can be written as:

For the radial direction

$$\bar{\epsilon}_r = \epsilon_r + zK_r \tag{18}$$

For the tangential or θ direction

$$\bar{\epsilon}_\theta = \epsilon_\theta + zK_\theta \tag{19}$$

where z is the distance from the midplane. The strains, ϵ_r and ϵ_θ, are the midplane strains and K_r and K_θ are the respective curvatures.

The curvatures are defined as

$$K_r = -\frac{\partial^2 w}{\partial r^2} \tag{20}$$

and

$$K_\theta = -\frac{1}{r}\frac{\partial w}{\partial r} \tag{21}$$

While the midplane strains are given by

$$\epsilon_r = \frac{\partial u}{\partial r} + \frac{1}{2}\left(\frac{\partial w}{\partial r}\right)^2 \tag{22}$$

and

$$\epsilon_\theta = \frac{u}{r} \tag{23}$$

where u is the displacement of the midplane in the r direction (u is considered positive when the displacements are in the positive r direction). If only small displacements are to be considered, the second term in equation (22) can be neglected. Note that the strains are written from a Lagrangian viewpoint and no nonlinearities due to radial displacements are considered.

Plastic Flow Considerations

Plastic behavior of the plate will be governed by the Tresca yield criteria. This criteria states that plastic yielding will begin when the maximum shear stress reaches a certain critical value, that is

$$\tau_{max} = \frac{\sigma_I - \sigma_{III}}{2} = \frac{\sigma_o}{2} \tag{24}$$

where σ_I and σ_{III} are, respectively, the maximum and minimum principal stresses and σ_o the critical yield stress of the material. With the assumption that the transverse normal stress is negligible ($\sigma_z = 0$), the Tresca condition can be graphically represented as shown in figure 8 in terms of σ_r and σ_θ.

Any combination of σ_r and σ_θ that falls on this boundary will initiate plastic flow. Any subsequent plastic flow will occur tangent to the surface of the yield diagram. For example, if σ_r and σ_θ fall on the line AB (see fig. 8), plastic flow will occur perpendicular to AB in a manner that the radial strain rate, $\dot{\epsilon}_r$, is zero. For stress combinations along AF, $\dot{\epsilon}_\theta$ will be zero. At the vertices of the diagrams the specific direction of plastic flow is not defined; both stresses, however, are defined. Thus, for all points on this diagram two conditions are specified: either both stresses or a direction of strain rate and a relationship between the stresses.

For pure bending of a plate the moment along a plastic flow line is unique and equal to $h^2\sigma_o$. Similarly when only midplane forces are considered the plastic membrane force is unique and equal to $2h\sigma_o$.

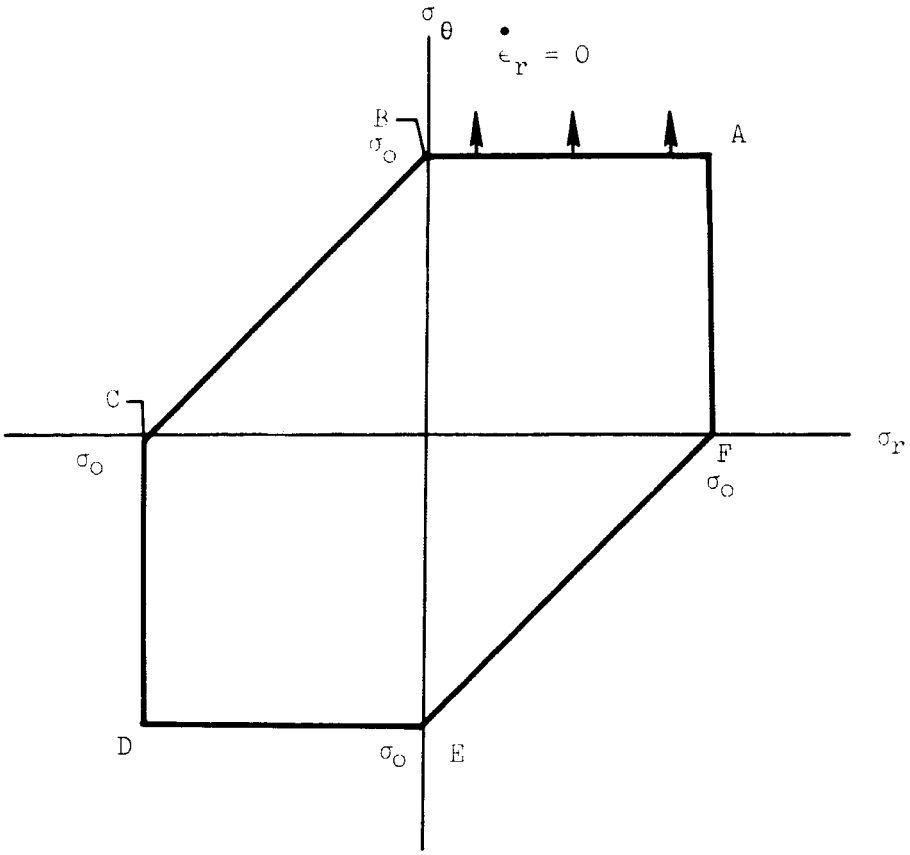

Figure 8.- Tresca yield diagram.

However, when both midplane forces and bending are permitted, then there are no unique values of $\bar{M}$ or $\bar{N}$ at the initiation of plastic flow.

A typical cross section for this case is shown in figure 9. Notice that the development of a midplane force causes the plastic stress distribution to create a neutral surface at some distance z_o from the midplane. The plastic moment and membrane force are then given by

$$\bar{M}_p = (h^2 - z_o^2)\sigma_o \tag{25}$$

and

$$\bar{N}_p = -2z_o\sigma_o \tag{26}$$

Notice that the plastic moment and membrane forces are coupled through z_o.

This coupling indicates that, while there is no unique value of the plastic midplane force, $\bar{N}_p$ or moment $\bar{M}_p$, there is an interaction of the two. Elimination of z_o from equations (25, and (26) gives the form of this interaction

$$\frac{\bar{M}_p}{M_o} + \left(\frac{\bar{N}_p}{N_o}\right)^2 = 1 \tag{27}$$

In nondimensional form equations (25), (26), and (27) can be written as

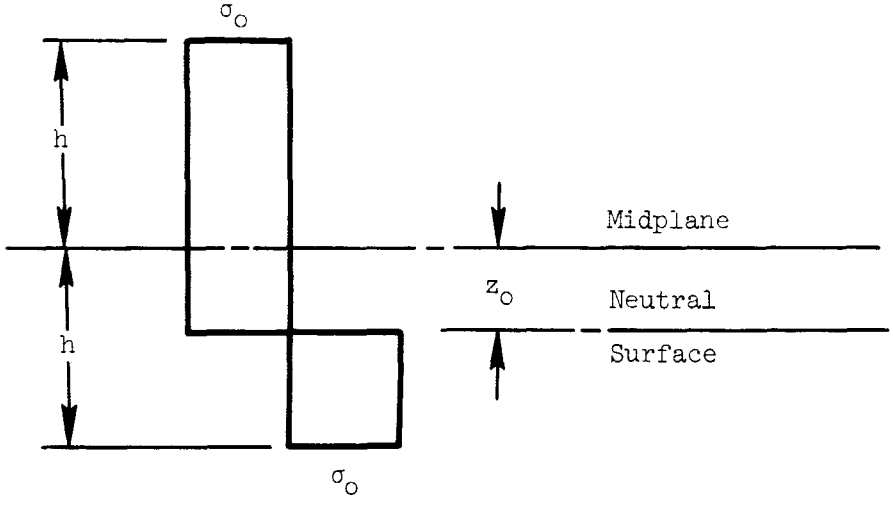

Figure 9.- Distribution of stresses in cross section of plate.

$$M_p = 1 - Z^2 \tag{28}$$

$$N_p = -Z \tag{29}$$

and

$$M_p + N_p^2 = 1 \tag{30}$$

where

$$Z = \frac{z_o}{h} \tag{31}$$

The interaction equation (eq. (27) or eq. (30)) gives a relationship between the plastic moment M_p and the plastic normal force N_p. As long as $\bar{N}_p$ is less than $\bar{N}_o (N_p < 1)$ a plastic moment exists. However, as soon as the plastic normal force becomes $\bar{N}_o (N_p = 1)$ then $\bar{M}_p$ becomes zero and the section no longer carries moment. These interaction relationships are especially useful if the value of the lateral load is prescribed, as in an analyses involving the bending behavior of a plastic plate with applied lateral loads.

When the deformations of the plate become large, lateral loads are generated by the stretching, $u(r,t)$, of the midplane.

With the condition that at the support $u(R,t)$ is zero, an integral expression for u can be written

$$u = \int_r^R du = \int_r^R (ds - dr) \tag{32}$$

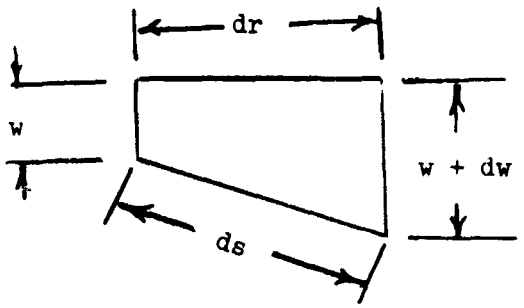

where s is the distance measured along the midplane. From the above sketch it can be seen that

$$ds^2 = dw^2 + dr^2 \tag{33}$$

Substitution of equation (33) in equation (32) results in

$$u = \int_r^R \left(\sqrt{1 + \left(\frac{\partial w}{\partial r}\right)^2} - 1 \right) dr \tag{34}$$

which, for the case where $\frac{\partial w}{\partial r} < 1$, can be approximated by

$$u = \int_r^R \frac{1}{2}\left(\frac{\partial w}{\partial r}\right)^2 dr \tag{35}$$

The separation of the neutral and midplane surfaces creates a coupling between slope and midplane distortion, u. This coupling is achieved through the previously mentioned assumption of straight normals. That is, a line perpendicular to the neutral surface before deformation will remain straight and normal after deformation. Consequently, in the radial direction the midplane distortion, u, is related to the radial slope by the equation

$$u = z_o \frac{\partial w}{\partial r} \tag{36}$$

With equations (35) and (36) z_o can be expressed in terms of the slope as

$$z_o = \frac{\int_r^R \frac{1}{2}\left(\frac{\partial w}{\partial r}\right)^2 dr}{\frac{\partial w}{\partial r}} \tag{37}$$

or in nondimensional terms

$$Z = \frac{\frac{1}{2}\int_\xi^1 \left(\frac{\partial W}{\partial \zeta}\right)^2 d\zeta}{\frac{\partial W}{\partial \xi}} \tag{38}$$

The magnitude of Z depends on the shape of the displacement. From equation (29) and the knowledge that $|N_p| < 1$, $|Z|$ must also be less than 1. Consequently, those portions of the plate where the absolute value of Z is greater than unity must be acting as a membrane (that is, they carry no moment) and there is no valid unique relationship between slope and displacement.

IX. DERIVATION OF GOVERNING EQUATIONS

Discussion of Physical Behavior

The following section is a description of the physical behavior of a plate as it reacts to the initial impulse. It should not in any way be construed as a statement of assumptions. On the contrary, the mechanisms and behavior described all result from the basic assumptions and considerations discussed in the previous chapter. These will become evident as the analysis in the following sections proceeds.

The purpose of this approach is twofold: First, it will give the reader a clearer understanding of the motivation and significance of the analytical work that follows. Second, it will permit the author to define and classify certain regions and behaviors before proving their existence.

Just after the initial moment of impact, the plate is separated into two plastic regions by a hinge circle, as shown in figure 10. The hinge, which originates at the support, travels at a velocity ρ_τ until it reaches the center. The central portion of this plate ($0 < r < \rho R$) travels at a uniform transverse velocity equal to the initial velocity, V_o. Such motion has been observed experimentally (see ref. 26). The stress conditions are such that $\sigma_r = \sigma_\theta = \sigma_o$. At any time, t, the displacement w in the central region is $V_o t$. In nondimensional terms the central displacement is

$$W(0,\tau) = A(\tau) = 2\tau \qquad 0 < \xi < \rho \tag{39}$$

Thus the nondimensional velocity in the central region is

$$W_\tau(0,\tau) = A_\tau(\tau) = 2 \qquad 0 < \xi < \rho \tag{40}$$

In the outer region ($\rho < \xi < 1$) only the tangential stress, σ_θ, is plastic. The velocities are linear with

$$W_\tau(\rho,\tau) = 2 \tag{41}$$

and

$$W_\tau(1,\tau) = 0 \tag{42}$$

This phase of the motion will be referred to as Phase 1. Note that the displacement of any point on the plate during this phase depends only on the function $\rho(\tau)$. Thus the parameter ρ could be thought of as a time parameter.

Once the hinge circle reaches the center of the plate, Phase 2 of the motion begins (see fig. 10). This phase of motion is similar to that occurring in the outer region for Phase 1. The stress, σ_θ, is plastic and the velocity distribution linear.

If during either Phase 1 or Phase 2 the motion and loading of the plate is such that midplane force N becomes 1, the behavior of the plate is changed.

A hinge circle, which will be referred to as a membrane hinge, forms at this point ($\xi = n$) (see fig. 10). This hinge divides the plate into two regions. The outer region, $n < \xi < 1$, carries both midplane forces and moments and behaves as before. The inner portion

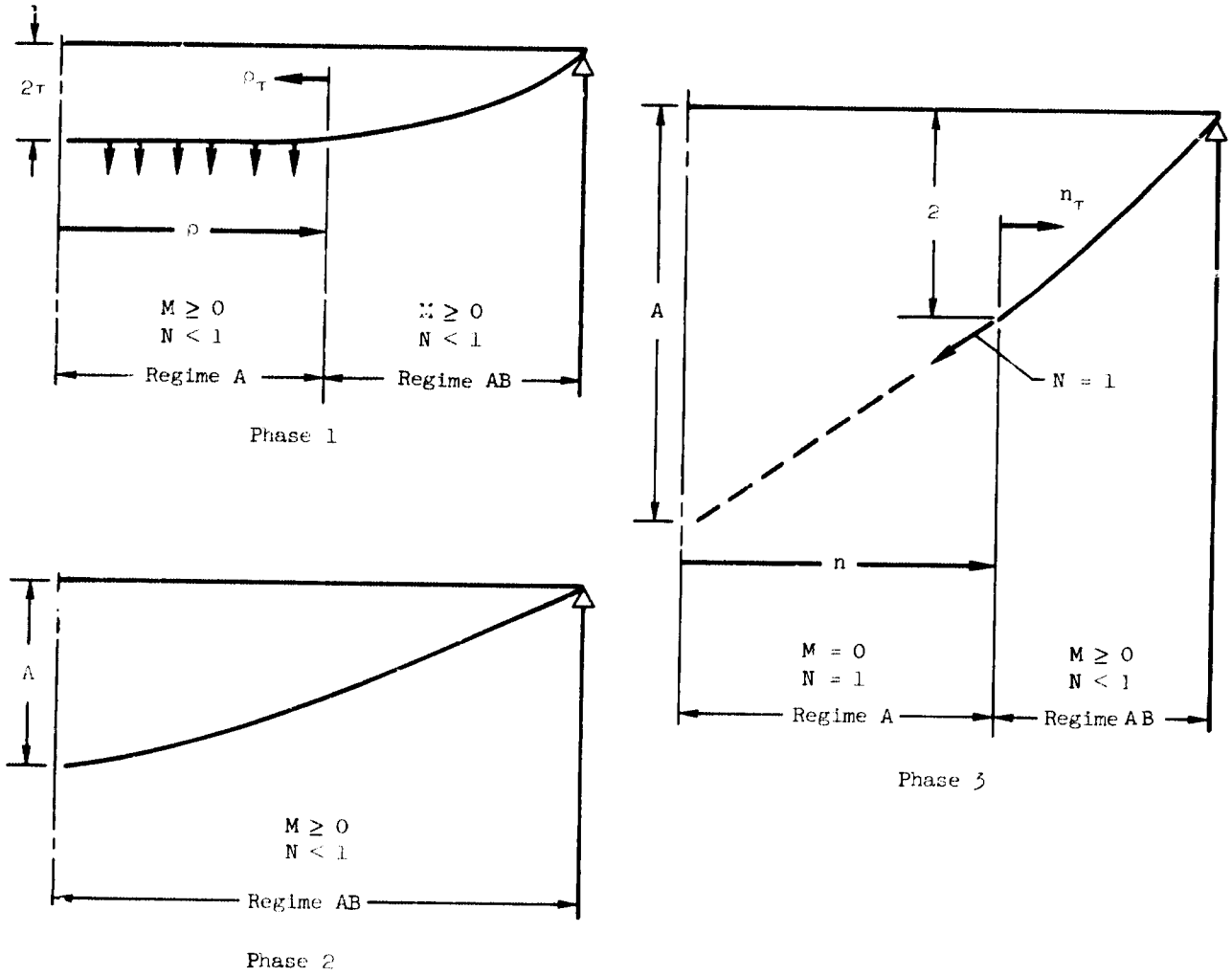

Figure 10.- Three possible phases of motion of plastic plates.

$0 < \xi < n$ behaves like a membrane. It carries no bending and transmits only a constant tensile load. This membrane hinge then travels at a velocity, n_T, toward the support. This phase of the motion will be referred to as Phase 3.

Analysis of Phase 1 Behavior

This phase of the plate behavior is typical of the initial phase of motion used by all of the previously mentioned investigators of ideally plastic, circular plate behavior (see, for example, refs. 10 and 11). Because of the rotational symmetry of the loading the maximum stress in a circular plate must occur at the center. Thus the plate cannot reach the flow limit without becoming plastic at the center. Due to rotational symmetry the radial and tangential stresses must be equal, thus $\sigma_r = \sigma_\theta = \sigma_o$. Therefore, the material at this point is in regime A of the Tresca yield hexagon (see fig. 8). At the simply supported boundary, the radial moment must vanish so that $\sigma_r = 0$. This portion of the plate must be in regime AB of the Tresca yield hexagon.

Consequently, the plate is assumed divided into two regions: a central portion in which the material is in regime A, and an outer region where the material is in regime AB. These two regions are separated at $\xi = \rho$ by a plastic hinge.

The inner portion of the plate ($\xi \leq \rho$) forms a circular plate with midplane forces at its outer edge ($\zeta = \rho$). The magnitude of these radial midplane forces, N_r, is taken to be N_ρ. Because of the symmetrical

loading condition imposed on the plate, the stresses at the center must be such that $N_r = N_\theta$. A solution that satisfies these boundary conditions and the equilibrium equation (eq. (13)) is that the stresses are such that $N_r = N_\theta$ for all interior points. Therefore, N_r is not a function of position and

$$N_r = N_\theta = N_\rho \qquad 0 < \xi < \rho \tag{43}$$

for all points in the inner region. Since the midplane force, N_ρ, can be a function only of time, the plastic moments must also be a function only of time (see eq. (30) so that

$$M_r = M_\theta = M_\rho \qquad 0 < \xi < \rho \tag{44}$$

With equations (43) and (44) the equilibrium equation (eq. (4)) reduces to

$$6I \int_0^\xi W_{\tau\tau} \zeta \, d\zeta = 2\xi N_\rho \frac{\partial W}{\partial \xi} \qquad 0 < \xi < \rho \tag{45}$$

In order to solve this governing equation a separation of variables technique will be used in which

$$W(\xi,\tau) = A(\tau)\bar{W}(\xi) \tag{46}$$

Substitution of equation (46) into the integral differential equation (eq. (45)) results, after some simplification, in

$$\frac{\xi \dfrac{\partial \bar{W}}{\partial \xi}}{\displaystyle\int_0^{\xi} \bar{W}\zeta \, d\zeta} = \frac{3I \dfrac{\partial^2 A}{\partial \tau^2}}{N_\rho A} \tag{47}$$

Since the left side of equation (47) is a function of ξ and the right side a function of τ, both must be equal to some constant, λ,

$$\frac{\xi \dfrac{\partial \bar{W}}{\partial \xi}}{\displaystyle\int_0^{\xi} \bar{W}\zeta \, d\zeta} = -\frac{3I \dfrac{\partial^2 A}{\partial \tau^2}}{N_\rho A} = -\lambda^2 \tag{48}$$

Hence the governing equation for $\bar{W}$ is

$$\xi \frac{\partial \bar{W}}{\partial \xi} + \lambda^2 \int_0^{\xi} \bar{W}\zeta \, d\zeta = 0 \tag{49}$$

Differentiating equation (49) gives

$$\xi \frac{d^2 \bar{W}}{d\xi^2} + \frac{d\bar{W}}{d\xi} + \lambda^2 \bar{W}\xi = 0 \tag{50}$$

Solution of equation (50) results in

$$\bar{W} = J_0(\lambda \xi) \tag{51}$$

The deflection in this inner region can now be written as

$$W(\xi\tau) = AJ_0(\lambda \xi) \qquad 0 < \rho < \xi \tag{52}$$

The initial condition of the problem states that the velocity everywhere is equal to 2 so that

$$W_T(\xi,0) = A_T J_0(\lambda\xi) = 2 \tag{53}$$

Thus λ must be zero and the velocity in the inner region is

$$W_T = 2 \qquad 0 < \xi < \rho \tag{54}$$

so that

$$W_{TT} = 0 \qquad 0 < \xi < \rho \tag{55}$$

$$W = 2\tau \qquad 0 < \xi < \rho \tag{56}$$

In the outer region ($\rho < \xi < 1$) the following conditions apply. At the hinge, $\xi = \rho$, the stresses are continuous, so that $\sigma_r = \sigma_\theta = \sigma_o$. At the support, $\xi = 1$, $\sigma_r = 0$. This portion of the plate, therefore, is in regime AB of the Tresca yield criteria. In this regime the plastic flow is such that the strain rate in the radial direction $\dot{\bar{\epsilon}}_r$, is zero for all points in the cross section (see eq. (18)) so that

$$\dot{\bar{\epsilon}}_r = \dot{\epsilon}_r + z\dot{K}_r = 0 \tag{57}$$

Since this equation must hold for all values of z

$$\dot{\epsilon}_r = \dot{K}_r = 0 \tag{58}$$

This condition coupled with equation (20) gives

$$\frac{\partial^3 W}{\partial \xi^2 \partial \tau} = 0 \tag{59}$$

As the velocity is continuous across the hinge

$$W_\tau(\rho,\tau) = 2 \tag{60}$$

While at the support $\xi = 1$

$$W_\tau(1,\tau) = 0 \tag{61}$$

The solution of equation (59) consistent with boundary conditions, equations (60) and (61), gives

$$W_\tau = 2\left(\frac{1 - \xi}{1 - \rho}\right) \qquad \rho < \xi < 1 \tag{62}$$

Equation (62) represents the velocity distribution of the plate in the outer region. Since ρ is a function of τ the acceleration of the plate in this region is

$$W_{\tau\tau} = 2\,\frac{(1 - \xi)}{(1 - \rho)^2}\,\rho_\tau \qquad \rho < \xi < 1 \tag{63}$$

where ρ_τ is the velocity of the hinge circle.

A relationship for ρ_τ can be obtained through the use of the equilibrium expressions.

Integration of the midplane-force equilibrium equation (eq. (13)) with the boundary condition that $N_r = N_\theta = N_\rho$ at the hinge (see eq. (43)) gives

$$\xi N_r = \int_\rho^\xi N_\theta \, d\zeta + \rho N_\rho \tag{64}$$

Integration of the moment equation (eq. (15)) with the boundary conditions for moment at the hinge, $M_r = M_\theta = M_\rho$, (see eq. (44)) gives

$$\xi M_r = \rho M_\rho + \int_\rho^\xi M_\theta \, d\zeta - 2\int_\rho^\xi \zeta N_r \frac{\partial W}{\partial \zeta} \, d\zeta + 6I \int_\rho^\xi \left[\int_o^\psi W_{\tau\tau} \, \zeta \, d\zeta \right] d\psi \tag{65}$$

The third term on the right side of equation (65) can be rewritten through the use of integration by parts as follows

$$\int \xi N_r \frac{\partial W}{\partial \xi} \, d\xi = \xi W N_r - \int W \frac{\partial (\xi N_r)}{\partial \xi} \, d\xi \tag{66}$$

This integral can now be written in terms of N_ρ and N_θ through the use of equations (13) and (64)

$$\int \xi N_r \frac{\partial W}{\partial \xi} \, d\xi = \rho W N_\rho + W \int_\rho^\xi N_\theta \, d\zeta - \int W N_\theta \, d\xi \tag{67}$$

Substitution of equation (67) in equation (65) gives

$$\xi M_r = \rho M_\rho + \int_\rho^\xi M_\theta \, d\zeta - 2\rho W N_\rho + 2\rho W(\rho) N_\rho - 2W \int_\rho^\xi N_\theta \, d\zeta$$

$$+ 2\int_\rho^\xi W N_\theta \, d\zeta + 6I \int_\rho^\xi \left[\int_o^\psi W_{\tau\tau} \, \zeta \, d\zeta \right] d\psi \qquad (68)$$

Equation (68) gives the value of the radial moment at any point ξ. The governing equation for ρ_τ is obtained by evaluation of equation (68) at the support $\xi = 1$.

At the support

$$W(1,\tau) = 0 \qquad (69)$$

and

$$M_r(1,\tau) = 0 \qquad (70)$$

Thus

$$\rho M_\rho + 2\rho W(\rho) N_\rho + \int_\rho^1 M_\theta \, d\xi + 2\int_\rho^1 W N_\theta \, d\xi = -6I \int_\rho^1 \left[\int_o^\psi W_{\tau\tau} \, \zeta \, d\zeta \right] d\psi \qquad (71)$$

Through the use of equations (55) and (63) the inertia term of equation (71) can be evaluated

$$\int_\rho^1 \left[\int_o^\psi W_{\tau\tau} \, \zeta \, d\zeta \right] d\psi = \frac{1}{6} \rho_\tau (1 - \rho)(1 + 3\rho) \qquad (72)$$

Substitution of equation (72) into equation (71) gives

$$I(1 - \rho)(1 + 3\rho)\rho_\tau = -\rho M_\rho - 2\rho W(\rho)N_\rho - \int_\rho^1 M_\theta \, d\xi - 2\int_\rho^1 WN_\theta \, d\xi \tag{73}$$

From the interaction equation between plastic normal forces and plastic moments (eq. (30)) and the expression for $W(\rho)$ from equation (56) ($W(\rho) = 2\tau$), equation (73) becomes

$$I(1 - \rho)(1 + 3\rho)\rho_\tau = -1 - 4\rho N_\rho \tau + \rho N_\rho{}^2 + \int_\rho^1 N_\theta{}^2 d\xi - 2\int_\rho^1 WN_\theta \, d\xi \tag{74}$$

Equation (74) can also be written in terms of the displacement of the neutral surface with the use of equation (29)

$$I(1 - \rho)(1 + 3\rho)\rho_\tau = -1 + 4\rho Z\tau + \rho Z_\rho{}^2 + \int_\rho^1 Z^2 d\xi + 2\int_\rho^1 WZ \, d\xi \tag{75}$$

Equations (74) and (75) are the governing equations for the hinge circle in the Phase 1 motion. The equations are dependent on the shape of the displacements and the values of the midplane forces. If only bending is considered, that is $N_\theta = 0$ or $Z = 0$, the equation reduces to that obtained by Wang in his bending solution for impulsively loaded plates (see ref. 3).

Analysis of Phase 2 Behavior

Phase 1 motion will continue until one of two conditions occurs. Either the hinge circle reaches the center of the plate or a portion of the plate becomes a membrane (that is, the plastic moment vanishes). The former case will be considered in this section.

Let τ_1 be the time it takes the hinge circle in Phase 1 to reach the center of the plate. Then the displacement and velocity at that time will be (see eqs. (54) and (56))

$$W(0,\tau_1) = 2\tau_1 \tag{76}$$

and

$$W_\tau(0,\tau_1) = 2 \tag{77}$$

Hence these conditions form the initial conditions for the Phase 2 motion.

The radial stresses in this phase range from σ_o at the center to zero at the support. Hence the material behaves in a manner similar to that in the outer region of the Phase 1 motion. The radial strain rates are zero and the velocity varies linearly from A_τ at the center to zero at the support. Thus

$$W_\tau = A_\tau(1 - \xi) \tag{78}$$

and

$$W_{\tau\tau} = A_{\tau\tau}(1 - \xi) \tag{79}$$

where A represents the deflection at the center of the plate.

The governing equations for this phase are identical to equation (71) in Phase 1 with ρ set equal to zero.

$$6I\int_o^1\left[\int_o^\psi W_{\tau\tau}\,\zeta\,d\zeta\right]d\psi = -\int_o^1 M_\theta\,d\xi - 2\int_o^1 WN_\theta\,d\xi \tag{80}$$

The inertia term for this phase becomes (see eq. (79)

$$6I\int_o^1\left[\int_o^\psi W_{\tau\tau}\,\zeta\,d\zeta\right]d\psi = \frac{1}{2}\,IA_{\tau\tau} \tag{81}$$

Substituting equation (81) into equation (80) gives

$$\frac{1}{2}\,IA_{\tau\tau} = -\int_o^1 M_\theta\,d\xi - 2\int_o^1 WN_\theta\,d\xi \tag{82}$$

which in terms of N_θ is

$$\frac{1}{2}\,IA_{\tau\tau} = -1 + \int_o^1 N_\theta{}^2 d\xi - 2\int_o^1 WN_\theta\,d\xi \tag{83}$$

and in terms of Z is

$$\frac{1}{2}\,IA_{\tau\tau} = -1 + \int_o^1 Z^2 d\xi + 2\int_o^1 WZ\,d\xi \tag{84}$$

Equations (83) and (84), as in Phase 1, reduce to the pure bending case for $N_\theta = Z = 0$. These governing equations apply until either the motion of the plate stops or a portion of the plate becomes a membrane.

Equations (74) and (83) (or eqs. (75) and (84)) are sufficient to define the motion of plates where the applied impulse, I, is small. When the impulse becomes large enough to cause a portion of the plate to be a membrane, an additional phase of motion must be considered.

Analysis of Phase 3 Behavior

As the deformations increase the midplane forces also increase. If the initial impulse, I, is large enough, the midplane forces in the central portion of the plate will become equal to one. Thus the bending moment vanishes and this portion of the plate behaves as a membrane.

Let the time at which a portion of the plate becomes a membrane be τ_2. As time increases, the size of the membrane region also increases. The plate is thus separated into two regions: one in which there is no moment and a second in which there is an interaction of moment and midplane force.

In the inner region, $0 < \xi < n$, $M_\theta = 0$ and $N_\theta = 1$. In addition, $N_r = N_\theta$ at the center. These conditions along with equilibrium equation (eq. (13)) result in

$$N_r = N_\theta = 1 \qquad 0 < \xi < n \tag{85}$$

for the entire inner region. Consequently, this region is in regime A of the Tresca yield diagram. The point of separation of the membrane portion of the plate, $\xi = n$, can then be thought of as a membrane hinge.

The moment equilibrium equation (eq. (15)) reduces at $\xi = n$ to

$$n \left.\frac{\partial W}{\partial \xi}\right|_n = 3I \int_o^n W_{TT}\, \xi \, d\xi \tag{86}$$

where the slope $\left.\frac{\partial W}{\partial \xi}\right|_n$ is evaluated at $\xi = n$.

The governing equations for the motion of this hinge can be obtained from the governing equation for the outer portion of the plate $(n < \xi < 1)$. This governing equation is identical to that for outer portion of Phase 1 motion with n substituted for ρ (see eq. (71)).

$$2nW(n) + \int_n^1 M_\theta \, d\xi + 2\int_n^1 WN_\theta \, d\xi = -6I \int_n^1 \left[\int_o^\psi W_{TT}\, \zeta \, d\zeta\right] d\psi \tag{87}$$

(Note that the conditions $N_\rho = N_n = 1$ and $M_\rho = M_n = 0$ were used.) With the use of equation (30), equation (87) becomes

$$6I \int_n^1 \left[\int_o^\psi W_{TT}\, \zeta \, d\zeta\right] d\psi = -(1 - n) - 2nW(n) + \int_n^1 N_\theta{}^2 d\xi - 2\int_n^1 WN_\theta \, d\xi \tag{88}$$

In terms of Z (see eq. (29))

$$6I \int_n^1 \left[\int_o^\psi W_{TT}\, \zeta \, d\zeta\right] d\psi = -(1 - n) - 2nW(n) + \int_n^1 Z^2 d\xi + 2\int_n^1 WZ \, d\xi$$

$$n < \zeta < 1 \tag{89}$$

As in Phase 1 motion, $W_{\xi\xi\tau} = 0$, so that the velocity is linear

$$W_\tau = (W_\tau)_n\left(\frac{1 - \xi}{1 - n}\right) \qquad n < \xi < 1 \tag{90}$$

where $(W_\tau)_n$ is the velocity at the membrane hinge.

X. SOLUTIONS OF GOVERNING EQUATIONS

In Chapter IX the governing equations for the bending hinge, ρ, the membrane hinge, n, and the center deflection, A, were derived. No assumptions were made in this section so that these equations are exact within the framework of the basic assumptions, equilibrium equations, and flow conditions discussed in Chapter VIII.

Note that these governing equations contain either a N_θ or Z and a deflection W. Consequently, a solution can be obtained if some assumptions concerning these terms are made.

The deflection term appears only in a definite integral. Furthermore, the value of the deflection is always known at both endpoints of the definite integral, that is, $W(\rho) = 2$, $W(0) = A$, and $W(1) = 0$. Consequently, only the assumption of shape of the deflection profile is necessary.

An assumption of conical surfaces will be made in the sections to follow. Such deformational surfaces have been observed experimentally for dynamic loading (see ref. 26) and have been used by others in solving membrane type problems. For example, both Hudson in reference 1 and Frederick in reference 2 made this assumption in their treatment of impulsively loaded membranes. Onat and Haythornthwaite (ref. 25) also made the same assumption in a study dealing with the influence of midplane forces on plastic plates under static loading.

In order to solve the governing equations in the form of equations (74) and (83), some knowledge of the value of N_θ is also necessary. If one recalls that in the elastic solution a circular plate

uniformly loaded at its supports has constant midplane stresses throughout the plate, it is tempting to assume that the plastic plate has a similar distribution. Applying this reasoning to the plastic plates with large impulses, the entire plate could be assumed a membrane and N_θ set equal to one.

This approach, however, does not take into account midplane forces that are developed by the distortion of the midplane of the plate. The failure to recognize this fact reflects itself in two ways: First the midplane forces are a constant. Second, and more important, no portion of the plate is permitted to become a membrane. Thus an accurate solution to impulsively loaded plates must be based on the governing equations that contain the neutral surface displacement Z (eqs. (75) and (84)). It also must, when appropriate, utilize the Phase 3 governing equations (eqs. (89) and (90)). Solutions using the assumption of constant midplane forces are of interest. They can serve as an evaluation of the influence of midplane forces on the deflections of plastic plates. In addition, the solution for $N_\theta = 1$ gives a limiting case of maximum midplane force. Thus both solutions will be developed in the following sections.

Bending of Plates Under Lateral Loads

In the analysis to follow the midplane forces will be assumed constant throughout the plate. With the exception of the limiting case of $N_\theta = 1$, the plate will always carry a plastic moment and at no time will the plate become a membrane. Consequently, this case can be thought

of as an analysis of the bending behavior of a plastic plate that has been loaded by lateral loads, N_θ, prior to the application of the impulse. This analysis will not recognize midplane deformations due to large deflections.

The governing equation for Phase 1 (eq. (74)) reduces for this case to

$$I(1 - \rho)(1 + 3\rho)\rho_\tau = N_\theta^2 - 1 - 4\rho N_\theta \tau - 2N_\theta \int_\rho^1 W \, d\xi \tag{91}$$

If the deflected surface is assumed to be a conical surface

$$\left.\begin{aligned} W &= 2\tau && 0 < \xi < \rho \\ W &= 2\tau\left(\frac{1 - \xi}{1 - \rho}\right) && \rho < \xi < 1 \end{aligned}\right\} \tag{92}$$

so that $W(\rho) = 2\tau$ and $W(1) = 0$. Substitution of equation (92) into equation (91) results in a nonlinear differential equation

$$I(1 - \rho)(1 + 3\rho)\rho_\tau = -(1 - N_\theta^2) - 2N_\theta \tau(1 + \rho) \tag{93}$$

This equation is solved in appendix A through the use of a finite difference approach. Numerical results are given for values of N_θ ranging from 0 to 1.0 and for a range of impulses, I, from 0.4 to 11.6. Exact solutions are obtained for the limiting cases of N_θ equal to zero and 1. Time histories of the hinge circle, ρ, are tabulated in appendix A for a wide range of I and N_θ.

Phase 1 motion will continue until the hinge circle reaches the center. Let τ_1 be the time at which this occurs. At $\tau = \tau_1$ the deformation at the center will be

$$W(0,\tau_1) = A(\tau_1) = 2\tau_1 \tag{94}$$

The velocity at the center will be

$$W_\tau(0,\tau_1) = A_\tau(\tau_1) = 2 \tag{95}$$

The value of τ_1 is tabulated in appendix A as a function of impulse I and midplane force N_θ. The values of τ_1 with the corresponding values of displacement $A(\tau_1)$ and velocity 2 serve as the initial values of the Phase 2 motion.

The governing equation for Phase 2 (eq. (83)) reduces to

$$\frac{1}{2} IA_{\tau\tau} = -(1 - N_\theta{}^2) - 2N_\theta \int_0^1 W \, d\xi \tag{96}$$

Consistent with the assumption of conical surfaces

$$W = A(1 - \xi) \tag{97}$$

Thus the governing equation becomes

$$IA_{\tau\tau} = -2(1 - N_\theta{}^2) - 2N_\theta A \tag{98}$$

The first integration of equation (98) can be achieved by multiplying the equation by A_τ.

$$IA_\tau A_{\tau\tau} = -\left[2(1 - N_\theta{}^2) + 2N_\theta A\right]A_\tau \tag{99}$$

The integral of equation (99) can now be written as

$$\frac{1}{2} IA_\tau{}^2 = -2(1 - N_\theta{}^2)A - N_\theta A^2 + C_1 \tag{100}$$

where C_1 is the constant of integration.

The initial conditions for Phase 2 are

$$A(\tau_1) = 2\tau_1 \tag{101}$$

$$A_\tau(\tau_1) = 2 \tag{102}$$

Therefore

$$C_1 = 2I + 4\tau_1(1 - N_\theta{}^2) + 4\tau_1{}^2 N_\theta \tag{103}$$

Substitution of equation (103) into equation (100) gives the expression for the velocity of the center of the plate as

$$IA_\tau{}^2 = -4(1 - N_\theta{}^2)A - 2N_\theta A^2 + 4I + 8\tau_1(1 - N_\theta{}^2) + 8\tau_1{}^2 N_\theta \tag{104}$$

The final deformation at the center of the plate, A_F, can now be obtained from equation (104) by setting $A_\tau = 0$.

$$N_\theta A_F{}^2 + 2(1 - N_\theta{}^2)A_F = 2I + 4\tau_1(1 - N_\theta{}^2) + 4\tau_1{}^2 N_\theta \tag{105}$$

Large Deflection of Plates

The analyses in this section will consider the midplane forces that are developed by large deformations of the plate. Consequently, governing equations (75), (84), and (89) will be used as these equations contain the parameter Z. As previously discussed, this parameter is a measure of the displacement of the neutral surface from the midplane.

The definition of Z is given in equation (38) in terms of the midplane displacement W. For the assumption of conical surfaces equation (38) reduces to

$$Z = -\frac{W}{2} \tag{106}$$

For Phase 1

$$W = 2\tau \qquad 0 < \xi < \rho$$

and (107)

$$W = 2\tau\left(\frac{1 - \xi}{1 - \rho}\right) \qquad \rho < \xi < 1$$

Thus

$$Z = -\tau \qquad 0 < \xi < \rho$$

(108)

$$Z = -\tau\left(\frac{1 - \xi}{1 - \rho}\right) \qquad \rho < \xi < 1$$

The governing equation for Phase 1 can now be written as

$$I(1 - \rho)(1 + 3\rho)\rho_\tau = -1 - (2\rho + 1)\tau^2 \tag{109}$$

A numerical solution of equation (109) using a finite difference approach is given in appendix B. Numerical values are calculated for a range of impulses from I equal to 0.2 to 12.

Note that at $\tau = 0$ equation (109) reduces to the differential equation for pure bending (see ref. 3). Thus for small values of τ the behavior of the hinge approximates that obtained for a plastic plate in bending. As time becomes large, however, the magnitude of the hinge velocity ρ_τ increases over that for the bending case. This increase in hinge velocity results in a decrease in final deformation.

Phase 1 motion continues until the hinge circle reaches the center of the plate. At this time, $\tau = \tau_1$, deformation of the center is

$$W(0,\tau_1) = A(\tau_1) = 2\tau_1 \tag{110}$$

and its velocity is

$$W_\tau(0,\tau_1) = A_\tau(\tau_1) = 2 \tag{111}$$

Thus equations (110) and (111) serve as initial conditions for Phase 2. The governing equations for this phase are given by equation (84). Using equation (106), equation (84) becomes

$$\frac{1}{2} IA_{\tau\tau} = -1 - \frac{3}{4} \int_0^1 W^2 d\xi \tag{112}$$

which can be approximated with the use of the conical surface assumption by

$$2IA_{\tau\tau} = -4 - A^2 \tag{113}$$

By a procedure similar to that used for the solution of equation (98), equation (113) can be integrated to get

$$IA_\tau^2 = -\frac{A}{3}(12 + A^2) + C_2 \tag{114}$$

The constant of integration C_2 can be evaluated by use of the initial conditions (eqs. (110) and (111))

$$C_2 = 4I + \frac{2\tau_1}{3}(12 + 4\tau_1^2) \tag{115}$$

Substitution of equation (115) into equation (114) gives an expression for the velocity of the center of the plate during Phase 2 motion

$$IA_\tau^2 = 4I + \frac{(2\tau_1)}{3}\left\{12 + (2\tau_1)^2\right\} - \frac{A}{3}(12 + A^2) \tag{116}$$

The final deformation of the center A_F can be evaluated from equation (116) by setting A_τ equal to zero. Thus

$$A_F(12 + A_F^2) = 12I + (2\tau_1)\left\{12 + (2\tau_1)^2\right\} \tag{117}$$

At first glance it would seem that equation (117) can provide a solution for the final deformation of the center of all impulsively loaded plates. There are, however, restrictions on the use of this equation.

Equation (117) is based on the assumption that only Phase 1 and Phase 2 behavior occurs during the deformation of the plate. Both of these phases assume that an interaction of bending and midplane forces occurs. It has been shown that as the plastic midplane forces, N, increased the value of the plastic moments, M, decreased until a value of N equal to one is reached. The moment at that time is zero and that portion of the plate became a membrane. Thus the behavior described under Phase 1 and Phase 2 is correct only for that portion of the deformation that does not generate a midplane force such that N^2 is greater than one. In terms of Z this condition states that Z^2 is less than one, and hence the deflection W must be less than 2 (see eq. (106)).

Consequently, equation (117) can be used to calculate the final deformation of the plate only if the impulse, I, is small enough so that the deformation of the plate is less than 2. When the plate is subjected to impulses greater than this value, a Phase 3 motion will begin. The plate will be separated into two parts. In the central region where the deflection is greater than two, no bending moments are present and the plate behaves as a membrane. In the outer region a coupling of midplane forces and bending moments occurs and the plate

in this region behaves as it did in Phase 1. The point of separation of these regions, $\xi = n$, is defined by

$$W(n,\tau) = 2 \tag{118}$$

This point then forms a membrane hinge. This portion of the motion of the plate is referred to as Phase 3.

The time, τ_2, at which the Phase 3 motion begins is defined as

$$W(\rho,\tau_2) = 2 \tag{119}$$

Using the expression for Z given in equation (106) and the value of the deflection at the membrane hinge, n, given by equation (119), the governing equation for Phase 3 (eq. (89)) becomes

$$6I\int_n^1 \left[\int_o^\psi W_{\tau\tau}\,\zeta\,d\zeta\right]d\psi = -(1 + 3n) - \frac{3}{4}\int_n^1 W^2 d\xi \tag{120}$$

In order to evaluate the left side of equation (120) the acceleration of the outer region ($n < \xi < 1$) must be evaluated. The velocity of the region is given in equation (90) in terms of the position of hinge and the transverse velocity at the hinge point $W_\tau(n,\tau)$.

Since the displacement at the hinge is by definition equal to a constant 2 (see eq. (118)), the transverse velocity is dependent on the slope of the deflection curve at the hinge and the velocity of the hinge, n_τ. In addition, as the deformation of the plate is monotonically increasing, the membrane hinge must be traveling toward the support. Thus

$$W_\tau(n,t) = \frac{2}{1 - n}\, n_\tau \tag{121}$$

With equations (90) and (121) the velocity of the plate in the outer region is given by

$$W_\tau = \frac{2n_\tau}{(1 - n)^2}(1 - \zeta) \qquad n < \zeta < 1 \tag{122}$$

The acceleration can now be written as

$$W_{\tau\tau} = \left[\frac{2}{(1 - n)^3}\left\{(1 - n)n_{\tau\tau} + 2n_\tau^2\right\}\right](1 - \zeta) \qquad n < \zeta < 1 \tag{123}$$

Substitution of equation (123) into equation (120) and performing the necessary integration results in the following differential equation

$$I\left[(1 - n)n_{\tau\tau} + 2n_\tau^2\right](1 + 3n) = -(1 + 3n) - \frac{3}{4}\int_n^1 W^2 d\zeta \tag{124}$$

Equation (124) can now be approximated with the assumption of conical surfaces in which $W(n,\tau) = 2$ and $W(1,\tau) = 0$, to give

$$I\left[(1 - n)n_{\tau\tau} + 2n_\tau^2\right](1 + 3n) = -2(1 - n) \tag{125}$$

The solution to this differential equation results in the velocity and position of the membrane hinge. The integrating factor for the above equation is

$$\frac{2n_\tau}{(1 + n)^5(1 + 3n)}$$

Multiplying equation (125) by this factor gives

$$I \frac{d}{d\tau}\left[\frac{n_\tau^2}{(1 - n)^4}\right] = - \frac{4}{(1 + 3n)(1 - n)^4} \frac{dn}{d\tau} \tag{126}$$

Hence the integral of equation (126) is

$$I\left[\frac{n_\tau^2}{(1 - n)^4}\right] = - \frac{1}{192}\left[\frac{108}{(1 - n)} + \frac{72}{(1 - n)^2} + \frac{64}{(1 - n)^3} + 81 \log \frac{1 + 3n}{1 - n}\right] + C_3 \tag{127}$$

If the Phase 3 behavior begins while the plate is in Phase 2, the membrane hinge occurs at the center of the plate, that is, at $n = 0$. The hinge velocity at that time is (from eq. (121))

$$(n_\tau)_o = \frac{1}{2} A_\tau(\tau_2) \tag{128}$$

The constant of integration, C_3, in equation (127) can now be evaluated and is given by

$$C_3 = I(n_\tau)_o^2 + \frac{1}{192}(244) \tag{129}$$

Substituting equation (129) into equation (127) gives

$$I\left[\frac{n_\tau^2}{(1-n)^4}\right] = -F(n) + I(n_\tau)_o^2 \tag{130}$$

where

$$F(n) = \frac{1}{192}\left[\frac{108}{(1-n)} + \frac{72}{(1-n)^2} + \frac{64}{(1-n)^3} + 81\log\left(\frac{1+3n}{1-n}\right) - 244\right] \tag{131}$$

Values of this function for a range of n from 0 to 1.0 are given in appendix C. The motion of the plate stops when $n_\tau = 0$, therefore, the final position of the membrane hinge is given by

$$F(n_F) = I(n_\tau)_o^2 \tag{132a}$$

or with equation (128)

$$F(n_F) = \frac{I}{4} A_\tau^2(\tau_2) \tag{132b}$$

The velocity, $A_\tau(\tau_2)$, can be evaluated from equation (116), since the deflection A is known to be 2 at $\tau = \tau_2$. Therefore

$$A_\tau^2(\tau_2) = 4 + \left[(2\tau_1)\left\{12 + (2\tau_1)^2\right\} - 32\right]\frac{1}{3I} \tag{133}$$

Equation (132) applies to the condition where the membrane behavior is initiated during the Phase 2 motion of the plate. If the impulse is great enough, membrane behavior can be initiated during Phase 1, that is,

before the bending hinge reaches the center of the plate. Since membrane behavior occurs when deflections are greater than 2 (see eq. (118)) and from equation (107)

$$W(\xi,\tau) = 2\tau \qquad 0 < \xi < \rho \tag{134}$$

the Phase 3 behavior of the plate is initiated directly from Phase 1 for all impulses where τ becomes greater than unity.

For this case the midplane forces are constant in the central region $(0 < \xi < \rho)$. The membrane hinge must thus originate at the point $\xi = \rho_1 = n_o$.

The differential equation for Phase 3 in this case is identical to the previous case. The solution to the differential equation is given by equation (127). The initial conditions, however, are different. The initial position of the membrane hinge, n_o, is equal to the position of the bending hinge, ρ_1, at time, $\tau = 1$. Thus

$$n_o = \rho(1) = \rho_1 \tag{135}$$

The transverse velocity of the plate at the hinge is 2. Thus from equation (121)

$$(n_\tau)_o = (1 - n_o) = (1 - \rho_1) \tag{136}$$

Evaluation of the constant of equation (127) for the above condition gives

$$C_3 = I\frac{(n_T)_o^2}{(1-n_o)^4} + \frac{1}{192}\left[\frac{108}{1-n_o} + \frac{72}{(1-n_o)^2} + \frac{64}{(1-n_o)^3} + 81\log\left(\frac{1+3n_o}{1-n_o}\right)\right] \tag{137}$$

With equation (137) and noting that $n_o = \rho_1$, the expression for the velocity can be written as

$$I\left[\frac{n_T^2}{(1-n)^4}\right] = I\left[\frac{(n_T)_o^2}{(1-\rho_1)^4}\right] - F(n) + F(\rho_1) \tag{138}$$

where $F(n)$ is defined by equation (131).

The motion stops when n_T is zero, hence the position of the hinge when the plate comes to rest, n_F, is given by

$$F(n_F) = I\left[\frac{(n_T)_o^2}{(1-\rho_1)^4}\right] + F(\rho_1) \tag{139}$$

With the use of equation (136)

$$F(n_F) = I\left[\frac{1}{(1-\rho_1)^2}\right] + F(\rho_1) \tag{140}$$

The final position of the membrane hinge is now known. If the center portion of the plate does not turn into a membrane until the plate is in Phase 2, equations (132) and (133) apply. If the center turns into a membrane during the first phase of the motion, equation (140) applies.

The inner portion of the plate ($0 < \xi < n$) during this time behaves like a membrane. That is, it carries no bending and transmits only a constant tensile load in the direction of its midplane. A very detailed and thorough discussion of such behavior is given by Hudson (ref. 1) and by Frederick (ref. 2). Some of the more pertinent aspects of the motion are repeated herein.

When Phase 3 motion is initiated during Phase 1 motion, the membrane portion of the plate behaves as follows. The bending hinge that originated during Phase 1 continues to travel inward toward the center of the plate. As the hinge sweeps over each annular material element in the flat central region, it tilts it into the shape of an annular truncated conical element behind the hinge. As the material cannot support bending, it is assumed no significant amount of work is done in bending. In addition, it is assumed that no thinning of the plate takes place. The portion of the plate passed over by the hinge is assumed to move in a manner that makes its slope agree with the slope of the outer portion of the plate. Thus when the motion of the membrane portion of the plate stops, which occurs after the hinge reaches the center, that portion forms a cone with a slope equal to the slope of the outer portion.

This conical behavior is also assumed if the Phase 3 motion is initiated from Phase 2 motion. Thus

$$\frac{A_F - 2}{n_F} = \frac{2}{1 - n_F} \tag{141}$$

or

$$A_F = 2 + \frac{2n_F}{1 - n_F} = \frac{2}{1 - n_F} \tag{142}$$

XI. DISCUSSION OF NUMERICAL RESULTS

Experimental Results

Before proceeding with a discussion of the numerical results and the all-important comparisons with experimental data, it would seem appropriate to first discuss the details of the experiments. All of the data used herein were obtained from an extensive experimental investigation performed by Florence. The details of the experiments and the resulting data were discussed in reference 4 from which much of the following discussion is taken. It is being repeated here for the sake of completeness.

The experiments were very thorough, covering a wide range of impulsive loadings and plates of two different materials: aluminum and steel. The aluminum plates were 6061-T6 and the steel plates were 1018 cold rolled steel.

A sketch of the experimental setup is shown in figure 11. The plates were all nominally 1/4-inch thick and 8-1/2 inches in diameter. The specimens were supported on an annular steel plate with an 8-inch inside diameter. The impulse was generated by the detonation of an 8-inch diameter of sheet explosive (DuPont EL-506D). The sheet explosive was cut to fit the opening in the upper support. A similar disk of solid neoprene, 1/8 of an inch in thickness, was placed between the explosive and the specimen. This served to reduce the high peak pressure in the shock wave entering the plate and tended to eliminate plastic waves, possible changes of material properties, and spallation.

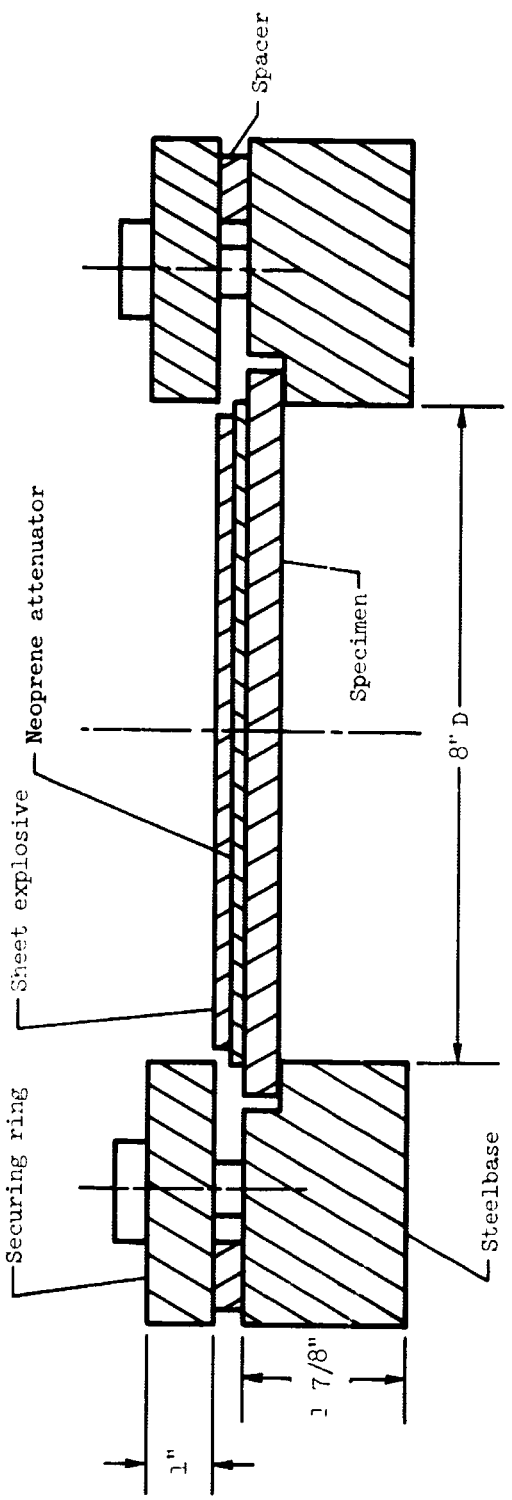

Figure 11.- Experimental setup used by Florence.

The upper support was used to control the rebound. An outside steel ring served as a spacer to prevent the edge of the plate from striking the upper support during the rebound.

Dimensions and properties of the plate used in the experiment are given in table I. The yield stress was taken to be the average value of static tensile tests of both with and across grain specimens. Each experimental stress-strain curve was replaced by a bilinear stress-strain curve. The strain-hardening portion of the curves was obtained by fitting a straight line through data points above 3- to 4-percent strain.

Twenty-two aluminum and 20 steel plates were tested. The values of the initial impulse imparted to the plate were obtained by firing free plates in front of a double-flash X-ray unit. The rigid-body displacement in the predetermined time between X-ray pictures gave the initial plate velocity.

The permanent central deflections were obtained through the use of a traveling microscope. The values of this permanent deflection along with the measured initial dimensional impulses are tabulated in table II. Also shown in this table are the corresponding values of nondimensional impulse I.

Large Deflection Effects

The analyses based on consideration of large deflectional effects will be used to predict the behavior of the experimental specimens.

TABLE I.- DIMENSIONS AND PROPERTIES OF SPECIMENS*

Material	Yield stress, lb/in^2	Density, $lb\text{-}sec^2/in^2$	Depth, in.	Radius, in.
Aluminum 6061-T6	42,000	0.000253	0.251	4.0
C.R. Steel 1018	79,000	0.000732	0.241	4.0

TABLE II.- EXPERIMENTAL RESULTS*

Steel plates			Aluminum plates		
Impulse I	Exper. A_F	μV_o $lb\text{-}sec/m^2$	Impulse I	Exper. A_F	μV_o $lb\text{-}sec/m^2$
6.97	8.66	0.505	12.71	13.42	0.317
6.86	8.43	0.501	10.56	9.94	0.289
5.54	7.44	0.450	10.49	10.96	0.288
5.20	7.14	0.436	10.13	10.61	0.283
4.69	7.00	0.414	7.53	8.06	0.244
3.52	6.41	0.359	7.28	8.54	0.240
3.33	5.81	0.349	7.28	8.32	0.240
3.24	5.54	0.344	7.28	8.41	0.240
3.00	5.05	0.331	6.17	8.06	0.221
2.70	4.48	0.314	6.07	7.75	0.219
2.66	4.75	0.312	4.66	6.34	0.192
2.02	3.78	0.272	4.61	7.08	0.191
1.82	3.22	0.258	4.28	5.99	0.184
1.26	2.56	0.215	2.81	4.94	0.149
0.67	1.06	0.157	2.62	4.84	0.144
0.67	1.03	0.156	2.55	4.05	0.142
0.67	1.20	0.156	2.52	4.69	0.141
0.64	1.49	0.153	2.44	4.27	0.139
0.41	0.80	0.123	2.34	3.89	0.136
0.40	0.83	0.121	1.91	3.12	0.123
			1.76	3.70	0.118
			1.47	3.16	0.108

*Data taken from reference 4.

Examination of the experimental setup shows that there are no mechanisms to provide a midplane force prior to impulse. Thus the plates must begin their motion in the pure bending mode. All specimens must, therefore, start with a deformational behavior similar to the Phase 1 behavior discussed herein.

The governing equation for the motion of the hinge circle during Phase 1 is given by equation (109). A solution to this equation is given in appendix B. Numerical results for the position of the hinge circle at any time τ are given for a range of impulses I from 0.2 to 12. Typical plots of these values are shown in figure 12.

The discussion in Chapter X pointed out that Phase 1 motion continues until one of two possible conditions occurs. Either the hinge circle reaches the center of the plate ($\rho = 0$) or the time τ reaches a value of one. From figure 12 it can be seen that the former condition applies to the smaller values of impulse ($I < 1.5$) while the latter occurs for the larger impulses where I is greater than 1.5.

In this phase of motion (Phase 1) the nondimensional displacement of the central portion of the plate is equal to twice the time τ. Thus for impulses greater than 1.5 the deflection of the central portion reaches a value of 2 (Z of one) before the hinge circle reaches the center. Once this value of deflection is reached the central portion of the plate becomes a membrane. (A nondimensional displacement of 2 is equivalent to an actual displacement of $2h$, that is, the thickness of the plate.) The position of the hinge, ρ_1, when the central portion

TABLE III.- THEORETICAL RESULTS

I	ρ_1	τ_1	n_F	A_F
0.2	---	0.192	---	0.56
0.3	---	0.280	---	0.83
0.4	---	0.366	---	1.07
0.5	---	0.447	---	1.27
0.6	---	0.520	---	1.46
0.7	---	0.595	---	1.65
0.8	---	0.651	---	1.80
0.9	---	0.710	---	1.94
1.0	---	0.768	0.044	2.09
1.1	---	0.820	0.103	2.23
1.2	---	0.868	0.156	2.37
1.3	---	0.910	0.210	2.50
1.4	---	0.953	0.240	2.63
1.5	---	0.992	0.274	2.75
1.6	0.044	---	0.326	2.97
1.7	0.085	---	0.368	3.17
1.8	0.120	---	0.403	3.35
1.9	0.151	---	0.434	3.53
2.0	0.179	---	0.460	3.71
4.0	0.455	---	0.694	6.54
6.0	0.564	---	0.773	8.81
8.0	0.627	---	0.816	10.85
10.0	0.668	---	0.842	12.67
12.0	0.699	---	0.862	14.50
14.0	0.722	---	0.875	16.00

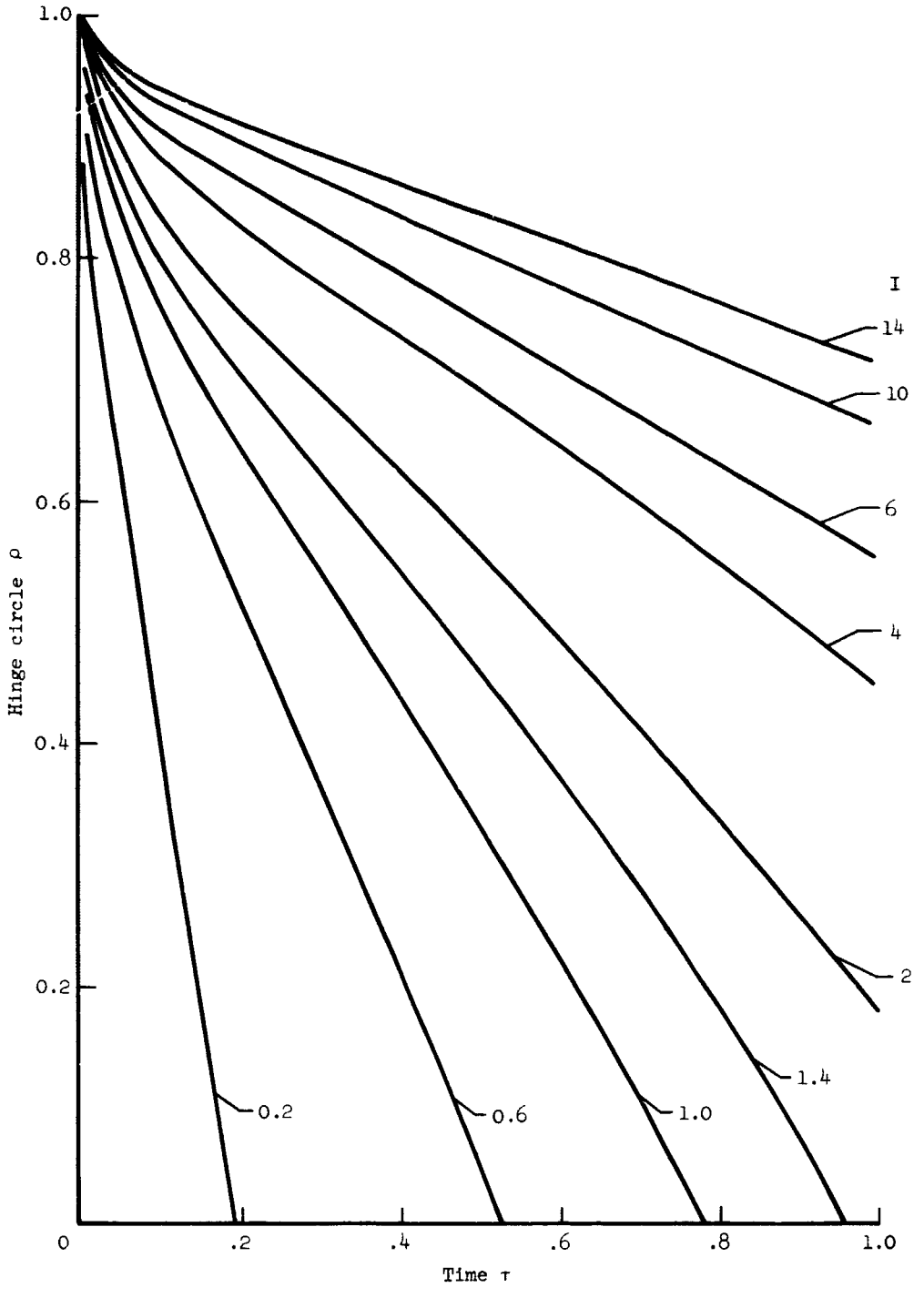

Figure 12.- Motion of bending hinge for various values of impulse.

initially becomes a membrane is a function of I as shown in figure 13 (see also table III).

For impulses less than 1.5 the hinge circle reaches the center of the plate before any portion of the plate can become a membrane ($\tau < 1$). The value of the time, τ_1, at which this occurs is plotted as a function of I in figure 14 (see also table III).

Subsequent motion of the plate depends on the magnitude of the impulse. For the large impulses ($I > 1.5$) the plate goes directly from Phase 1 to Phase 3 behavior. The initial location of the membrane is given by ρ_1 in table III. The displacement at the hinge point at this time, $W(n,\tau_2)$ is two and the velocity, $W_\tau(n,\tau_2)$ is also two (see eqs. (118) and (41)). The final position of the membrane hinge is calculated from equation (140) and its values are tabulated in table III for various values of I. It is also plotted as a function of I in figure 15. The final plastic deformations of the center of the plates are calculated from equation (142) and are tabulated in table III.

For impulses less than 1.5 the plate goes from the Phase 1 tc the Phase 2 motion. The initial center deflection for this phase is given by $2\tau_1$ and the velocity by 2. The values of τ_1 are obtained from table III for the appropriate values of I. If the impulse on the plate is small enough, the motion of the plate will stop before the central part of the plate becomes a membrane. The final deformation is then calculated from equation (117). This happens for all impulses smaller than 0.95.

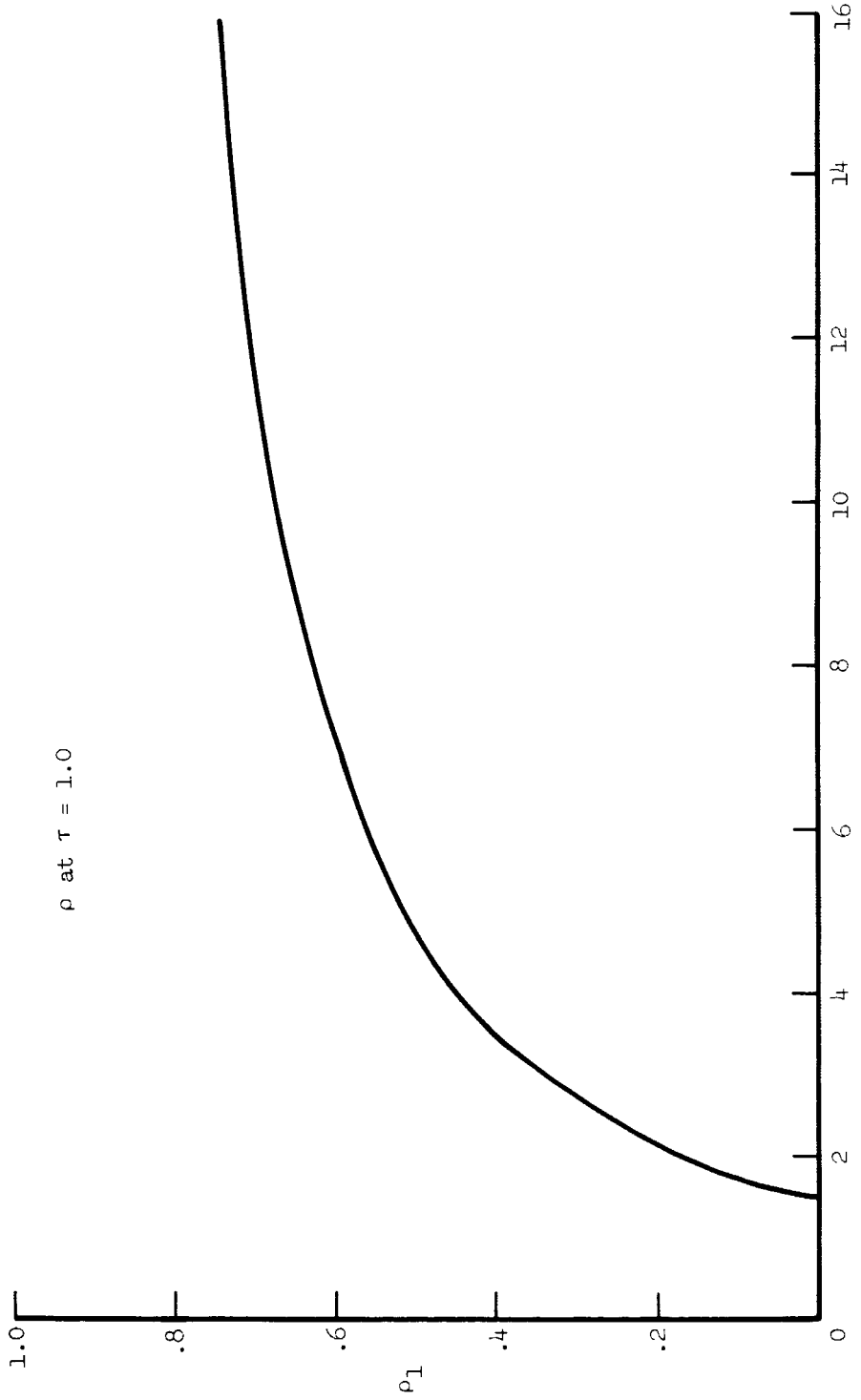

Figure 13.- Position of hinge at initiation of membrane behavior as a function of impulse.

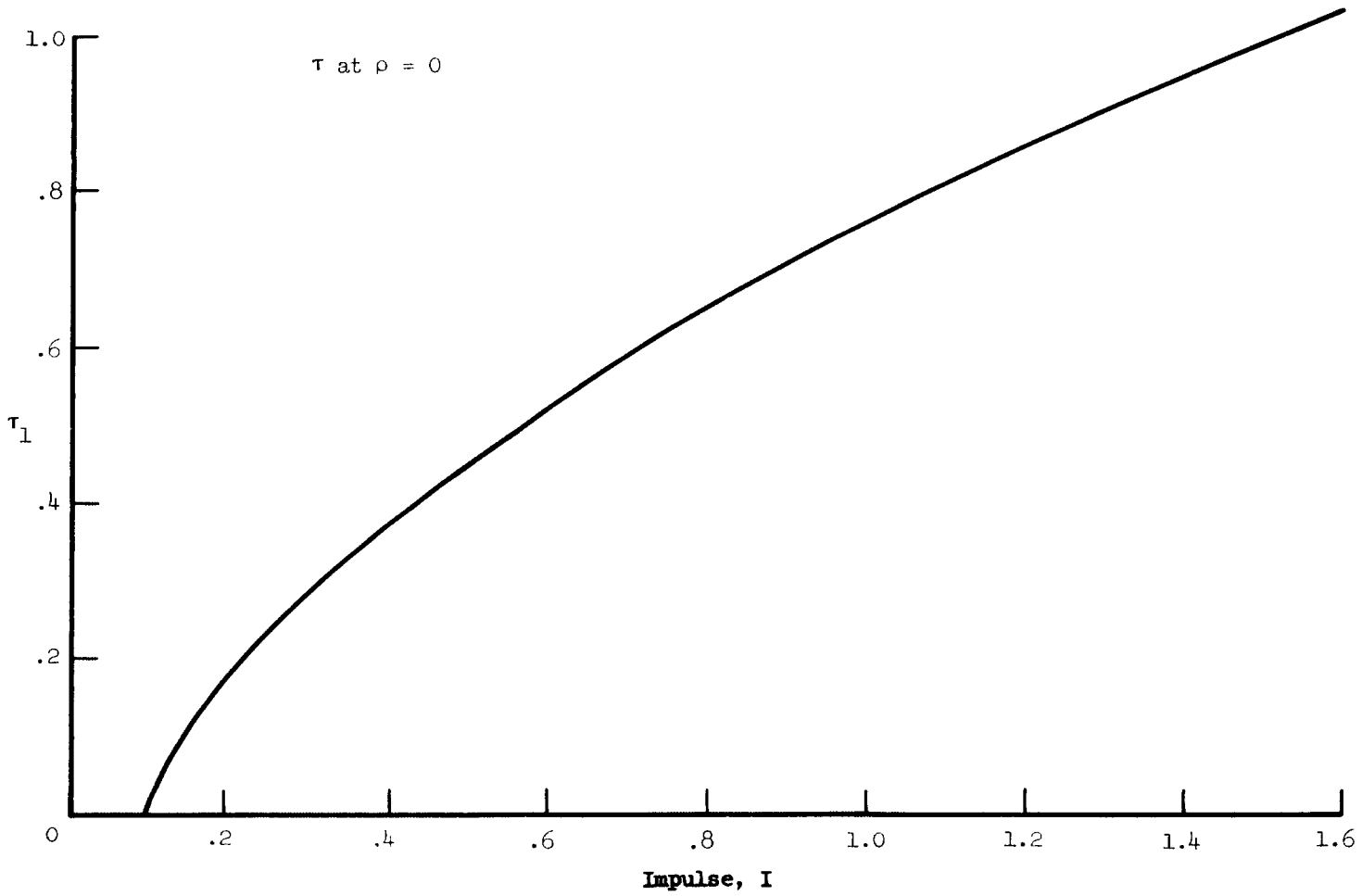

Figure 14.- Time for hinge circle to reach center of plate as a function of impulse.

If the impulse is in the intermediate range ($0.95 < I < 1.5$), the center of the plate turns into a membrane before the motion of the plate ends. For this case the final position of the membrane hinge is calculated from equation (132). These values are shown in table III and figure 15. The final deformation as calculated from equation (142) is also tabulated in table III.

A comparison of the calculated deformations at the center of the simply supported plate to those obtained experimentally is shown in figure 16 for the small and intermediate impulses and in figure 17 for the complete range of impulses from 0 to 14. The circles represent the experimental data from the 22 aluminum plates; the squares are from the data of the 20 steel plates. The solid curve was obtained from the present large deformation theory. The dashed curve is based on Wang's plastic bending theory.

The comparisons between the calculated and experimental deformations are very good, especially in the small and intermediate impulse range. For impulses less than 4-1/2 the agreement between theory and experiment is within experimental scatter. As the impulse increases above 5, the calculated deformations become larger than those measured. This deviation from experiment can be attributed, at least in part, to the omission of strain hardening effects. Inclusion of strain hardening effects certainly would cause a reduction in calculated permanent deformation. Furthermore, these effects would become increasingly important with the additional strains caused by increased impulse.

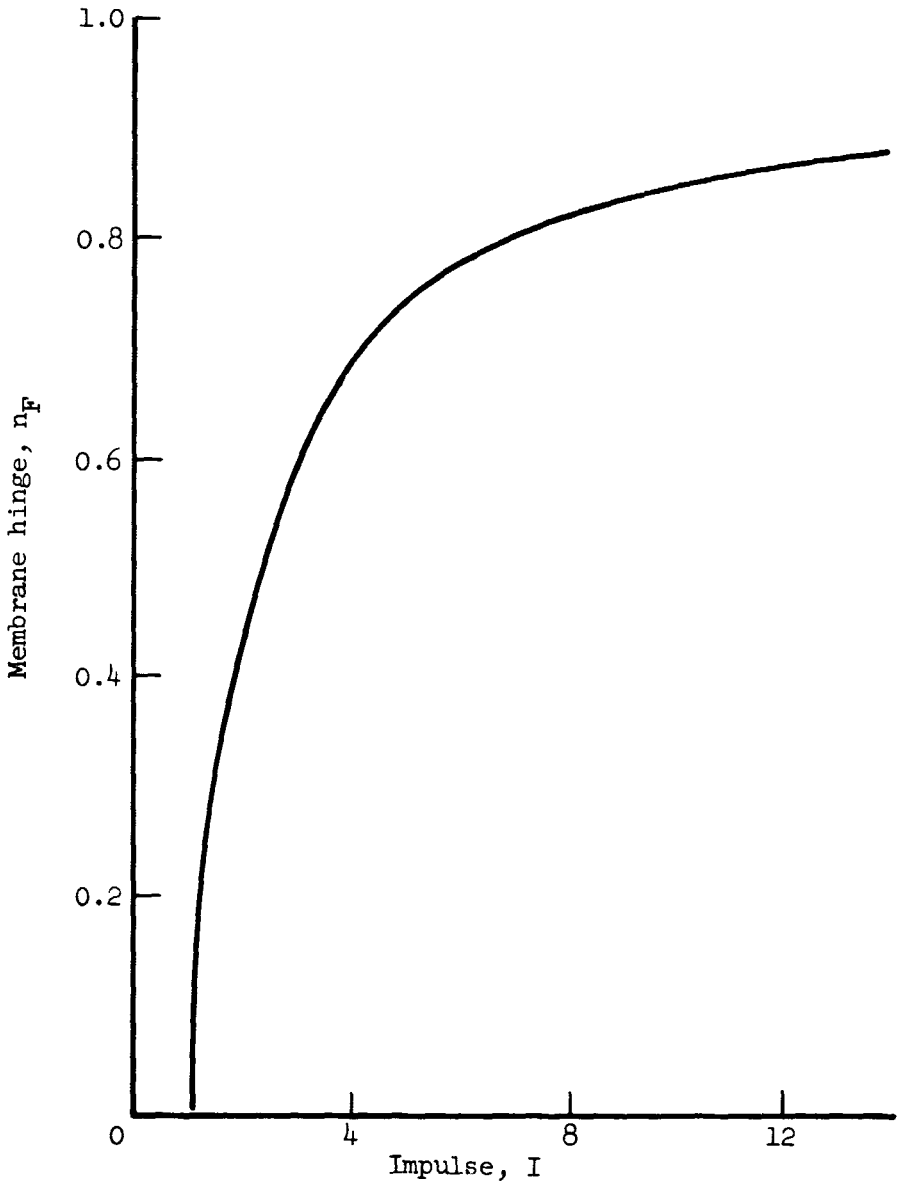

Figure 15. Final position of membrane hinge as a function of impulse.

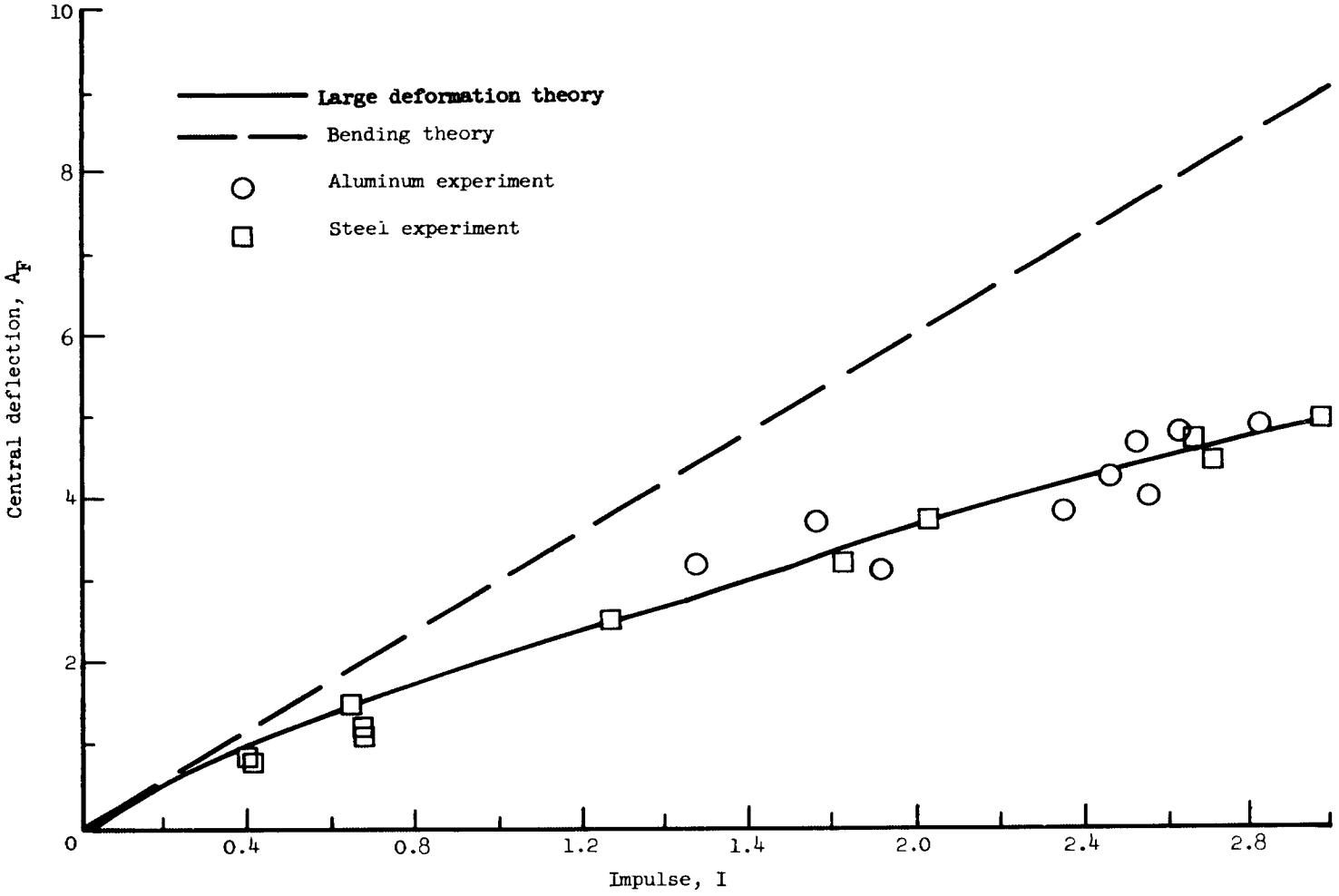

Figure 16.- Central deflection for small and intermediate impulses and comparisons with experimental data.

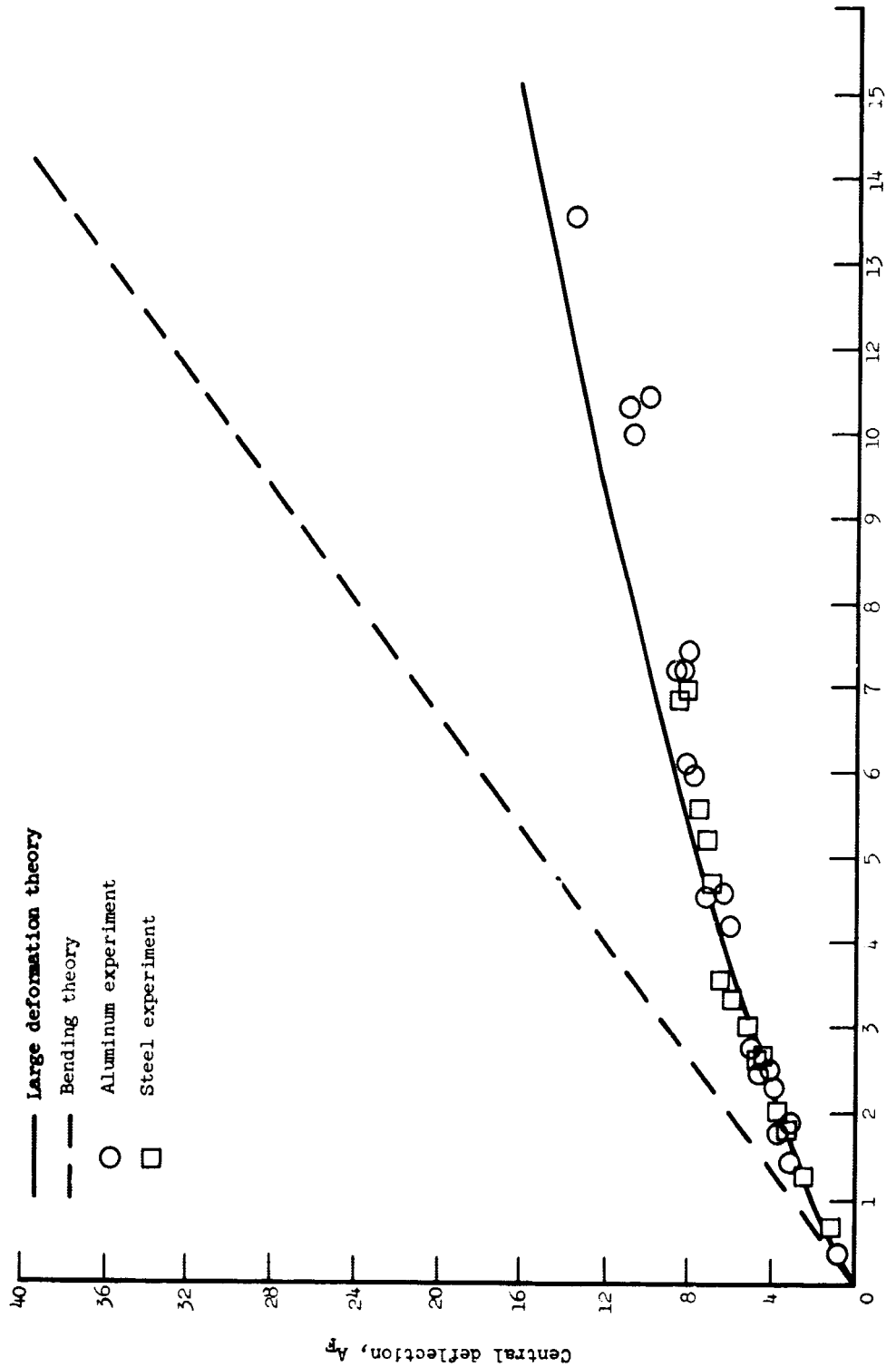

Figure 17.- Central deflection for large impulses and comparisons with experimental data.

The bending theory of Wang gives poor agreement even for the low values of impulse where no membrane behavior is present. As the value of the impulse is increased so that portions of the plate turn into a membrane, the difference between the bending and large deformation theories becomes substantial. This difference is largely due to the neglect of the restraints provided by the midplane forces. This effect will be further discussed in the next section.

Lateral Load Effects

The influence of the lateral loads on the deformational behavior of plastic plates can be seen by examining some of the numerical results given in appendix A for the case of plate bending with lateral loads.

The governing equations for Phase 1 motion for this case were given by equation (93). The equation was solved numerically in appendix A for various assigned values of N_θ. As the values of N_θ are assumed to be constant in the analyses, a plastic bending moment is present at all times. Thus no membrane behavior is considered regardless of the magnitude of the deformation. Even for the limiting case of $N_\theta = 1$, the plate does not behave as a membrane as the flow conditions for the interaction case is used, that is, $\dot{\epsilon}_r = 0$. Consequently, equation (93) is considered to be the governing equation for the motion of the hinge even after the deformation becomes greater than 2 ($\tau > 1$).

The final deformation of the plate was calculated from equation (105). The results are shown in figure 18, where the central deflection of the plate is plotted as a function of the uniform lateral loads, N, for

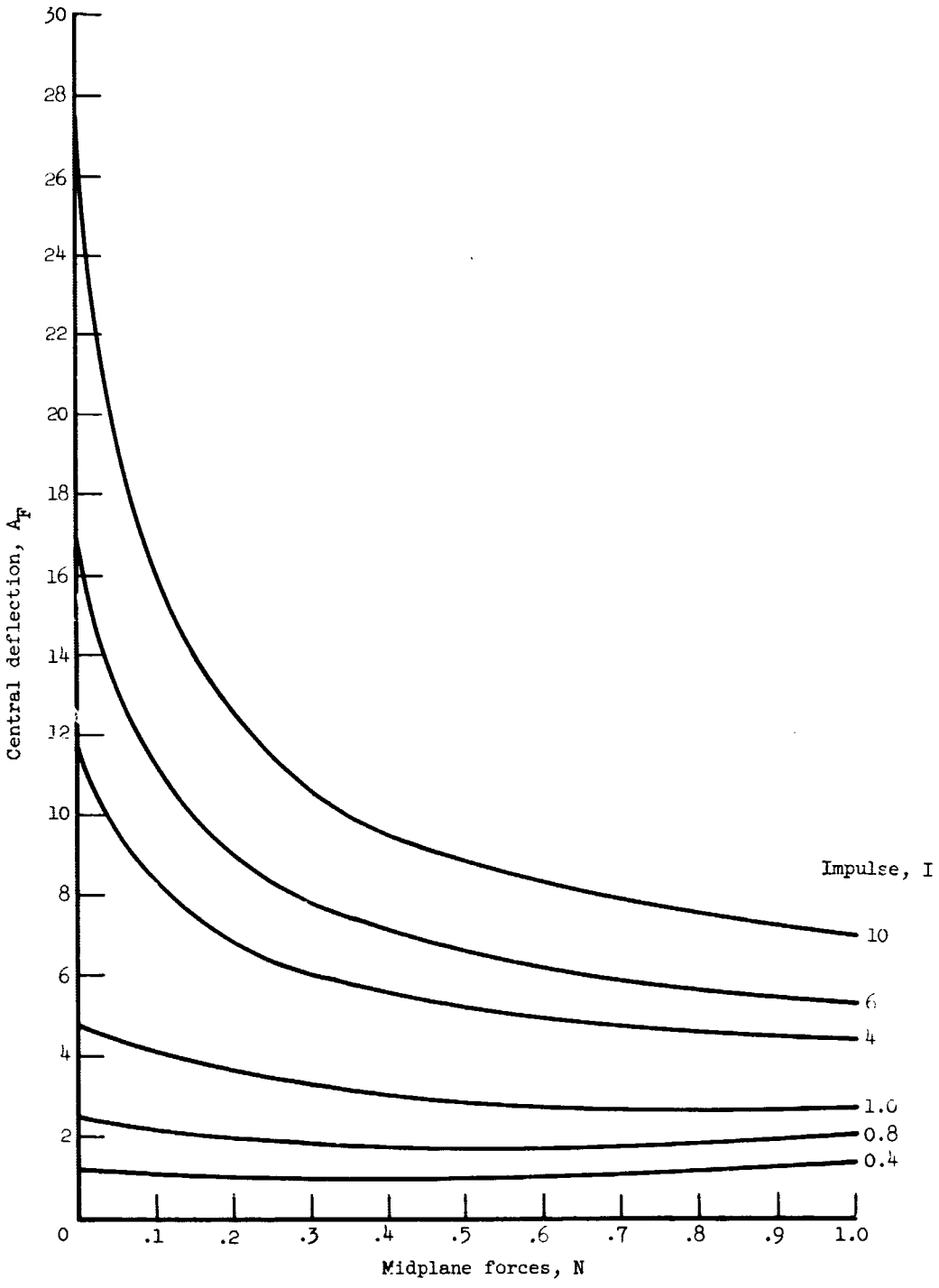

Figure 18.- Influence of midplane forces on central deflection.

various values of the impulse, I. Examination of these curves shows that for small impulses where the deformations are also relatively small, the midplane forces do not significantly influence the final deformation. However, with increasing values of impulse and correspondingly larger deformations, the influence of the midplane forces is greatly increased.

For example, for an impulse of 10 the calculated central deformation of the plate is reduced by almost 60 percent with the introduction of a midplane force of only 0.2 of the maximum (N = 0.2). Once the midplane forces reach a value in the range of 0.2 to 0.3, further increases of this force are not as effective in reducing the central deformation. In the case of an impulse of 10 in the above example, an introduction of a midplane force of 0.2 caused a reduction of deformation from 30 to 12.5. Further increase of the force to its maximum of 1.0, however, reduces the deformation only to a value of 7.0.

XII. COMPARISON OF LARGE DEFORMATION THEORY TO EXPERIMENTAL RESULTS AND OTHER METHODS OF ANALYSES

This section will be devoted to a critical examination of the various methods of analyses that have possible application to deformations of plastic plates. Conclusions as to the accuracy of these methods are based on the deformational results for impulsively loaded plates. These conclusions, however, are believed to be valid for other loading conditions when applied on a deformational basis.

Five methods of analysis will be discussed.

1. The large deformation theory developed herein.
2. The bending theory of Wang from reference 3.
3. An analysis based on maximum midplane forces.
4. The membrane theory of Frederick from reference 2.
5. The midplane interaction analysis of Jones from reference 5.

The calculated central deflections are shown in figure 19 as a function of impulse from all five of these analyses. In addition, the experimental results from Florence (ref. 4) are plotted for comparison.

Large Deformation Theory

The results from this analysis, replotted from figure 17, are shown as a solid line in figure 19. Recall that in this analysis the interaction between plastic bending moments and midplane forces are based entirely on the deflectional behavior of the plate. As long as the displacements are less than the thickness of the plate ($W < 2$) this interaction is present. However, when the deflections become greater

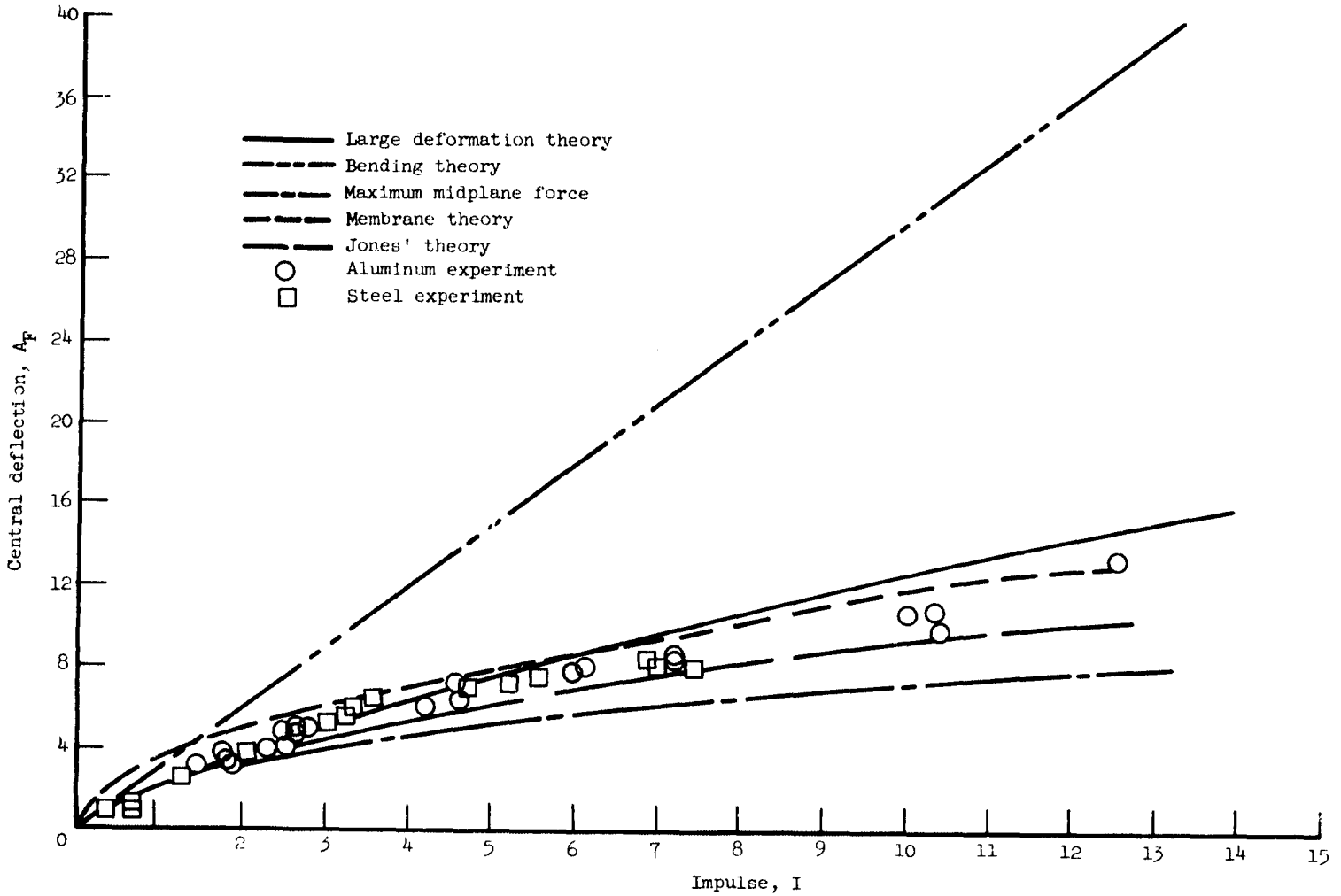

Figure 19.- Comparison of the large deformation theory to other methods of analyses.

than the thickness, the central portion of the plate becomes a membrane and thereafter supports no bending moment. The motion of the bending and membrane hinges, which are the governing factors of the final deformation, is obtained from solutions of appropriate governing equations.

From figure 19, it can be seen that the comparisons to theory are excellent for deformations of the order of 2 to 3 times the thickness (W of 4 to 6). For larger deformations the theory becomes slightly conservative. This, however, should be expected in the light of the basic assumptions of the theory. The assumption that the plate material is a rigid plastic neglects both elasticity and strain-hardening effects. Each of these would tend to reduce the calculated final deformation if included. In addition, the assumption that the shape of the outer region of the plate is conical tends to underestimate the speed of the hinge circles and thus increases the calculated deflection. The inclusion of all three of these effects would, therefore, bring the theoretical calculations into even better agreement with the experiment.

Bending Theory

The results from this analysis are shown in figure 19 as a dash—double-dot line. In terms of the parameters used herein, the central deflection is based on the equation

$$A_F = 3I \tag{143}$$

Figure 19 shows that the comparison between the bending theory and experiment is extremely poor even for the lower values of permanent deformation. Because of this poor comparison it would seem ill advised

to use this approach when accurate deflections are desired. As the method always gives permanent deformations that are above that obtained experimentally, the results of a bending analysis can be used to give very conservative estimates of permanent deformations.

It has been previously pointed out that the behavior of the bending hinge circle in Phase 1 is directly related to the final deformation of the plate. The larger the speed of the bending hinge the smaller the permanent deformation. Thus the conservativeness of the bending theory is due primarily to a calculated hinge circle speed that is too low.

Maximum Midplane Force Analysis

The results of this analysis are shown in figure 19 as a dot-dashed line. This analysis is identical to that for the large deformation except for the interaction relationship of moments and midplane forces. The interaction relationship used in the midplane force analysis is not dependent on deformations. Instead, it is based on the assumption that the deflections will be so large that the entire plate will carry the maximum midplane force of $\bar{N}_o(N = 1)$. This, therefore, necessitates that the bending moment vanish. The final deformation results for this case were discussed in a previous section and correspond to the values of A_F for $N = 1.0$ in figure 18.

The comparison of the central deformation calculated by the maximum midplane force assumption to the experimental results show that this method of analysis is unconservative, for the large deformations where the method should be most applicable. This unconservativeness in calculated

deformation reflects a calculated hinge circle velocity that is too large. The assumption that only midplane forces are present is, therefore, as poor an assumption as one where only bending moments are permitted.

Membrane Theory of Frederick

The results from this analysis are shown in figure 19 as a short dashed line. In terms of the parameters used herein the central deflection as calculated in reference 2 is given by

$$A_F = \sqrt{\frac{12I}{1 - 12I\left(\frac{h}{R}\right)^2}} \qquad (144)$$

The comparison of the experimental data and the theoretical results shows excellent agreement for the larger deformations. For small deformations the agreement is very poor. However, it should be noted that the theoretical model used by Frederick was never intended to be used for small deformations.

As the analysis has many assumptions it is difficult for the author to fully understand the theoretical reasons for the good agreement obtained for larger impulses as opposed to the very poor agreement in the lower impulse range.

The analysis does assume that only membrane forces are present which is the same assumption used by the maximum midplane force analysis just described. The behavior of the membrane is also assumed to be similar to the Phase 1 and Phase 2 behavior described herein.

The outer portion of the membrane in Phase 1 and the total membrane in Phase 2, however, are assumed to be rigid in Frederick's approach. Both of these assumptions should cause the membrane analysis to underestimate the final deformation. The third important difference of the two methods is that the membrane analysis assumes that the hinge velocity is uniform and dependent only on the initial velocity and the yield stress and density of the plate material. Thus it must be this assumption that compensates for the unconservatism of the other two.

Interaction Analysis of Jones

The results of Jones' analysis are shown in figure 19 as a long dashed curve. The data for this curve were taken from a figure in reference 5.

As can be seen from figure 19, Jones' analysis gives slightly unconservative results in the higher impulse or deformation range. Addition of the neglected strain hardening and elasticity effects would result in even more unconservative results. His calculations for small permanent deformations are in very poor agreement.

Jones assumed in his analysis that since the deformations were large, the midplane forces would always be at their maximum. He also permitted the plate to carry bending moments during the Phase 1 motion. These moments ranged from the maximum $\bar{M}_o$ at the bending hinge to zero at the support. Therefore, he violated the interaction relationship based on the Tresca yield condition. His flow conditions were the same as those used in the constant midplane-force analysis. Thus it would

seem that his calculated deformations should be smaller than those showed by the dot-dashed line. The fact that they are not smaller is due to an additional assumption used by Jones concerning the hinge velocity. In particular, he assumed the hinge velocity to be the same as that obtained by Wang for the bending case. As was shown in the section dealing with the comparison of the bending theory, this predicted hinge velocity is very much smaller than it should be. This lower value of velocity must then be responsible for increasing the value of his calculated deformation above that of the dot-dashed curve.

XIII. CONCLUDING REMARKS

An analysis of a simply supported circular plate under an impulsive loading has been presented. The analysis considers the influence of both bending and midplane forces and includes large deformation effects. Shear and rotary inertia effects are neglected. The plate material is assumed to be isotropic and a rigid plastic. The yield criteria are based on the Tresca condition.

Governing equations were developed and solved for three phases of motion. The initial Phase 1 included a bending hinge that traveled from the support to the center of the plate. Phase 2, which was initiated when the hinge reached the center, continued until either the motion ceased or a portion of the plate became a membrane. Phase 3 described the motion of the membrane hinge from its initial point to its final resting position.

Two types of bending-moment—midplane-force interaction relationships were studied: One was based on displacement of the neutral surface from the midplane surface. The second was based on the magnitude of midplane forces only. The former relationship took account of large deformations and midplane distortions and hence allowed regions of the plate to behave as a membrane. The latter only considered the lateral forces and no membrane behavior was permitted.

Comparisons of the analytical results with experimental data resulted in the following conclusions.

1. Interaction relationships based on large deformations should be used in order to get reliable data for a complete range of deflections and impulses.

2. Analyses of plastic plates based on bending behavior alone give highly conservative results and hence should only be used to get conservative estimates of the permanent deformations.

3. Even a small amount of midplane force has a significant effect on the final deformations of plastic plates.

4. Analyses of plastic plates based on maximum membrane forces throughout the plate tend to be seriously unconservative. This method should not be used unless accompanied by a conservative assumption to counteract this influence. Under no conditions should this assumption be used to study deformational behaviors of plates with deformations of the order of one to two plate thicknesses.

5. For final deformations of the order of five thicknesses and greater the influence of strain hardening and elasticity becomes important.

Elasticity effects can be approximately accounted for in the present analyses by incorporating an elastic phase of motion prior to the Phase 1 motion considered herein. This elastic phase could be used to evaluate the energy dissipated in elastic deformational behavior and correct the initial velocity conditions on Phase 1, accordingly.

A more accurate and sophisticated approach, however, would be to permit the plastic behavior to initiate at the center of the plate and

then spread toward the supports. To do this it would be necessary to define another hinge circle separating the elastic and plastic portions of the plate.

Another possible area of refinement is in the analysis of the membrane portion of the plate. An initial effort in this area should deal with the influence of reduced thickness.

XIV. REFERENCES

1. Hudson, G. E.: Theory of the Dynamic Plastic Deformation of a Thin Diaphragm. Journal of Applied Physics. Vol. 22, No. 1, Jan. 1951.

2. Frederick, Daniel: Simplified Analysis of Circular Membranes Subjected to an Impulsive Loading Producing Large Plastic Deformations. 4th Mid Western Conference in Solid Mechanics, 1959.

3. Wang, A. J.: Permanent Deflection of a Plastic Plate Under Blast Loading. Journal of Applied Mechanics. Sept. 1955.

4. Florence, A. L.: Circular Plates Under a Uniformly Distributed Impulse. International Journal of Solids and Structures. Vo . 2, No. 1, Jan. 1966.

5. Jones, N.: Impulse Loading of a Simply Supported Circular Plate. Division of Engineering, Brown Univeristy. Report No. 37, Feb. 1967.

6. Timoshenko, S.: Theory of Plates and Shells. McGraw-Hill Book Company, Inc., 1940.

7. Hodge, Phillip G., Jr.: Plastic Analysis of Structures. McGraw-Hill Book Company, Inc., 1959.

8. Florence, A. L.: Annular Plate Under a Transverse Line Impulse. AIAA Journal, Vol. 3, No. 9, Sept. 1965.

9. Prager, William: On the Use of Singular Yield Conditions and Associated Flow Rules. Journal of Applied Mechanics. Vol. 20, No. 3, Sept. 1953.

10. Hopkins, H. Geoffrey; and Prager, William: On the Dynamics of Plastic Circular Plates. Z.A.M.P. Vol. 5, 1954.

11. Hopkins, H. G.; and Prager, W.: Load Carrying Capacities of Circular Plates. Journal of the Mechanics and Physics of Solids. Vol. 2, Oct. 1953.

12. May, Gerald W.; and Gerstle, Kurt H.: Elastic Plastic Behavior of Axisymmetric Plates. ASCE Structural Conference, May 1967.

13. Symonds, P. S.; and Mentel, T. J.: Impulsive Loading of Plastic Beams With Axial Constraints. Journal Mech. Physics. Solids. Vol. 6, 1958.

14. Symonds, P. S.: Survey of Methods of Analysis for Plastic Deformation of Structures Under Dynamic Loading. Division of Engineering, Brown University. Rept. BU/NSRDC/1-67, June 1967.

15. Olszak, W.; Mroz, Z.; and Perzyna, P.: Recent Trends in the Development of the Theory of Plasticity. Macmillan Co., 1963.

16. Lepik, Yu R.: Plastic Flow of Thin Circular Plates Made of the Rigid-Plastic Material. Izv. Aked. Nank SSSR, OTN Mech., Wash. 1960, No. 2, 78-87.

17. Sawczuk, Antoni: On Initiation of the Membrane Action in Rigid Plastic Plates. Journal de Mecanique. Vol. 3, No. 1, March 1965.

18. Thomson, Robert G.: Plastic Deformation of Plates Subjected to a General Gaussian Distribution of Impulse. PhD Thesis, Virginia Polytechnic Inst., June 1966.

19. Thomson, Robert G.: Plastic Behavior of Circular Plates Under Transverse Impulse Loading of Gaussian Distribution. NASA TR R-279, Jan. 1968.

20. Perzyna, P.: Dynamic Load Carrying Capacity of a Circular Plate. Arch. Mech. Stos., Vol. 10, 1958.

21. Wang, A. J.; and Hopkins, H. G.: On the Plastic Deformation of Built-in Circular Plates Under Impulsive Load. J. Mech. and Physics of Solids, Vol. 3, 1954.

22. Shapiro, G. S.: On a Rigid Plastic Annular Plate Under Impulsive Load. Prikl. Mat. Mehk., Vol. 23, 1959.

23. Mroz, A.: Plastic Deformations of Annular Plates Under Dynamic Loads. Arch. Mech. Stos., Vol. 10, 1952.

24. Reissner, Eric: Rotationally Symmetric Problems in the Theory of Thin Elastic Shells. Third U.S. Nat. Congress of Applied Mechanics, 1958.

25. Onat, E. T.; and Haythornthwaite, R. M.: Load Carrying Capacity of Circular Plate at Large Deflection. Journal of Applied Mechanics. Vol. 23, 1956.

26. Munday, G.; and Newitt, D. M.: Deformations of Transversely Loaded Disks Under Dynamic Loads. Philosophical Transactions of The Royal Society of London - Series A - Vo. 256, Dec. 1963.

XV. VITA

The author was born in [redacted] on [redacted], [redacted] He attended public schools in Pittsburgh. He received a B.S. degree in Civil Engineering from Carnegie Institute of Technology in 1942. He attended Virginia Polytechnic Institute, where he received a M.S. degree in Applied Mechanics in 1956. He was elected to both the Sigma Xi and the Phi Kappa Phi fraternities. The first 2 years after his B.S. degree he spent in aircraft industry as a stress analyst. Since then the author has been engaged in research at the Langley Research Laboratories of the National Advisory Committee for Aeronautics which became the National Aeronautics and Space Administration. During this time he has carried out research in the areas of solids and dynamics authoring 28 technical papers and talks. For the past 12 years he has been responsible for the planning and direction of research in the area of structural mechanics and for the supervision of the research personnel. The author is also an instructor for the University of Virginia Extension at Hampton, Virginia, teaching graduate courses in Applied Mathematics.

XVI. APPENDIX A

SOLUTION OF GOVERNING EQUATIONS FOR BENDING OF PLATES UNDER UNIFORM LATERAL LOADS

The governing equation for Phase 1 in terms of the impulse I and the lateral load, N_θ, is (see eq. (93)

$$\rho_\tau = \frac{-(1 - N_\theta^2) - 2N_\theta\tau(1 + \rho)}{I(1 - \rho)(1 + 3\rho)} \tag{A-1}$$

The initial condition for this phase is that $\rho = 1$ for $\tau = 0$. This phase ends at $\tau = \tau_1$ when $\rho = 0$. Phase 2 motion then begins and continues until a final deformation is reached. The equation for the final deformation is given by equation (105) as

$$N_\theta A_F^2 + 2(1 - N_\theta^2)A_F = 2I + 4\tau_1(1 - N_\theta^2) + 4\tau_1^2 N_\theta \tag{A-2}$$

For the case of pure bending ($N_\theta = 0$) the solutions for equation (A-1) can be found in closed form as

$$1 - \rho - \rho^2 + \rho^3 = \frac{\tau}{1} \tag{A-3}$$

so that

$$\tau_1 = I \tag{A-4}$$

The solution of equation (A-2) for $N_\theta = 0$ is then

$$A_F = 3I \tag{A-5}$$

For the case of the maximum midplane force ($N_\theta = 1$) the solution of equation (A-1) is

$$\tau^2 = I\left[\frac{3}{2}(1 + \rho)^2 - 8(1 + \rho) + 4 \log \frac{(1 + \rho)}{2} + 10\right] \tag{A-6}$$

so that

$$\tau_1^2 = 0.7274I \tag{A-7}$$

The solution of equation (A-2) then can be written as

$$A_F^2 = 2I + 4\tau_1^2 \tag{A-8}$$

$$A_F = 2.21\sqrt{I} \tag{A-9}$$

For the general case equation (A-1) is solved numerically for τ_1 and the value of A_F calculated from equation (A-2). The flow diagrams, computer program, and numerical results follow.

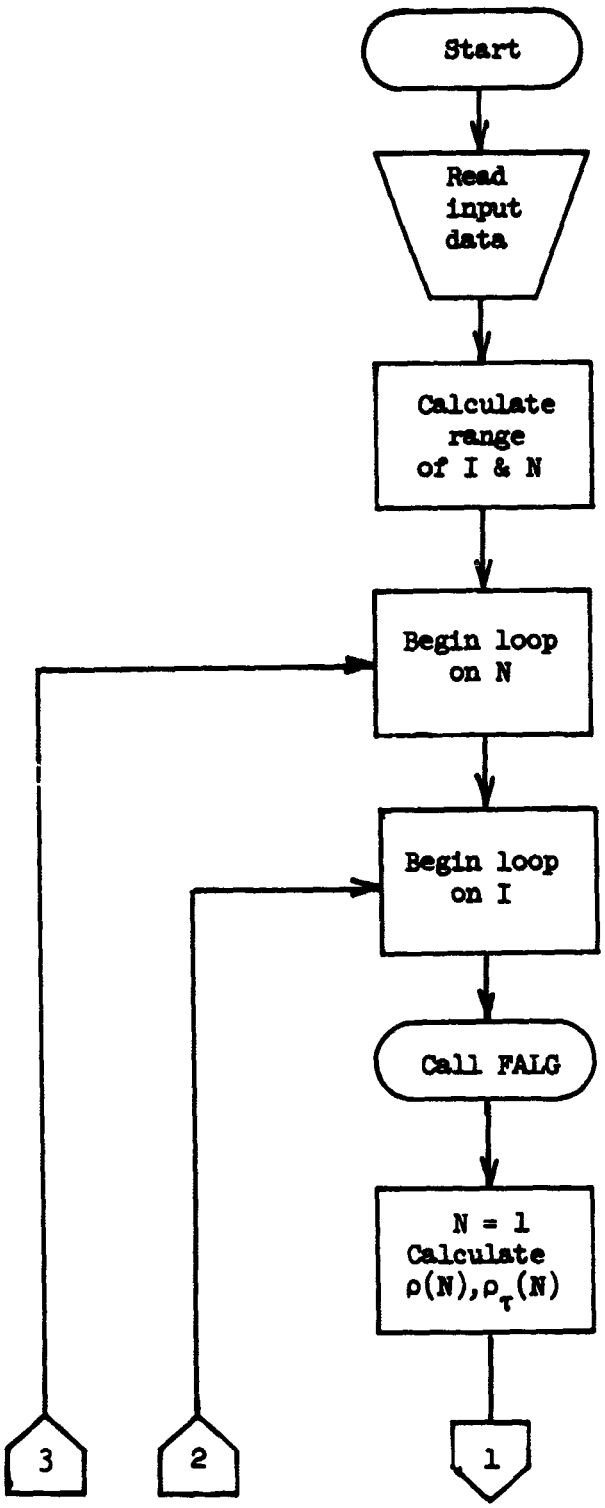
Start
Read input data
Calculate range of I & N
Begin loop on N
Begin loop on I
Call FALG
N = 1
Calculate
ρ(N), ρ_τ(N)
1
2
3

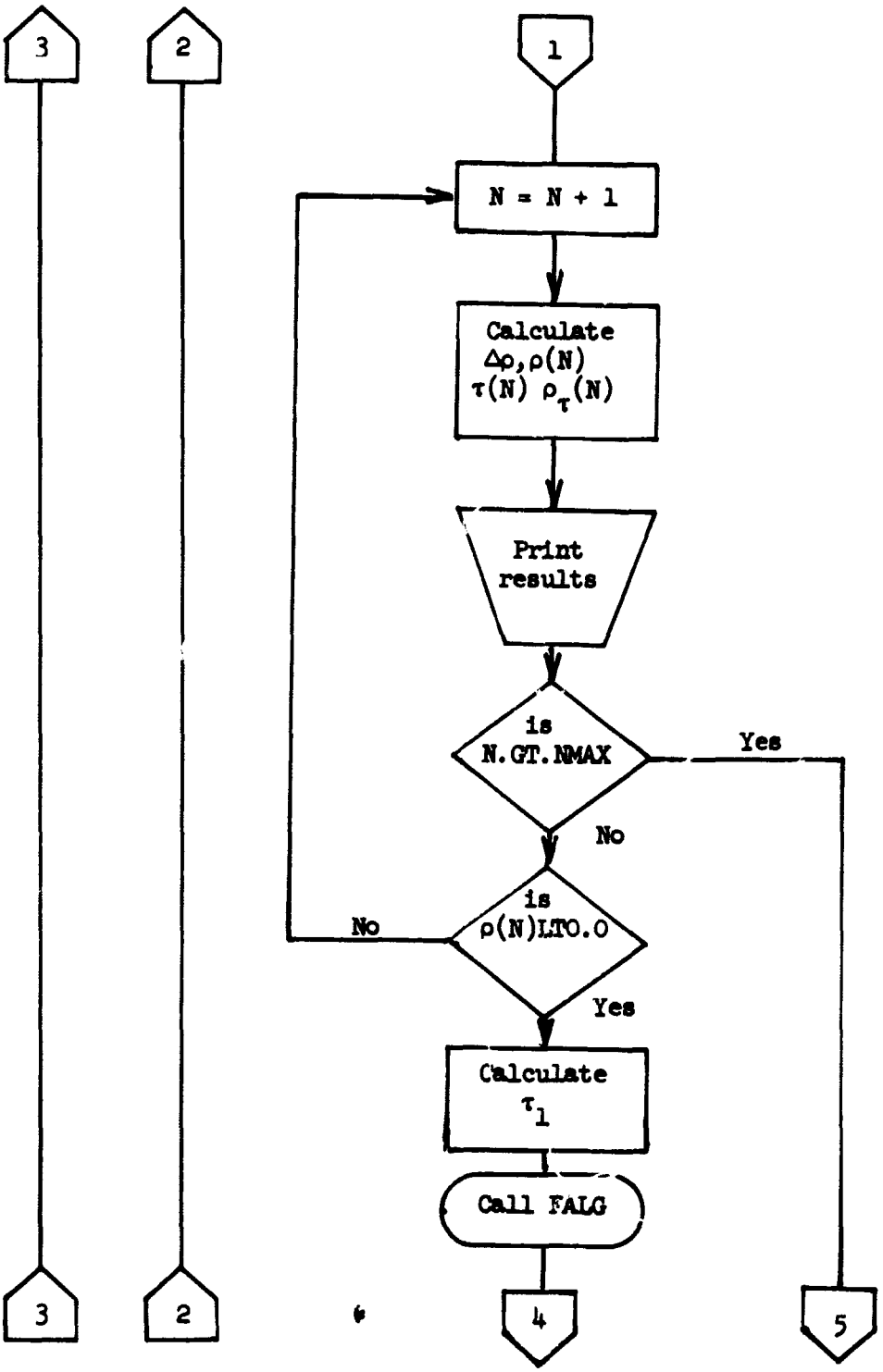
3
2
1
N = N + 1
Calculate
Δρ, ρ(N)
τ(N) ρ_τ(N)
Print
results
is
N.GT.NMAX
Yes
No
is
ρ(N)LTO.0
No
Yes
Calculate
τ_1
Call FALG
3
2
4
5

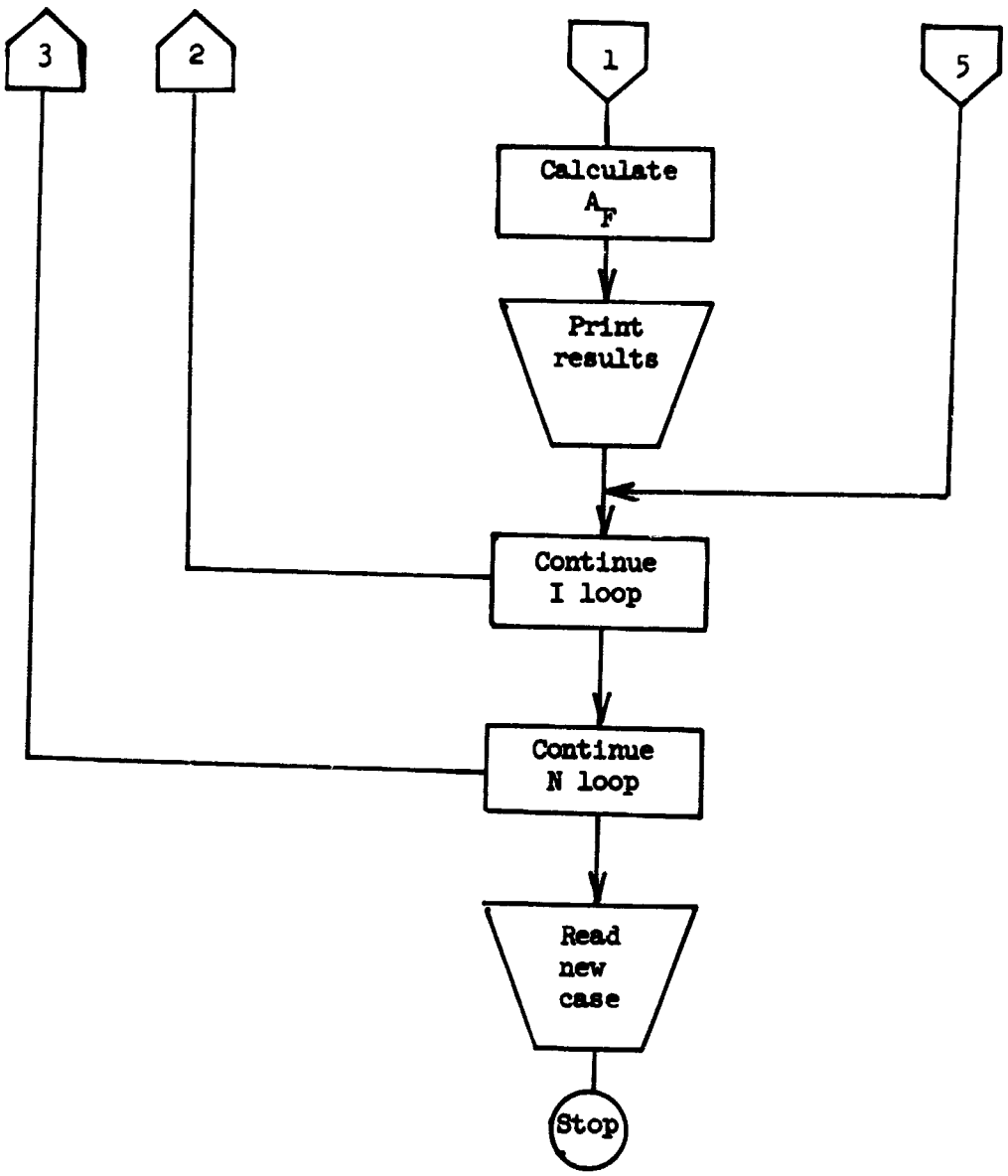
3
2
1
5
Calculate A_F
Print results
Continue I loop
Continue N loop
Read new case
Stop

FINAL DEFORMATION OF IMPULSIVELY LOADED PLATES

WITH MIDPLANE FORCES

I \ N_θ	0	0.1	0.2	0.3	0.4	0.6	0.8	1.0
0.4	1.20	---	1.10	---	1.09	1.15	1.25	1.40
0.8	2.40	---	2.01	---	1.88	1.85	1.90	1.98
1.2	3.60	---	2.80	---	2.52	2.41	2.39	2.42
1.6	4.80	---	3.51	---	3.07	2.88	2.81	2.80
4.0	12.00	8.19	6.83	6.06	5.56	4.96	4.63	4.42
6.0	18.00	10.03	8.95	7.83	7.11	6.24	5.74	5.41
8.0	24.00	13.50	10.77	9.33	8.43	7.32	6.68	6.25
10.0	30.00	15.71	12.38	10.67	9.58	8.27	7.50	6.99
12.0	36.00	17.73	13.84	11.87	10.63	9.13	8.25	7.66

```
SRD4924.                                                    LRC COMPUTER COMPLEX
JOB,1,0644,40000.          A1998,      2, MARTHA ROBINSON,RDV122, 1148 2011

      PROGRAM PLATES2 (INPUT,OUTPUT,TAPE21)
000003      DIMENSION COEFS(4),TAU(500),RHO(500),RHOT(500),RESULT(2)
000003      DIMENSION CO(3),IN(2),XM1(5),YM1(1),F(100),A(100),YM2(1),XM2(3)
000003      COMPLEX R(3),TEMP(8)
000003      COMPLEX TEM(6),AF(2)
000003      REAL NTHETA,IB,IE,INC
000003      NAMELIST/INPUT/DTAU,IB,IE,INC,MAXN,IPFN,IPLOT
000003      PRINT 1
000007    1 FORMAT(*1INFLUENCE OF UNIFORM MID-PLANE FORCES ON*/* PLASTIC BENDI
           1NG UNDER IMPULSIVE LOADING*/* ROBINSON-KRUSZEWSKI, SRD-A1998, FEBR
           2UARY 1968, RDV-122*)
000007 1000 CALL DAYTIM (RESULT)
000011      PRINT 2, RESULT
000017    2 FORMAT(*0DATE*A10,5X*TIME*A10)

      C INPUT DATA
      *   DTAU - TIME INCREMENT
      *   IB - INITIAL IMPULSE LOAD
      *   IE - FINAL IMPULSE LOAD
      *   INC - INCREMENT ON IMPULSE LOAD
      *   MAXN - MAXIMUM NUMBER OF ITERATIONS ON TIME, RADIUS AND VELOCITY
      *   IPFN - PRINT FREQUENCY
      *   IPLOT - PLOTTING INDICATOR

000017    3 READ INPUT
      CALCULATE TOTAL NUMBER OF IMPULSE LOADS AND SET INITIAL TIME
000022      TAU(1)=DTAU
000024      NN=ABS((IE-IB)/INC)+1.0
000033      DO 15 J=1,3,2
      CALCULATE THE NORMAL FORCE (NTHETA)
000034      NTHETA=.1*FLOAT(J)
000037      DO 14 I=1,NN
000041      IF (I.EQ.1) FI=IB
000044      IF (I.GT.1) FI=FI+INC
000050      F(I)=FI
000052      N=1
000053      IF (I.GT.1) PRINT 41
000061   41 FORMAT(*1*)
000061      PRINT 4, DTAU,FI,NTHETA
000073    4 FORMAT(///* DTAU=*F5.3,5X*I=*F5.1,5X*NTHETA=*F5.2//)
      CALCULATE INITIAL RHO VALUE
000073      COEFS(1)=1.0
```

```
000075          COEFS(2)=-1.0
000076          COEFS(3)=-1.0
000077          COEFS(4)=1.0-DTAU/FI
000102          CALL FALG (COEFS,3,0,R,TEMP,IERR)
000106          IF (IERR.NE.0) PRINT 5, IERR
000115        5 FORMAT(//10X*ERROR IN FALG SUBROUTINE*/)
000115          DO 6 M=1,3
000117          IF (AIMAG(R(M)).EQ.0.0) GO TO 8
000123        6 CONTINUE
000125          PRINT 7
000130        7 FORMAT(//10X*ALL ROOTS COMPLEX*/)
000130        8 RHO(1)=REAL(R(M))
          CALCULATE INITIAL RHOT VALUE
000133          RHOT(1)=-(2.*NTHETA*TAU(1)*(1.+RHO(1))+(1.-NTHETA**2))/(FI*(1.-
               1RHO(1))*(1.+3.*RHO(1)))
000156          PRINT 9, N,TAU(N),RHO(N),RHOT(N)
000172        9 FORMAT(4X*N*,11X*TAU*,17X*RHO*,17X*RHOT*//2XI3,3(5XE15.8))
          C BEGIN ITERATION ON RHO, TAU, RHOT
000172       10 N=N+1
000174          DELRHO=RHOT(N-1)*DTAU
000176          RHO(N)=RHO(N-1)+DELRHO
000200          TAU(N)=TAU(N-1)+DTAU
000202          RHOT(N)=-(2.*NTHETA*TAU(N)*(1.+RHO(N))+(1.-NTHETA**2))/
               1(FI*(1.-RHO(N))*(1.+3.*RHO(N)))

          C OUTPUT
          *    RHO -RADIUS OF HINGE CIRCLE
          *    RHOT - VELOCITY OF HINGE CIRCLE
          *    TAU - TIME OF HINGE CIRCLE

000227          IF (MOD(N,IPFN).EQ.0) PRINT 11, N,TAU(N),RHO(N),RHOT(N)
000247       11 FORMAT(2XI3,3(5XE15.8))
          C IF MAXIMUM NUMBER OF ITERATIONS IS REACHED OR RADIUS (RHO)
          C BECOMES NEGATIVE -- STOP
000247          IF (N.GT.MAXN) GO TO 12
000253          IF (RHO(N).LT.0.0) GO TO 20
000254          GO TO 10
000254       12 PRINT 13
000260       13 FORMAT(//10X*MAXIMUM N REACHED*//)
000260          GO TO 14
          C INTERPOLATE FOR TIME AT WHICH RHO=0
000261       20 TAUA=TAU(N-1)+RHO(N-1)*DTAU/(RHO(N-1)-RHO(N))
          CALCULATE AF
```

```
000270          CO(1)=NTHETA
000272          CO(2)=2.*(1.-NTHETA**2)
000276          CO (3)=-2.*FI-4.*TAUA*(1.-NTHETA**2)-4.*TAUA**2*NTHETA
000310          CALL FALG (CO,2,0,AF,TEM,IERR)
000314          IF (IERR.NE.0) PRINT 5, IERR
000323          DO 19 M=1,2
000325          IF ((REAL(AF(M)).GT.0.0).AND.(AIMAG(AF(M)).EQ.0.0)) GO TO 21
000340       19 CONTINUE
000342          PRINT 22
000345       22 FORMAT(5X*NO REAL POSITIVE ROOTS FOR AF*)
000345       21 A(I)=REAL(AF(M))
000352          PRINT 16, TAUA,AF
000362       16 FORMAT(/10X*TAUA=*E15.8,5X*AF(1)=*E15.8,E16.8,5X*AF(2)=*E15.8,E16.
                8)
            C PLOT RESULTS IF IPLOT=1
000362          IF (IPLOT.EQ.0) GO TO 14
000363          DATA IN/2HSRDMPR TUBKRUSZEWSKI/
000363          IT=6LTAPE21
000365          DATA XM1(1)/10HTAU        /
000365          DATA YM1(1)/10HRHO        /
000365          DATA XM1(2)/10H          I=/
000365          ENCODE (10,18,XM1(3)) FI
000374       18 FORMAT(F5.1)
000374          DATA XM1(4)/10H   NTHETA=/
000374          ENCODE (10,18,XM1(5)) NTHETA
000404          CALL DDIPLT (1,IN,N,TAU,RHO,0.,TAU(N),0.,1.,5,XM1,1,YM1,14,IT)
000425       14 CONTINUE
000430          IF (IPLOT.EQ.0) GO TO 15
000431          XM2(1)=10HI
000432          XM2(2)=10H   NTHETA=
000434          ENCODE (10,18,XM2(3)) NTHETA
000443          DATA YM2(1)/10HAF         /
000443          CALL DDIPLT (1,IN,NN,F ,A,IB,FI,0.,0.,3,XM2,1,YM2,14,IT)
000462       15 CONTINUE
000464          GO TO 1000
000465          STOP
000467          END
```

PROGRAM LENGTH INCLUDING I/O BUFFERS
012364

FUNCTION ASSIGNMENTS

STATEMENT ASSIGNMENTS

1	-	000530	2	-	000551	3	-	000017	4	-	000562
5	-	000573	7	-	000600	8	-	000130	9	-	000606
10	-	000172	11	-	000615	12	-	000254	13	-	000620
14	-	000425	15	-	000462	16	-	000634	18	-	000646
20	-	000261	21	-	000345	22	-	000627	41	-	000560
1000	-	000007									

BLOCK NAMES AND LENGTHS

VARIABLE ASSIGNMENTS

A	-	004036	AF	-	004250	CO	-	003657	COEFS	-	000715
DELRHO	-	004273	DTAU	-	004260	F	-	003672	FI	-	004267
I	-	004266	IB	-	004255	IE	-	004256	IERR	-	004271
IN	-	003662	INC	-	004257	IPFN	-	004262	IPLOT	-	004263
IT		004275	J	-	004265	M	-	004272	MAXN	-	004261
N	-	004270	NN	-	004264	NTHETA	-	004254	R	-	004206
RESULT	-	003655	RHO	-	001705	RHOT	-	002671	TAU	-	000721
TAUA	-	004274	TEM	-	004234	TEMP	-	004214	XM1	-	003664
XM2	-	004203	YM1	-	003671	YM2	-	004202			

START OF CONSTANTS
000520

START OF TEMPORARIES
000664

START OF INDIRECTS
000705

UNUSED COMPILER SPACE
002400

```
CORE MAP  19.16.56.  NORMAL                    CONTROL                                                    000100    023554    000000    000000
      ---TIME---LOAD MODE --L1--L2-----TYPE----------USER---++---CALL----------FWA LOAD--LWA LOAD--BLNK COMN--LENGTH--
      FWA LOADER  034454  FWA TABLES  034042
      -PROGRAM----ADDRESS-                  --LABELED---COMMON--
      PLATES2     000100
      SYSTEM      012464
      OUTPTC      013427
      DAYTIM      013564
      INPUTN      013615
      FALG        015061
      OUTPTS      016137
      DDIPLT      016444
      SION        021106
      GETBA       021732
      KODER       021751
      CPC         023144
      DISBCD      023373
      OUTPTB      023504
      --ENTRY-----ADDRESS-                                        REFERENCES
      PLATES2     000101
      Q8NTRY      012465          PLATES2     000102

      SYSTEM      012650          OUTPTC      013443
                                  INPUTN      014266    014276
                                  OUTPTS      016204
                                  KODER       022755
                                  OUTPTB      023545

      SYSTEMC     012615
      SYSTEMP     012643
      END         012537          PLATES2     000570
                                  FALG        015766
                                  DDIPLT      020442

      STOP        012570          PLATES2     000566

      EXIT        012562          INPUTN      015055

      ABNORML     012600          OUTPTC      013444
                                  INPUTN      014277
                                  OUTPTS      016205
                                  KODER       022756
                                  OUTPTB      023546

      OUTPTC      013431          PLATES2     000105    000106    000113    000115    000116    000157    000160
                                              000163    000165    000167    000171    000172    000211    000213
                                              000214    000226    000227    000260    000262    000264    000266
                                              000270    000271    000335    000337    000341    000343    000345
                                              000346    000356    000357    000417    000421    000422    000443
                                              000444    000454    000456    000460    000461
```

DAYTIM	013565	PLATES2	000110						
INPUTN	013616	PLATES2	000121						
FALG	015062	PLATES2	000205	000413					
OUTPTS	016141	PLATES2	000466	000470	000472	000473	000476	000500	000502
			000503	000535	000537	000541	000542		
		DDIPLT	016726	016730	016732	016733	016741	016743	016745
			016746	017342	017350	017356	017357	017440	017446
			017454	017455	017775	020003	020005	020006	020050
			020056	020060	020061	020311	020316	020320	020321
			020343	020350	020352	020353			
DDIPLT	016456	PLATES2	000511	000524	000546	000561			
RKSPRU.	021401								
FIZBAK.	021412								
POSFIL.	021450	OUTPTC	013461						
RDPRU.	021460								
DAT.	021502	OUTPTC	013464	013503	013517				
CIOI.	021346	OUTPTB	023532	023542	023535	023524			
OPEN.	021112	SYSTEM	013125						
		OUTPTC	013451						
		INPUTN	014160						
		OUTPTB	023536						
SIO.	021224	OUTPTC	013516						
		OUTPTB	023513						
GETBA	021732	OUTPTC	013437						
		INPUTN	013624						
		OUTPTB	023517						
KODER	021752	OUTPTC	013433	013467					
		OUTPTS	016144	016161					
CPC	023212	DAYTIM	013572	013576	013604				
CPC02	023256								
CPC03	023144								
CPC04	023163								
CPC999	023363								
DISBCD	023374	DDIPLT	016476	016531	016652	016712	017372	017466	017761
			020016	020034	020071	020327	020361		
OUTPTB	023506	DDIPLT	016506	016510	016511	020233	020243	020246	020263
			020273	020277	020376	020406	020411	020417	020427
			020432						

----UNSATISFIED EXTERNALS----- REFERENCES

INFLUENCE OF UNIFORM MID-PLANE FORCES ON
PLASTIC BENDING UNDER IMPULSIVE LOADING
ROBINSON-KRUSZEWSKI, SRD-A1998, FEBRUARY 1968, RDV-122

DATE 03/07/68 TIME 19.16.59.

DTAU= .010 I= 4.0 NTHETA= .10

N	TAU	RHO	RHOT
1	1.00000000E-02	9.64325054E-01	-1.78916444E+00
10	1.00000000E-01	8.80608619E-01	-5.90849807E-01
20	2.00000000E-01	8.29276011E-01	-4.46368495E-01
30	3.00000000E-01	7.87761936E-01	-3.84295030E-01
40	4.00000000E-01	7.51066650E-01	-3.48865004E-01
50	5.00000000E-01	7.17286100E-01	-3.25934887E-01
60	6.00000000E-01	6.85452608E-01	-3.10040640E-01
70	7.00000000E-01	6.54993972E-01	-2.98576451E-01
80	8.00000000E-01	6.25537314E-01	-2.90128280E-01
90	9.00000000E-01	5.96822057E-01	-2.83859153E-01
100	1.00000000E+00	5.68655887E-01	-2.79242542E-01
110	1.10000000E+00	5.40890256E-01	-2.75932814E-01
120	1.20000000E+00	5.13405705E-01	-2.73696801E-01
130	1.30000000E+00	4.86102527E-01	-2.72375324E-01
140	1.40000000E+00	4.58894475E-01	-2.71860561E-01
150	1.50000000E+00	4.31704306E-01	-2.72082392E-01
160	1.60000000E+00	4.04460408E-01	-2.73000154E-01
170	1.70000000E+00	3.77094097E-01	-2.74597925E-01
180	1.80000000E+00	3.49537255E-01	-2.76882340E-01
190	1.90000000E+00	3.21720101E-01	-2.79882483E-01
200	2.00000000E+00	2.93568869E-01	-2.83651821E-01
210	2.10000000E+00	2.65003209E-01	-2.88272380E-01
220	2.20000000E+00	2.35933030E-01	-2.93862061E-01
230	2.30000000E+00	2.06254428E-01	-3.00586357E-01
240	2.40000000E+00	1.75844160E-01	-3.08677131E-01
250	2.50000000E+00	1.44551752E-01	-3.18463206E-01
260	2.60000000E+00	1.12187711E-01	-3.30421985E-01
270	2.70000000E+00	7.85050049E-02	-3.45270934E-01
280	2.80000000E+00	4.31682146E-02	-3.64140668E-01
290	2.90000000E+00	5.69841823E-03	-3.88931569E-01

TAUA= 2.91461683E+00 AF(1)= 8.19444091E+00 0.

DTAU= .010 I= 6.0 NTHETA= .10

N	TAU	RHO	RHOT
1	1.00000000E-02	9.70920305E-01	-1.45591684E+00
10	1.00000000E-01	9.03063513E-01	-4.76542157E-01
20	2.00000000E-01	8.61766565E-01	-3.57967732E-01
30	3.00000000E-01	8.28546299E-01	-3.06689398E-01
40	4.00000000E-01	7.99320530E-01	-2.77152995E-01
50	5.00000000E-01	7.72536510E-01	-2.57796503E-01
60	6.00000000E-01	7.47407232E-01	-2.44148330E-01
70	7.00000000E-01	7.23469545E-01	-2.34071958E-01
80	8.00000000E-01	7.00423916E-01	-2.26404202E-01
90	9.00000000E-01	6.78063379E-01	-2.20452673E-01
100	1.00000000E+00	6.56237641E-01	-2.15777627E-01
110	1.10000000E+00	6.34833178E-01	-2.12085787E-01
120	1.20000000E+00	6.13761395E-01	-2.09174050E-01
130	1.30000000E+00	5.92951187E-01	-2.06897600E-01
140	1.40000000E+00	5.72344043E-01	-2.05150854E-01
150	1.50000000E+00	5.51890703E-01	-2.03855581E-01
160	1.60000000E+00	5.31548791E-01	-2.02953236E-01
170	1.70000000E+00	5.11281098E-01	-2.02399863E-01
180	1.80000000E+00	4.91054284E-01	-2.02162642E-01
190	1.90000000E+00	4.70837881E-01	-2.02217512E-01
200	2.00000000E+00	4.50603495E-01	-2.02547533E-01
210	2.10000000E+00	4.30324150E-01	-2.03141766E-01
220	2.20000000E+00	4.09973721E-01	-2.03994533E-01
230	2.30000000E+00	3.89526432E-01	-2.05104988E-01
240	2.40000000E+00	3.68956381E-01	-2.06476927E-01
250	2.50000000E+00	3.48237078E-01	-2.08118830E-01
260	2.60000000E+00	3.27340963E-01	-2.10044133E-01
270	2.70000000E+00	3.06238895E-01	-2.12271744E-01
280	2.80000000E+00	2.84899565E-01	-2.14826851E-01
290	2.90000000E+00	2.63288822E-01	-2.17742100E-01
300	3.00000000E+00	2.41368855E-01	-2.21059267E-01
310	3.10000000E+00	2.19097184E-01	-2.24831598E-01
320	3.20000000E+00	1.96425369E-01	-2.29127129E-01
330	3.30000000E+00	1.73297335E-01	-2.34033422E-01
340	3.40000000E+00	1.49647132E-01	-2.39664469E-01
350	3.50000000E+00	1.25395857E-01	-2.46171003E-01
360	3.60000000E+00	1.00447334E-01	-2.53756336E-01
370	3.70000000E+00	7.46818134E-02	-2.62701583E-01
380	3.80000000E+00	4.79464922E-02	-2.73407601E-01
390	3.90000000E+00	2.00405872E-02	-2.86468443E-01

TAUA= 3.96887600E+00 AF(1)= 1.10328784E+01 0.

DTAU= .010 I= 8.0 NTHETA= .10

N	TAU	RHO	RHOT
1	1.00000000E-02	9.74841259E-01	-1.25834155E+00
10	1.00000000E-01	9.16326172E-01	-4.09768396E-01
20	2.00000000E-01	8.80865910E-01	-3.06837213E-01
30	3.00000000E-01	8.52424119E-01	-2.62193667E-01
40	4.00000000E-01	8.27465145E-01	-2.36378952E-01
50	5.00000000E-01	8.04644527E-01	-2.19375231E-01
60	6.00000000E-01	7.83281360E-01	-2.07306725E-01
70	7.00000000E-01	7.62975496E-01	-1.98320631E-01
80	8.00000000E-01	7.43468716E-01	-1.91407420E-01
90	9.00000000E-01	7.24583180E-01	-1.85965423E-01
100	1.00000000E+00	7.06190328E-01	-1.81611781E-01
110	1.10000000E+00	6.88193650E-01	-1.78090411E-01
120	1.20000000E+00	6.70518442E-01	-1.75223193E-01
130	1.30000000E+00	6.53105376E-01	-1.72882294E-01
140	1.40000000E+00	6.35906281E-01	-1.70973617E-01
150	1.50000000E+00	6.18881280E-01	-1.69426458E-01
160	1.60000000E+00	6.01996768E-01	-1.68186795E-01
170	1.70000000E+00	5.85223962E-01	-1.67212815E-01
180	1.80000000E+00	5.68537832E-01	-1.66471834E-01
190	1.90000000E+00	5.51916284E-01	-1.65938140E-01
200	2.00000000E+00	5.35339542E-01	-1.65591453E-01
210	2.10000000E+00	5.18789656E-01	-1.65415811E-01
220	2.20000000E+00	5.02250107E-01	-1.65398746E-01
230	2.30000000E+00	4.85705492E-01	-1.65530685E-01
240	2.40000000E+00	4.69141248E-01	-1.65804499E-01
250	2.50000000E+00	4.52543431E-01	-1.66215180E-01
260	2.60000000E+00	4.35898509E-01	-1.66759608E-01
270	2.70000000E+00	4.19193184E-01	-1.67436390E-01
280	2.80000000E+00	4.02414222E-01	-1.68245765E-01
290	2.90000000E+00	3.85548295E-01	-1.69189566E-01
300	3.00000000E+00	3.68581820E-01	-1.70271225E-01
310	3.10000000E+00	3.51500794E-01	-1.71495841E-01
320	3.20000000E+00	3.34290629E-01	-1.72870294E-01
330	3.30000000E+00	3.16935960E-01	-1.74403421E-01
340	3.40000000E+00	2.99420442E-01	-1.76106262E-01
350	3.50000000E+00	2.81726516E-01	-1.77992394E-01
360	3.60000000E+00	2.63835133E-01	-1.80078373E-01
370	3.70000000E+00	2.45725437E-01	-1.82384310E-01
380	3.80000000E+00	2.27374371E-01	-1.84934637E-01
390	3.90000000E+00	2.08756207E-01	-1.87759118E-01
400	4.00000000E+00	1.89841949E-01	-1.90894202E-01
410	4.10000000E+00	1.70598595E-01	-1.94384851E-01
420	4.20000000E+00	1.50988172E-01	-1.98287061E-01
430	4.30000000E+00	1.30966487E-01	-2.02671374E-01
440	4.40000000E+00	1.10481461E-01	-2.07627906E-01
450	4.50000000E+00	8.94708677E-02	-2.13273698E-01
460	4.60000000E+00	6.78591765E-02	-2.19763777E-01
470	4.70000000E+00	4.55530486E-02	-2.27308355E-01
480	4.80000000E+00	2.24346799E-02	-2.36200640E-01
490	4.90000000E+00	-1.64840441E-03	-2.46863946E-01

TAUA= 4.89329104E+00 AF(1)= 1.35000324E+01 0.

DTAU= .010 I= 10.0 NTHETA= .10

N	TAU	RHO	RHOT
1	1.00000000E-02	9.77512541E-01	-1.12396677E+00
10	1.00000000E-01	9.25325755E-01	-3.64759686E-01
20	2.00000000E-01	8.93789604E-01	-2.72570989E-01
30	3.00000000E-01	8.68543162E-01	-2.32520735E-01
40	4.00000000E-01	8.46423763E-01	-2.09312512E-01
50	5.00000000E-01	8.26228895E-01	-1.93983812E-01
60	6.00000000E-01	8.07349736E-01	-1.83066526E-01
70	7.00000000E-01	7.894 3712E-01	-1.74902351E-01
80	8.00000000E-01	7.72235296E-01	-1.68587443E-01
90	9.00000000E-01	7.55610935E-01	-1.63582866E-01
100	1.00000000E+00	7.39441233E-01	-1.59545450E-01
110	1.10000000E+00	7.23640529E-01	-1.56245431E-01
120	1.20000000E+00	7.08142740E-01	-1.53522768E-01
130	1.30000000E+00	6.92895607E-01	-1.51262375E-01
140	1.40000000E+00	6.77856930E-01	-1.49379298E-01
150	1.50000000E+00	6.62992005E-01	-1.47809448E-01
160	1.60000000E+00	6.48271829E-01	-1.46503596E-01
170	1.70000000E+00	6.33671807E-01	-1.45423346E-01
180	1.80000000E+00	6.19170799E-01	-1.44538372E-01
190	1.90000000E+00	6.04750412E-01	-1.43824476E-01
200	2.00000000E+00	5.90394448E-01	-1.43262190E-01
210	2.10000000E+00	5.76088482E-01	-1.42835757E-01
220	2.20000000E+00	5.61819528E-01	-1.42532377E-01
230	2.30000000E+00	5.47575765E-01	-1.42341639E-01
240	2.40000000E+00	5.33346325E-01	-1.42255089E-01
250	2.50000000E+00	5.19121108E-01	-1.42265905E-01
260	2.60000000E+00	5.04890634E-01	-1.42368641E-01
270	2.70000000E+00	4.90645910E-01	-1.42559032E-01
280	2.80000000E+00	4.76378326E-01	-1.42833847E-01
290	2.90000000E+00	4.62079550E-01	-1.43190771E-01
300	3.00000000E+00	4.47741444E-01	-1.43628325E-01
310	3.10000000E+00	4.33355983E-01	-1.44145803E-01
320	3.20000000E+00	4.18915180E-01	-1.44743235E-01
330	3.30000000E+00	4.04411012E-01	-1.45421362E-01
340	3.40000000E+00	3.89835349E-01	-1.46181636E-01
350	3.50000000E+00	3.75179885E-01	-1.47026235E-01
360	3.60000000E+00	3.60436062E-01	-1.47958086E-01
370	3.70000000E+00	3.45594994E-01	-1.48980920E-01
380	3.80000000E+00	3.30647383E-01	-1.50099337E-01
390	3.90000000E+00	3.15583429E-01	-1.51318898E-01
400	4.00000000E+00	3.00392729E-01	-1.52646240E-01
410	4.10000000E+00	2.85064160E-01	-1.54089229E-01
420	4.20000000E+00	2.69585754E-01	-1.55657145E-01
430	4.30000000E+00	2.53944540E-01	-1.57360928E-01
440	4.40000000E+00	2.38126370E-01	-1.59213471E-01
450	4.50000000E+00	2.22115701E-01	-1.61230013E-01
460	4.60000000E+00	2.05895347E-01	-1.63428623E-01
470	4.70000000E+00	1.89446164E-01	-1.65830838E-01
480	4.80000000E+00	1.72746669E-01	-1.68462488E-01
490	4.90000000E+00	1.55772562E-01	-1.71354782E-01
500	5.00000000E+00	1.38496132E-01	-1.74545767E-01
510	5.10000000E+00	1.20885483E-01	-1.78082300E-01
520	5.20000000E+00	1.02903542E-01	-1.82022784E-01
530	5.30000000E+00	8.45067381E-02	-1.86441014E-01
540	5.40000000E+00	6.56432367E-02	-1.91431731E-01
550	5.50000000E+00	4.62504968E-02	-1.97118842E-01
560	5.60000000E+00	2.62518380E-02	-2.03667968E-01
570	5.70000000E+00	5.55145305E-03	-2.11306288E-01

TAUA= 5.72618326E+00 AF(1)= 1.57110046E+01 0.

DTAU= .010 I= 12.0 NTHETA= .10

N	TAU	RHO	RHOT
1	1.00000000E-02	9.79482068E-01	-1.02501141E+00
10	1.00000000E-01	9.31942759E-01	-3.31818643E-01
20	2.00000000E-01	9.03273630E-01	-2.47589073E-01
30	3.00000000E-01	8.80353384E-01	-2.10957800E-01
40	4.00000000E-01	8.60294723E-01	-1.89702092E-01
50	5.00000000E-01	8.41999875E-01	-1.75639072E-01
60	6.00000000E-01	8.24913135E-01	-1.65601972E-01
70	7.00000000E-01	8.08708225E-01	-1.58076381E-01
80	8.00000000E-01	7.93174896E-01	-1.52236742E-01
90	9.00000000E-01	7.78168650E-01	-1.47590687E-01
100	1.00000000E+00	7.63585329E-01	-1.43824595E-01
110	1.10000000E+00	7.49347046E-01	-1.40728393E-01
120	1.20000000E+00	7.35393813E-01	-1.38155668E-01
130	1.30000000E+00	7.21678299E-01	-1.36001040E-01
140	1.40000000E+00	7.08162383E-01	-1.34186629E-01
150	1.50000000E+00	6.94814824E-01	-1.32653591E-01
160	1.60000000E+00	6.81609617E-01	-1.31356827E-01
170	1.70000000E+00	6.68524819E-01	-1.30260306E-01
180	1.80000000E+00	6.55541681E-01	-1.29336538E-01
190	1.90000000E+00	6.42644003E-01	-1.28562795E-01
200	2.00000000E+00	6.29817633E-01	-1.27920829E-01
210	2.10000000E+00	6.17050089E-01	-1.27395742E-01
220	2.20000000E+00	6.04330254E-01	-1.26975287E-01
230	2.30000000E+00	5.91648135E-01	-1.26649347E-01
240	2.40000000E+00	5.78994672E-01	-1.26409530E-01
250	2.50000000E+00	5.66361576E-01	-1.26248869E-01
260	2.60000000E+00	5.53741202E-01	-1.26161575E-01
270	2.70000000E+00	5.41126435E-01	-1.26142851E-01
280	2.80000000E+00	5.28510604E-01	-1.26188745E-01
290	2.90000000E+00	5.15887396E-01	-1.26296033E-01
300	3.00000000E+00	5.03250795E-01	-1.26462121E-01
310	3.10000000E+00	4.90595015E-01	-1.26684978E-01
320	3.20000000E+00	4.77914454E-01	-1.26963074E-01
330	3.30000000E+00	4.65203638E-01	-1.27295335E-01
340	3.40000000E+00	4.52457185E-01	-1.27681110E-01
350	3.50000000E+00	4.39669756E-01	-1.28120150E-01
360	3.60000000E+00	4.26836024E-01	-1.28612584E-01
370	3.70000000E+00	4.13950628E-01	-1.29158918E-01
380	3.80000000E+00	4.01008143E-01	-1.29760029E-01
390	3.90000000E+00	3.88003037E-01	-1.30417171E-01
400	4.00000000E+00	3.74929637E-01	-1.31131988E-01
410	4.10000000E+00	3.61782086E-01	-1.31906533E-01
420	4.20000000E+00	3.48554303E-01	-1.32743297E-01
430	4.30000000E+00	3.35239937E-01	-1.33645240E-01
440	4.40000000E+00	3.21832318E-01	-1.34615841E-01
450	4.50000000E+00	3.08324403E-01	-1.35659155E-01
460	4.60000000E+00	2.94708715E-01	-1.36779878E-01
470	4.70000000E+00	2.80977275E-01	-1.37983442E-01
480	4.80000000E+00	2.67121524E-01	-1.39276112E-01
490	4.90000000E+00	2.53132235E-01	-1.40665123E-01
500	5.00000000E+00	2.38999407E-01	-1.42158839E-01
510	5.10000000E+00	2.24712146E-01	-1.43766947E-01
520	5.20000000E+00	2.10258519E-01	-1.45500711E-01
530	5.30000000E+00	1.95625388E-01	-1.47373279E-01
540	5.40000000E+00	1.80798197E-01	-1.49400073E-01
550	5.50000000E+00	1.65760731E-01	-1.51599290E-01
560	5.60000000E+00	1.50494805E-01	-1.53992545E-01
570	5.70000000E+00	1.34979892E-01	-1.56605712E-01
580	5.80000000E+00	1.19192644E-01	-1.59470031E-01
590	5.90000000E+00	1.03106296E-01	-1.62623596E-01
600	6.00000000E+00	8.66898911E-02	-1.66113382E-01
610	6.10000000E+00	6.99072796E-02	-1.69998059E-01
620	6.20000000E+00	5.27157759E-02	-1.74351978E-01
630	6.30000000E+00	3.50643513E-02	-1.79270963E-01
640	6.40000000E+00	1.68911267E-02	-1.84880937E-01
650	6.50000000E+00	-1.88018629E-03	-1.91351228E-01

TAUA= 6.49013851E+00 AF(1)= 1.77316318E+01 0.

DTAU= .010 I= 4.0 NTHETA= .30

N	TAU	RHO	RHOT
1	1.00000000E-02	9.64325054E-01	-1.65930084E+00
10	1.00000000E-01	8.83079455E-01	-5.99399137E-01
20	2.00000000E-01	8.29850692E-01	-4.75617618E-01
30	3.00000000E-01	7.84796684E-01	-4.26411059E-01
40	4.00000000E-01	7.43433701E-01	-4.00713649E-01
50	5.00000000E-01	7.04096361E-01	-3.85810289E-01
60	6.00000000E-01	6.65954302E-01	-3.76899482E-01
70	7.00000000E-01	6.28521061E-01	-3.71755821E-01
80	8.00000000E-01	5.91477981E-01	-3.69217355E-01
90	9.00000000E-01	5.54596757E-01	-3.68634642E-01
100	1.00000000E+00	5.17700254E-01	-3.69636088E-01
110	1.10000000E+00	4.80640346E-01	-3.72017456E-01
120	1.20000000E+00	4.43283950E-01	-3.75687237E-01
130	1.30000000E+00	4.05503099E-01	-3.80640581E-01
140	1.40000000E+00	3.67166796E-01	-3.86950393E-01
150	1.50000000E+00	3.28133154E-01	-3.94771489E-01
160	1.60000000E+00	2.88240532E-01	-4.04358260E-01
170	1.70000000E+00	2.47296147E-01	-4.16100709E-01
180	1.80000000E+00	2.05059849E-01	-4.30590822E-01
190	1.90000000E+00	1.61219031E-01	-4.48745583E-01
200	2.00000000E+00	1.15346693E-01	-4.72047373E-01
210	2.10000000E+00	6.68252393E-02	-5.03055674E-01
220	2.20000000E+00	1.46928062E-02	-5.46639318E-01

TAUA= 2.22664656E+00 AF(1)= 6.06151369E+00 0.

DTAU= .010 I= 6.0 NTHETA= .30

N	TAU	RHO	RHOT
1	1.00000000E-02	9.70920305E-01	-1.35028152E+00
10	1.00000000E-01	9.05042592E-01	-4.83920921E-01
20	2.00000000E-01	8.62162169E-01	-3.82135256E-01
30	3.00000000E-01	8.26030295E-01	-3.41189167E-01
40	4.00000000E-01	7.92992244E-01	-3.19363167E-01
50	5.00000000E-01	7.61696653E-01	-3.06255518E-01
60	6.00000000E-01	7.31475909E-01	-2.97926021E-01
70	7.00000000E-01	7.01945258E-01	-2.92535572E-01
80	8.00000000E-01	6.72859333E-01	-2.89109391E-01
90	9.00000000E-01	6.44049382E-01	-2.87085491E-01
100	1.00000000E+00	6.15391936E-01	-2.86121024E-01
110	1.10000000E+00	5.86791596E-01	-2.85999355E-01
120	1.20000000E+00	5.58170838E-01	-2.86581688E-01
130	1.30000000E+00	5.29463555E-01	-2.87780342E-01
140	1.40000000E+00	5.00610699E-01	-2.89543450E-01
150	1.50000000E+00	4.71557143E-01	-2.91846087E-01
160	1.60000000E+00	4.42249235E-01	-2.94685360E-01
170	1.70000000E+00	4.12632710E-01	-2.98078142E-01
180	1.80000000E+00	3.82650744E-01	-3.02060868E-01
190	1.90000000E+00	3.52241934E-01	-3.06691195E-01
200	2.00000000E+00	3.21338031E-01	-3.12051730E-01
210	2.10000000E+00	2.89861181E-01	-3.18256398E-01
220	2.20000000E+00	2.57720374E-01	-3.25460577E-01
230	2.30000000E+00	2.24806645E-01	-3.33877088E-01
240	2.40000000E+00	1.90986271E-01	-3.43801812E-01
250	2.50000000E+00	1.56090749E-01	-3.55656067E-01
260	2.60000000E+00	1.19901286E-01	-3.70059969E-01
270	2.70000000E+00	8.21235722E-02	-3.87967205E-01
280	2.80000000E+00	4.23439742E-02	-4.10932380E-01
290	2.90000000E+00	-5.29385935E-05	-4.41698084E-01

TAUA= 2.89987918E+00 AF(1)= 7.83052918E+00 0.

DTAU= .010 I= 8.0 NTHETA= .30

N	TAU	RHO	RHOT
1	1.00000000E-02	9.74841259E-01	-1.16706206E+00
10	1.00000000E-01	9.18020904E-01	-4.16354678E-01
20	2.00000000E-01	8.41172035E-01	-3.27906352E-01
30	3.00000000E-01	8.50198230E-01	-2.92129600E-01
40	4.00000000E-01	8.21936426E-01	-2.72887229E-01
50	5.00000000E-01	7.95218984E-01	-2.61165355E-01
60	6.00000000E-01	7.69470951E-01	-2.53546516E-01
70	7.00000000E-01	7.44362849E-01	-2.48432740E-01
80	8.00000000E-01	7.19686461E-01	-2.44974077E-01
90	9.00000000E-01	6.95300531E-01	-2.42677274E-01
100	1.00000000E+00	6.71103719E-01	-2.41237796E-01
110	1.10000000E+00	6.47019816E-01	-2.40459059E-01
120	1.20000000E+00	6.22989064E-01	-2.40210177E-01
130	1.30000000E+00	5.93962751E-01	-2.40402386E-01
140	1.40000000E+00	5.74899682E-01	-2.40975216E-01
150	1.50000000E+00	5.50763761E-01	-2.41888063E-01
160	1.60000000E+00	5.26522261E-01	-2.43114938E-01
170	1.70000000E+00	5.02144521E-01	-2.44641152E-01
180	1.80000000E+00	4.77600925E-01	-2.46461266E-01
190	1.90000000E+00	4.52862026E-01	-2.48577913E-01
200	2.00000000E+00	4.27897776E-01	-2.51001265E-01
210	2.10000000E+00	4.02676769E-01	-2.53749043E-01
220	2.20000000E+00	3.77165474E-01	-2.56847033E-01
230	2.30000000E+00	3.51327379E-01	-2.60330135E-01
240	2.40000000E+00	3.25122014E-01	-2.64244060E-01
250	2.50000000E+00	2.98503763E-01	-2.68647859E-01
260	2.60000000E+00	2.71420375E-01	-2.73617609E-01
270	2.70000000E+00	2.43811036E-01	-2.79251781E-01
280	2.80000000E+00	2.15603800E-01	-2.85679159E-01
290	2.90000000E+00	1.86712063E-01	-2.93070750E-01
300	3.00000000E+00	1.57029579E-01	-3.01658248E-01
310	3.10000000E+00	1.26423176E-01	-3.11763669E-01
320	3.20000000E+00	9.47217110E-02	-3.23849055E-01
330	3.30000000E+00	6.16985354E-02	-3.38604492E-01
340	3.40000000E+00	2.70421116E-02	-3.57114905E-01

TAUA= 3.47422878E+00 AF(1)= 9.33474990E+00 0.

DTAU= .010 I= 10.0 NTHETA= .30

N	TAU	RHO	RHOT
1	1.00000000E-02	9.77512541E-01	-1.04244728E+00
10	1.00000000E-01	9.26830068E-01	-3.70767278E-01
20	2.00000000E-01	8.94041693E-01	-2.91498125E-01
30	3.00000000E-01	8.66524316E-01	-2.59331921E-01
40	4.00000000E-01	8.41449748E-01	-2.41943575E-01
50	5.00000000E-01	8.17774825E-01	-2.31268482E-01
60	6.00000000E-01	7.94986712E-01	-2.24247963E-01
70	7.00000000E-01	7.72792333E-01	-2.19450800E-01
80	8.00000000E-01	7.51007267E-01	-2.16114732E-01
90	9.00000000E-01	7.29507198E-01	-2.13796342E-01
100	1.00000000E+00	7.08203747E-01	-2.12220736E-01
110	1.10000000E+00	6.87031280E-01	-2.11209229E-01
120	1.20000000E+00	6.65939179E-01	-2.10641477E-01
130	1.30000000E+00	6.44887057E-01	-2.10434296E-01
140	1.40000000E+00	6.23841657E-01	-2.10529190E-01
150	1.50000000E+00	6.02774754E-01	-2.10884682E-01
160	1.60000000E+00	5.81661694E-01	-2.11471452E-01
170	1.70000000E+00	5.60480327E-01	-2.12269169E-01
180	1.80000000E+00	5.39210214E-01	-2.13264392E-01
190	1.90000000E+00	5.17832003E-01	-2.14449183E-01
200	2.00000000E+00	4.96326923E-01	-2.15820193E-01
210	2.10000000E+00	4.74676352E-01	-2.17378095E-01
220	2.20000000E+00	4.52861435E-01	-2.19127276E-01
230	2.30000000E+00	4.30862713E-01	-2.21075744E-01
240	2.40000000E+00	4.08659761E-01	-2.23235222E-01
250	2.50000000E+00	3.86230806E-01	-2.25621438E-01
260	2.60000000E+00	3.63552304E-01	-2.28254607E-01
270	2.70000000E+00	3.40598460E-01	-2.31160165E-01
280	2.80000000E+00	3.17340668E-01	-2.34369797E-01
290	2.90000000E+00	2.93746820E-01	-2.37922866E-01
300	3.00000000E+00	2.69780454E-01	-2.41868384E-01
310	3.10000000E+00	2.45399681E-01	-2.46267757E-01
320	3.20000000E+00	2.20555772E-01	-2.51198646E-01
330	3.30000000E+00	1.95191310E-01	-2.56760497E-01
340	3.40000000E+00	1.69237668E-01	-2.63082652E-01
350	3.50000000E+00	1.42611512E-01	-2.70336557E-01
360	3.60000000E+00	1.15209812E-01	-2.78754743E-01
370	3.70000000E+00	8.69024738E-02	-2.88661502E-01
380	3.80000000E+00	5.75210670E-02	-3.00524804E-01
390	3.90000000E+00	2.68407346E-02	-3.15049329E-01

TAUA= 3.98350950E+00 AF(1)= 1.06660980E+01 0.

DTAU= .010 I= 12.0 NTHETA= .30

N	TAU	RHO	RHOT
1	1.00000000E-02	9.79482068E-01	-9.50677410E-01
10	1.00000000E-01	9.33308355E-01	-3.37379753E-01
20	2.00000000E-01	9.03489370E-01	-2.64921333E-01
30	3.00000000E-01	8.78491927E-01	-2.35457041E-01
40	4.00000000E-01	8.55734784E-01	-2.19477010E-01
50	5.00000000E-01	8.34266320E-01	-2.09618146E-01
60	6.00000000E-01	8.13619147E-01	-2.03087304E-01
70	7.00000000E-01	7.93526577E-01	-1.98577062E-01
80	8.00000000E-01	7.73821202E-01	-1.95390653E-01
90	9.00000000E-01	7.54390578E-01	-1.93122307E-01
100	1.00000000E+00	7.35155168E-01	-1.91520002E-01
110	1.10000000E+00	7.16056312E-01	-1.90419417E-01
120	1.20000000E+00	6.97049185E-01	-1.89709340E-01
130	1.30000000E+00	6.78098445E-01	-1.89312306E-01
140	1.40000000E+00	6.59175420E-01	-1.89173175E-01
150	1.50000000E+00	6.40256216E-01	-1.89252100E-01
160	1.60000000E+00	6.21320411E-01	-1.89520038E-01
170	1.70000000E+00	6.02350111E-01	-1.89955810E-01
180	1.80000000E+00	5.83329264E-01	-1.90544120E-01
190	1.90000000E+00	5.64243133E-01	-1.91274204E-01
200	2.00000000E+00	5.45077891E-01	-1.92138902E-01
210	2.10000000E+00	5.25820286E-01	-1.93134015E-01
220	2.20000000E+00	5.06457372E-01	-1.94257872E-01
230	2.30000000E+00	4.86976267E-01	-1.95511045E-01
240	2.40000000E+00	4.67363936E-01	-1.96896191E-01
250	2.50000000E+00	4.47606988E-01	-1.98417984E-01
260	2.60000000E+00	4.27691473E-01	-2.00083141E-01
270	2.70000000E+00	4.07602675E-01	-2.01900529E-01
280	2.80000000E+00	3.87324886E-01	-2.03881360E-01
290	2.90000000E+00	3.66841162E-01	-2.06039482E-01
300	3.00000000E+00	3.46133041E-01	-2.08391785E-01
310	3.10000000E+00	3.25180215E-01	-2.10958752E-01
320	3.20000000E+00	3.03960141E-01	-2.13765192E-01
330	3.30000000E+00	2.82447565E-01	-2.16841217E-01
340	3.40000000E+00	2.60613937E-01	-2.20223552E-01
350	3.50000000E+00	2.38426674E-01	-2.23957302E-01
360	3.60000000E+00	2.15848221E-01	-2.28098377E-01
370	3.70000000E+00	1.92834824E-01	-2.32716863E-01
380	3.80000000E+00	1.69334917E-01	-2.37901814E-01
390	3.90000000E+00	1.45286929E-01	-2.43768207E-01
400	4.00000000E+00	1.20616263E-01	-2.50467328E-01
410	4.10000000E+00	9.52310032E-02	-2.58202753E-01
420	4.20000000E+00	6.90156399E-02	-2.67255892E-01
430	4.30000000E+00	4.18215542E-02	-2.78028639E-01
440	4.40000000E+00	1.34519527E-02	-2.91118574E-01

TAUA= 4.44577991E+00 AF(1)= 1.18731443E+01 0.

DATE 03/07/68 TIME 19.17.02.

```
03/07/68  LRC SCOPE 3.0       6600B--65K  02/16/68
19.16.44.SRD4924.
19.16.44.                          LRC COMPUTER COMPLEX
19.16.45.JOB,1,0644,40000.              A1998,      2,
19.16.45. MARTHA ROBINSON,RDV122, 1148 2011
19.16.45.RUN(S)
19.16.49.SETINDF.
19.16.50.LGO.
19.17.02.EOF ENCOUNTERED BY NAMELIST
19.17.02.EXIT
19.17.02.SPPRINT(OUTPUT,3)
19.17.03.CPU    002.206238 SEC.
19.17.03.PPU    011.701952 SEC.
  SRD4924. PRINT-PP 00806 LINES
```

XVII. APPENDIX B

SOLUTION OF GOVERNING EQUATIONS FOR PHASE 1

The governing equation for Phase 1 can be written as (see eq. (109)

$$\rho_{\tau} = - \frac{1 + (2\rho + 1)\tau^2}{I(1 - \rho)(1 + 3\rho)} \tag{B-1}$$

The initial conditions for this phase are that $\rho = 1$ at $\tau = 0$. The motion is terminated if either the hinge circle becomes zero or the time, τ, becomes one. The equation was solved numerically. The flow diagram, computer program, and numerical results follow.

In order to avoid the singular point at $\rho = 1$, the motion of the hinge during the first time interval ($\Delta\tau = 0.01$) was calculated from the bending case. This procedure is valid as at $\tau = 0$ when $\rho = 1.0$. The differential equation is exactly that obtained for the pure bending solution.

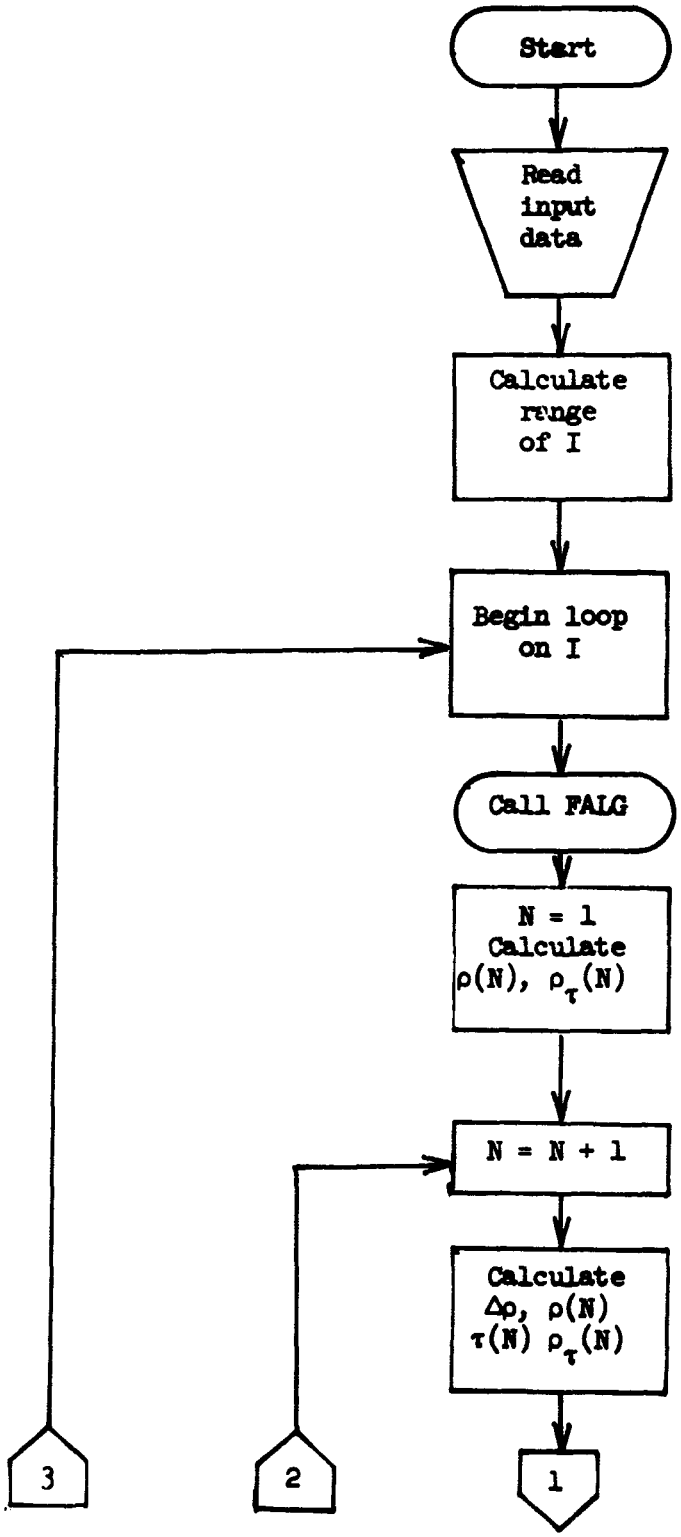
Start
Read input data
Calculate range of I
Begin loop on I
Call FALG
N = 1
Calculate ρ(N), ρτ(N)
N = N + 1
Calculate Δρ, ρ(N) τ(N) ρτ(N)
1
2
3

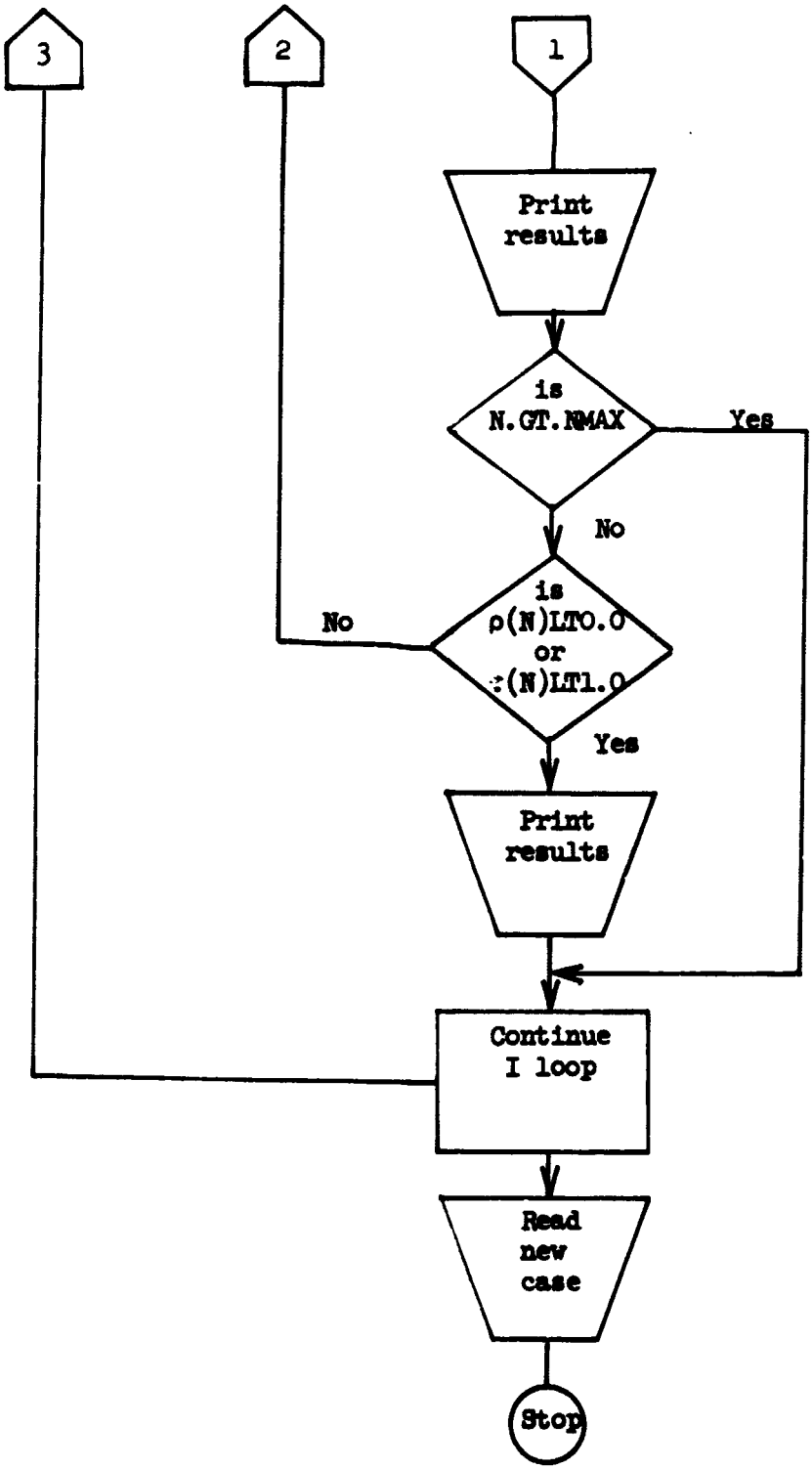
3
2
1
Print results
is N.GT.NMAX
Yes
No
is ρ(N)LT0.0 or :(N)LT1.0
No
Yes
Print results
Continue I loop
Read new case
Stop

```
SRD4911.                                                    LRC COMPUTER COMPLEX
JOB,1,0644,40000.          A1998,      2, MARTHA ROBINSON,RDV122, 1148 2011


                PROGRAM PLATES1 (INPUT,OUTPUT)
000003          DIMENSION COEFS(4),TAU(500),RHO(500),RHOT(500),RESULT(2)
000003          REAL IB,IE,INC
000003          COMPLEX R(3),TEMP(8)
000003          NAMELIST/INPUT/DTAU,IB,IE,INC,MAXN,IPFN
000003          PRINT 1
000007        1 FORMAT(*1LARGE DEFORMATIONAL ANALYSIS OF PLASTIC*/* PLATES UNDER I
                1MPULSIVE LOADING*/* ROBINSON-KRUSZEWSKI, SRD-A1998, FEBRUARY 1968,
                2 RDV-122*)
000007          CALL DAYTIM (RESULT)
000011          PRINT 2, RESULT
000017        2 FORMAT(*0DATE*A10,5X*TIME*A10)

              C INPUT DATA
              *   DTAU - TIME INCREMENT
              *   IB - INITIAL IMPULSE LOAD
              *   IE - FINAL IMPULSE LOAD
              *   INC - INCREMENT ON IMPULSE LOAD
              *   MAXN - MAXIMUM NUMBER OF ITERATIONS ON VELOCITY, TIME AND RADIUS
              *   IPFN - PRINT FREQUENCY

000017        3 READ INPUT
              CALCULATE TOTAL NUMBER OF IMPULSE LOADS AND INITIALIZE TIME
000022          NN=ABS((IE-IB)/INC)+1.0
000031          TAU(1)=DTAU
000033          DO 14 I=1,NN
000034          N=1
000035          IF (I.EQ.1) FI=IB
000040          IF (I.GT.1) FI=FI+INC
000044          IF ((I.GT.2).AND.(MOD(I,2).NE.0)) PRINT 41
000064       41 FORMAT(*1*)
000064          PRINT 4, DTAU,FI
000074        4 FORMAT(///* DTAU=*F5.3,5X*I=*F5.1//)
              CALCULATE INITIAL RHO VALUE
000074          COEFS(1)=1.0
000076          COEFS(2)=-1.0
000077          COEFS(3)=-1.0
000100          COEFS(4)=1.0-DTAU/FI
000103          CALL FALG (COEFS,3,0,R,TEMP,IERR)
000107          IF (IERR.NE.0) PRINT 5, IERR
000116        5 FORMAT(//10X*ERROR IN FALG SUBROUTINE*/)
000116          DO 6 M=1,3
```

```
0C0120          IF (AIMAG(R(M)).EQ.0.0) GO TO 8
000124        6 CONTINUE
0C0126          PRINT 7
000131        7 FORMAT(//10X*ALL ROOTS COMPLEX*/)
0C0131        8 RHO(1)=REAL(R(M))
          CALCULATE INITIAL RHOT VALUE
0C0134          RHOT(1)=-(1.+TAU(1)**2*(1.+2.*RHO(1)))/(FI*(1.-RHO(1))*(1.+3.*
               1RHO(1)))
0C0154          PRINT 9, N,TAU(N),RHO(N),RHOT(N)
0C0167        9 FORMAT(4X*N*,11X*TAU*,17X*RHO*,17X*RHOT*//2X I3,3(5XE15.8))
          C BEGIN ITERATION ON TAU, RHO, RHOT
0CC167       10 N=N+1
0C0171          DELRHO=RHOT(N-1)*DTAU
0C0173          RHO(N)=RHO(N-1)+DELRHO
0C0175          TAU(N)=TAU(N-1)+DTAU
000177          RHOT(N)=-(1.+TAU(N)**2*(1.+2.*RHO(N)))/(FI*(1.-RHO(N))*(1.+3.*
               1RHO(N)))

          C OUTPUT
          *    RHO - RADIUS OF HINGE CIRCLE
          *    TAU - TIME OF HINGE CIRCLE
          *    RHOT - VELOCITY OF HINGE CIRCLE
          *    N - ITERATION NUMBER

0C0220          IF (MOD(N,IPFN).EQ.0) PRINT 11, N,TAU(N),RHO(N),RHOT(N)
0C0240       11 FORMAT(2X I3,3(5XE15.8))
000240          IF (N.GT.NMAX) GO TO 12
0C0244          IF ((1.-RHO(N)).LT.0.0) GO TO 14
000247          IF (N.LE.2) GO TO 10
000251          IF ((TAU(N-2)-1.0).GT.0.0) GO TO 14
0CC255          GO TO 10
000255       12 PRINT 13
0C0261       13 FORMAT(//10X*MAXIMUM N REACHED*//)
0C0261       14 CONTINUE
000264          STOP
0C0266          END
```

```
PROGRAM LENGTH INCLUDING I/O BUFFERS
0C7516

FUNCTION ASSIGNMENTS

STATEMENT ASSIGNMENTS
1      -  CC0323    2      -  000343    3      -  000017    4      -  000353
5      -  000363    7      -  000370    8      -  C00131    9      -  000376
1C     -  000167    11     -  C00405    12     -  000255    13     -  0004C0
14     -  000261    41     -  000351

BLOCK NAMES AND LENGTHS

VARIABLE ASSIGNMENTS
COEFS  -  000444    DELRHO -  003450    DTAU   -  003437    FI     -  003445
I      -  003443    IB     -  0034C6    IE     -  003407    IERR   -  003446
INC    -  003410    IPFN   -  003441    M      -  003447    MAXN   -  003440
N      -  0C3444    NMAX   -  003451    NN     -  003442    R      -  003411
RESULT -  003404    RHO    -  001434    RHOT   -  002420    TAU    -  C00450
TEMP   -  003417

START OF CONSTANTS
0CC314

START OF TEMPORARIES
0C0415

START OF INDIRECTS
0C0434

UNUSED COMPILER SPACE
0C3400
```

```
CCPE MAP  20.41.41.  NORMAL              CONTROL                                    000100    015556    000000    000000
          ---TIME---LOAD MODE --L1--L7-----TYPE--------------USER-----*---CALL-------------FWA LOAD--LWA LOAD--BLNK COMN--LENGTH--
          FWA LOADER  034454  FWA TABLES  034202
          -PROGRAM----ADDRESS-                    --LABELED---COMMON--
          PLATES1     000100
          SYSTEM      007616
          OUTPTC      010561
          DAYTIM      010716
          INPUTN      011747
          FALG        012213
          SICN        013271
          CETMA       014115
          KODER       014134
          CPC         015327
          --ENTRY-----ADDRESS-                                  REFERENCES
          PLATES1     000101
          CRNTRY      007617              PLATES1     000102

          SYSTEM      010002              OUTPTC      010575
                                          INPUTN      011420    011430
                                          KODER       015140

          SYSTEML     007747
          SYSTEMP     007775
          ENC         007671              PLATES1     000367
                                          FALG        013120

          STOP        007722              PLATES1     000365

          EXIT        007714              INPUTN      012207

          APROPPL     007732              OUTPTC      010576
                                          INPUTN      011431
                                          KODER       015141

          OUTPTC      010563              PLATES1     000105    000106    000113    000115    000116    000162    000163
                                                      000166    000170    000172    000173    000212    000214    000215
                                                      000227    000230    000295    000297    000261    000263    000265
                                                      000266    000326    000330    000332    000334    000336    000337
                                                      000357    000360

          DAYTIM      010717              PLATES1     000110

          INPUTN      010750              PLATES1     000121

          FALG        012214              PLATES1     000206

          BKSPRU.     013564
          PIZPRK.     013575
          POSFIL.     013633              OUTPTC      010613

          RDPRU.      013643
          EAT.        013665              OUTPTC      010616    010635    010651

          CIOI.       013531
          OPEN.       013275              SYSTEM      010257
                                          OUTPTC      010603
                                          INPUTN      011312

          SIU.        013607              OUTPTC      010650

          CETMA       014115              OUTPTC      010571
                                          INPUTN      010756

          KODER       014135              OUTPTC      010565    010621

          CPC         015375              DAYTIM      010724    010730    010736

          CPCO2       015461
          CPC03       015327
          CPC04       015346
          CPC999      015546
          ----UNSATISFIED EXTERNALS-----                        REFERENCES
```

LARGE DEFORMATIONAL ANALYSIS OF PLASTIC
PLATES UNDER IMPULSIVE LOADING
ROBINSON-KRUSZEWSKI, SRD-A1998, FEBRUARY 1968, RDV-122

DATE 03/06/68 TIME 20.41.43.

DTAU= .010 I= 2.0

N	TAU	RHO	RHOT
1	1.00000000E-02	9.49354650E-01	-2.56633899E+00
10	1.00000000E-01	8.28503242E-01	-8.60407945E-01
20	2.00000000E-01	7.52748293E-01	-6.82851812E-01
30	3.00000000E-01	6.87216597E-01	-6.33697190E-01
40	4.00000000E-01	6.24269401E-01	-6.29870185E-01
50	5.00000000E-01	5.60554158E-01	-6.49277874E-01
60	6.00000000E-01	4.94198799E-01	-6.83213669E-01
70	7.00000000E-01	4.23944539E-01	-7.27998205E-01
80	8.00000000E-01	3.48763533E-01	-7.82825860E-01
90	9.00000000E-01	2.67592104E-01	-8.49573709E-01
100	1.00000000E+00	1.79012621E-01	-9.34323791E-01

DTAU= .010 I= 4.0

N	TAU	RHO	RHOT
1	1.00000000E-02	9.64325054E-01	-1.80062063E+00
10	1.00000000E-01	8.80607841E-01	-5.90846328E-01
20	2.00000000E-01	8.28619291E-01	-4.62953323E-01
30	3.00000000E-01	7.84379886E-01	-4.25719558E-01
40	4.00000000E-01	7.42234159E-01	-4.20060823E-01
50	5.00000000E-01	6.99375986E-01	-4.29964743E-01
60	6.00000000E-01	6.56090243E-01	-4.48754404E-01
70	7.00000000E-01	6.10157480E-01	-4.73056340E-01
80	8.00000000E-01	5.61618031E-01	-5.01038204E-01
90	9.00000000E-01	5.10152761E-01	-5.31739944E-01
100	1.00000000E+00	4.55510761E-01	-5.64785698E-01

DTAU= .01C I= 6.0

N	TAU	RHO	RHOT
1	1.00000000E-02	9.7C920305E-01	-1.46522169E+00
10	1.COCC0000E-01	9.03C65367E-01	-4.76550575E-01
20	2.00000000E-01	8.61227120E-01	-3.71626288E-01
30	3.C00CCCC0E-01	8.25765008E-01	-3.40734513E-01
40	4.00CC0000E-01	7.92C63572E-01	-3.35563586E-01
50	5.00000000E-01	7.58248952E-01	-3.42970621E-01
6C	6.000000C0E-C1	7.23345159E-01	-3.57429945E-01
70	7.00000000E-01	6.86786771E-01	-3.76101593E-01
80	8.00000CC0E-01	6.48237901E-01	-3.97382427E-01
90	9.00000000E-01	6.07477632E-01	-4.20343948E-01
10C	1.CC0C0C00E+00	5.64365818E-01	-4.444706C5E-01

DTAU= .01C I= 8.0

N	TAU	RHO	RHOT
1	1.00000000E-02	9.74E41259E-01	-1.26637469E+00
10	1.C0C00000E-01	9.16329031E-01	-4.09781482E-01
20	2.00000CC0E-01	8.8C297088E-01	-3.18725378E-01
30	3.00000000E-01	8.50C05267E-01	-2.91793207E-01
40	4.C0CC0CC0E-Ci	8.21156722E-01	-2.87118176E-01
50	5.00000C0E-01	7.92231636E-01	-2.93291285E-01
6C	6.00CC0000E-01	7.62390448E-01	-3.05500383E-01
70	7.00000CC0E-01	7.31153606E-01	-3.21258145E-01
8C	8.00C00C0E-01	6.98236316E-01	-3.39145222E-01
90	9.C00C00C0E-01	6.63467C96E-01	-3.58320151E-01
100	1.00000000E+00	6.26741673E-01	-3.78288098E-01

DTAU= .C1C I= 10.0

N	TAU	RHO	RHCT
1	1.COOCOOOOE-02	9.77512541E-01	-1.13113659E+00
10	1.00000000E-01	9.25329065E-01	-3.64774921E-01
20	2.OCCCOCCOE-01	8.93369278E-01	-2.832400S6E-01
30	3.00000000E-01	8.66373491E-01	-2.59066132E-01
40	4.OCCOOOOOE-01	8.40766777E-01	-2.54792094E-01
50	5.OOOCOCOCE-01	8.15101715E-01	-2.60199397E-01
60	6.00000000E-01	7.88630139E-01	-2.70970510E-01
70	7.CCCCOOCOE-01	7.6C927210E-01	-2.84867606E-01
80	8.00000000E-01	7.31743604E-01	-3.00607661E-01
90	9.CCCCOOOOE-01	7.00932761E-01	-3.17422915E-01
100	1.000000C0E+00	6.6E4098 74E-01	-3.3485246 2E-01

DTAU= .C1C I= 12.0

N	TAU	RHO	RHOT
1	1.OOOCOOCOE-02	9.79482068E-01	-1.03154632E+00
10	1.00C00000E-01	9.31946283E-01	-3.31834924E-01
20	2.OOOOOOCOE-01	9.C2889257E-01	-2.57352622E-01
30	3.00000000E-01	8.7E3686C1E-01	-2.35238060E-01
40	4.OCCCOOOOE-01	8.55120781E-01	-2.31285649E-01
50	5.OOOCOCOOE-01	8.31E25262E-01	-2.36158683E-01
6C	6.00000000E-01	8.C7800665E-01	-2.45907867E-01
70	7.OCCCOOCOE-01	7.82661535E-01	-2.58482927E-01
80	8.00000000E-01	7.56183372E-01	-2.72705358E-01
9C	9.000000C0E-01	7.28236227E-01	-2.87866609E-01
100	1.OOOCOOCOE+00	6.9E747338E-01	-3.03537076E-01

DTAU= .C1C I= 14.0

N	TAU	RHO	RHOT
1	1.00CC0000E-02	9.81011420E-01	-9.54283778E-01
10	1.00CC0000E-01	9.37C73938E-01	-3.06396242E-01
20	2.00000000E-01	9.10256151E-01	-2.37407313E-01
30	3.000C00C0E-01	8.87641213E-01	-2.16904737E-01
40	4.00000000E-01	8.662C7594E-01	-2.13214769E-01
50	5.C0CC0000E-01	8.44733200E-01	-2.17687642E-01
60	6.00000000E-01	8.22588230E-01	-2.26661812E-01
70	7.00000C00E-01	7.99417352E-01	-2.38234367E-01
80	8.00000CC0E-C1	7.75C14706E-01	-2.513C9793E-01
90	9.00000000E-01	7.49262413E-01	-2.65227619E-01
100	1.C0C000C0E+00	7.22096001E-01	-2.79585154E-01

DTAU= .01C I= 16.0

N	TAU	RHO	RHOT
1	1.00000000E-02	9.82243330E-01	-8.92092324E-01
10	1.C00C00C0E-01	9.41197612E-01	-2.85992394E-01
20	2.00000000E-01	9.16174345E-01	-2.21438253E-01
30	3.C00000C0E-01	8.95084436E-01	-2.02241395E-01
40	4.0C0000C0E-C1	8.75101421E-01	-1.98769786E-01
50	5.00000000E-01	8.55082496E-01	-2.02928337E-01
60	6.0C0CC000E-01	8.34439220E-01	-2.11288325E-01
70	7.00000000E-01	8.12640285E-01	-2.22066497E-01
80	8.0C0000C0E-01	7.9CC94500E-01	-2.34235152E-01
90	9.C00C0000E-01	7.66093258E-C1	-2.47173616E-01
100	1.C0CC00CCE+00	7.4C778205E-01	-2.60502145E-01

DTAU= .C1C I= 18.0

N	TAU	RHO	RHOT
1	1.COCCOOOOE-02	9.83263156E-01	-8.40637554E-01
10	1.00000000E-01	9.44606869E-01	-2.69159456E-01
20	2.000000C0E-01	9.21C63053E-01	-2.08282849E-01
30	3.00000000E-01	9.01228986E-01	-1.90171210E-01
40	4.00000000E-01	8.82439802E-01	-1.86884508E-01
50	5.00000000E-01	8.63618262E-01	-1.90787597E-01
60	6.00000000E-01	8.44210132E-01	-1.98645141E-01
70	7.00000000E-01	8.23903819E-01	-2.08773523E-01
80	8.00000000E-01	8.02520068E-01	-2.20201743E-01
90	9.C0000000E-01	7.79957682E-01	-2.32342675E-01
100	1.00000000E+00	7.56163042E-01	-2.44836267E-01

DTAU= .C1C I= 20.0

N	TAU	RHO	RHOT
1	1.0CCCCOC0E-02	9.84125486E-01	-7.97150195E-01
10	1.000000C0E-01	9.47486469E-01	-2.54966813E-01
20	2.C0000000E-01	9.25189353E-01	-1.97203850E-01
30	3.000C0000E-01	9.06412573E-01	-1.80012680E-01
40	4.00000000E-01	8.8662796E-01	-1.76884950E-01
50	5.CCCC00C0E-01	8.7C813749E-01	-1.80575023E-01
60	6.00000000E-01	8.52444531E-01	-1.88011519E-01
70	7.00000000E-01	8.33225301E-01	-1.97595440E-01
80	8.00CC0000E-01	8.12586759E-01	-2.08404089E-01
9C	9.00000000E-01	7.91633808E-01	-2.19879C69E-01
100	1.0CCCCCC0E+00	7.69116623E-01	-2.31677393E-01

```
02/06/68  LRC SCOPE 3.0       6600B--65K  02/16/68
20.41.33.SRD4911.
20.41.33.                          LRC COMPUTER COMPLEX
20.41.33.JOB,1,0644,40000.              A1998,      2,
20.41.33. MARTHA ROBINSON,RDV122, 1148 2011
20.41.34.RUN(S)
20.41.38.SETINDF.
20.41.39.LGO.
20.41.45.STOP
20.41.45.SPPRINT(OUTPUT,3)
20.41.47.CPU    000.950224 SEC.
20.41.47.PPU    006.358400 SEC.
  SRD4911. PRINT-PP 00392 LINES
```

XVIII. APPENDIX C

VALUES OF F(n)

The value of the function F(n) is needed to evaluate the final deformation. Since the argument of F(n) is limited between 0 and 1, it was expedient to generate a table for this function.

X	F(X)
0.00	0.
.01	4.02093263E-02
.02	8.08746017E-02
.03	1.22051904E-01
.04	1.63797750E-01
.05	2.06169417E-01
.06	2.49225241E-01
.07	2.93024925E-01
.08	3.37629834E-01
.09	3.83103291E-01
.10	4.29510892E-01
.11	4.76920811E-01
.12	5.25404131E-01
.13	5.75035184E-01
.14	6.25891907E-01
.15	6.78056228E-01
.16	7.31614470E-01
.17	7.86657786E-01
.18	8.43282629E-01
.19	9.01591261E-01
.20	9.61692300E-01
.21	1.02370132E+00
.22	1.08774151E+00
.23	1.15394437E+00
.24	1.22245053E+00
.25	1.29341057E+00
.26	1.36698601E+00
.27	1.44335031E+00
.28	1.52269007E+00
.29	1.60520631E+00
.30	1.69111587E+00
.31	1.78065300E+00
.32	1.87407114E+00
.33	1.97164490E+00
.34	2.07367220E+00
.35	2.18047681E+00
.36	2.29241109E+00
.37	2.40985908E+00
.38	2.53324005E+00
.39	2.66301240E+00
.40	2.79967822E+00
.41	2.94378828E+00
.42	3.09594788E+00
.43	3.25682332E+00
.44	3.42714951E+00
.45	3.60773845E+00
.46	3.79948909E+00
.47	4.00339864E+00
.48	4.22057561E+00
.49	4.45225484E+00
.50	4.69981495E+00
.51	4.96479867E+00
.52	5.24893643E+00
.53	5.55417411E+00
.54	5.88270543E+00
.55	6.23701027E+00
.56	6.61989978E+00
.57	7.03457006E+00
.58	7.48466593E+00
.59	7.97435731E+00
.60	8.50843084E+00
.61	9.09240044E+00
.62	9.73264126E+00
.63	1.04365528E+01
.64	1.12127588E+01
.65	1.20713527E+01
.66	1.30242020E+01
.67	1.40853277E+01
.68	1.52713783E+01
.69	1.66022301E+01
.70	1.81017486E+01
.71	1.97987645E+01
.72	2.17283338E+01
.73	2.39333795E+01
.74	2.64668506E+01
.75	2.93945880E+01
.76	3.27991738E+01
.77	3.67851575E+01
.78	4.14862437E+01
.79	4.70753123E+01
.80	5.37785952E+01
.81	6.18960611E+01
.82	7.18312529E+01
.83	8.41358234E+01
.84	9.95774710E+01
.85	1.19246106E+02
.86	1.44724337E+02
.87	1.78369766E+02
.88	2.23799110E+02
.89	2.86752518E+02
.90	3.76710856E+02
.91	5.10094046E+02
.92	7.17020114E+02
.93	1.05679676E+03
.94	1.65723304E+03
.95	2.82847838E+03
.96	5.45742996E+03
.97	1.27818794E+04
.98	4.26332497E+04
.99	3.37140837E+05